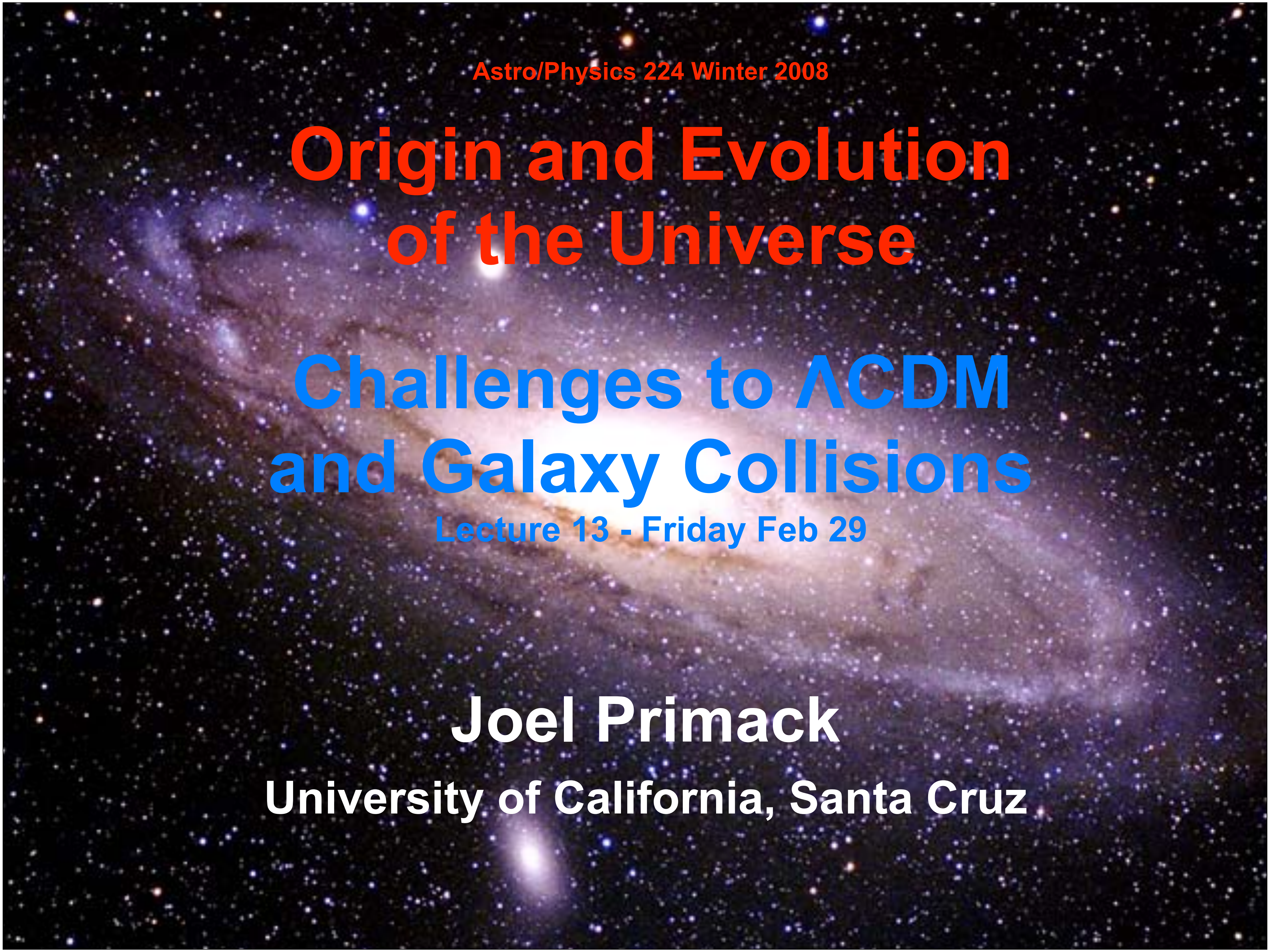

Astro/Physics 224 Winter 2008

Origin and Evolution of the Universe

Challenges to ΛCDM and Galaxy Collisions

Lecture 13 - Friday Feb 29

Joel Primack

University of California, Santa Cruz

Continue from my lecture at the Dark Matter 2008 meeting at Marina del Rey:

DM2008-Primack.pdf

at
http://physics.ucsc.edu/~joel/Cosmology224/Lectures

The Antennae colliding galaxies - HST

GALAXY COLLISIONS: Simulations vs. Observations

Joel R. Primack (UCSC)
Thomas J. Cox (CfA)
Patrik Jonsson (UCSC)
Jennifer Lotz (Arizona)
Avishai Dekel (Hebrew U)
Matt Covington (UCSC)
Greg Novak (UCSC)
Christy Pierce (UCSC)

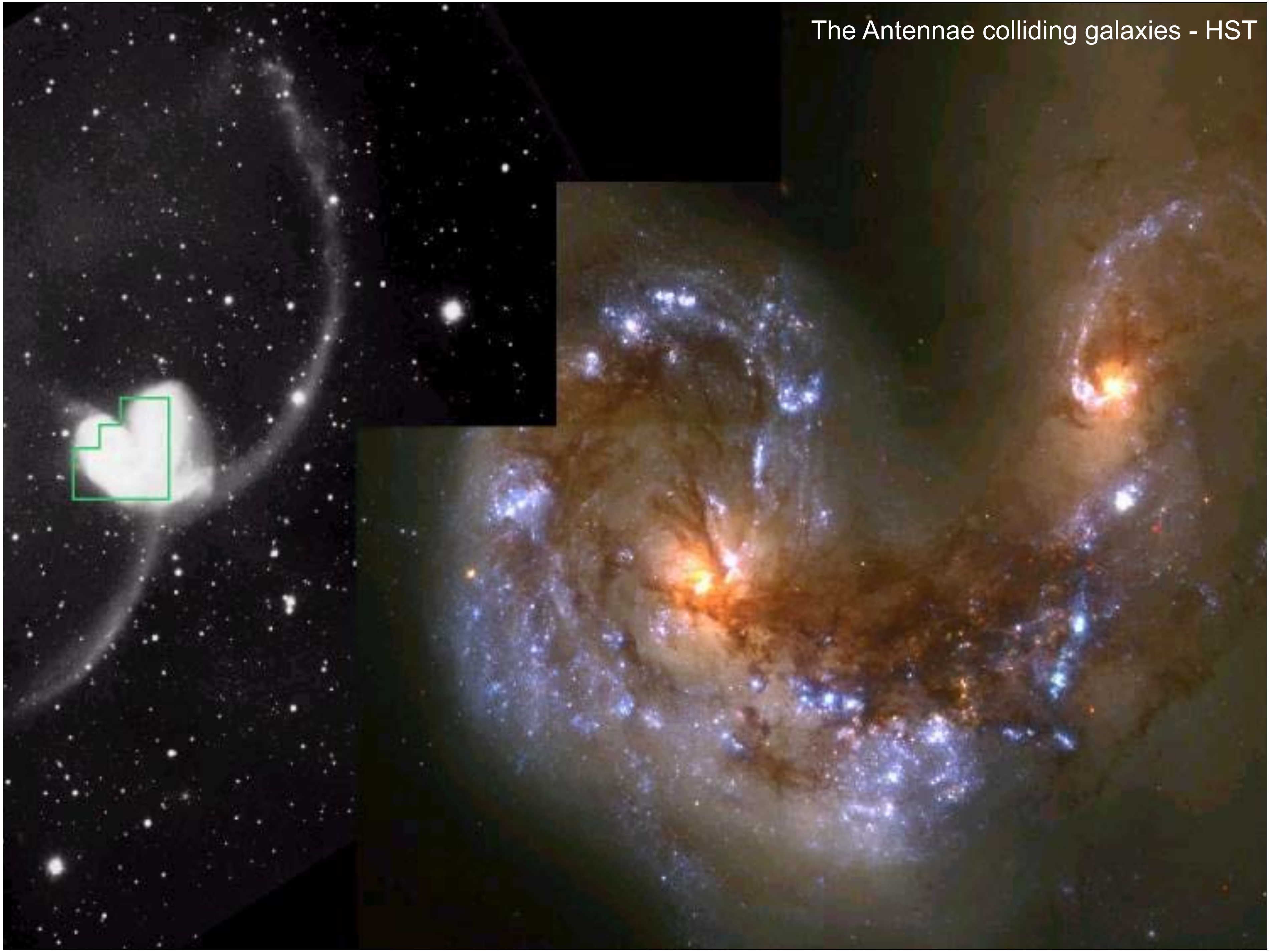
The Antennae colliding galaxies - HST

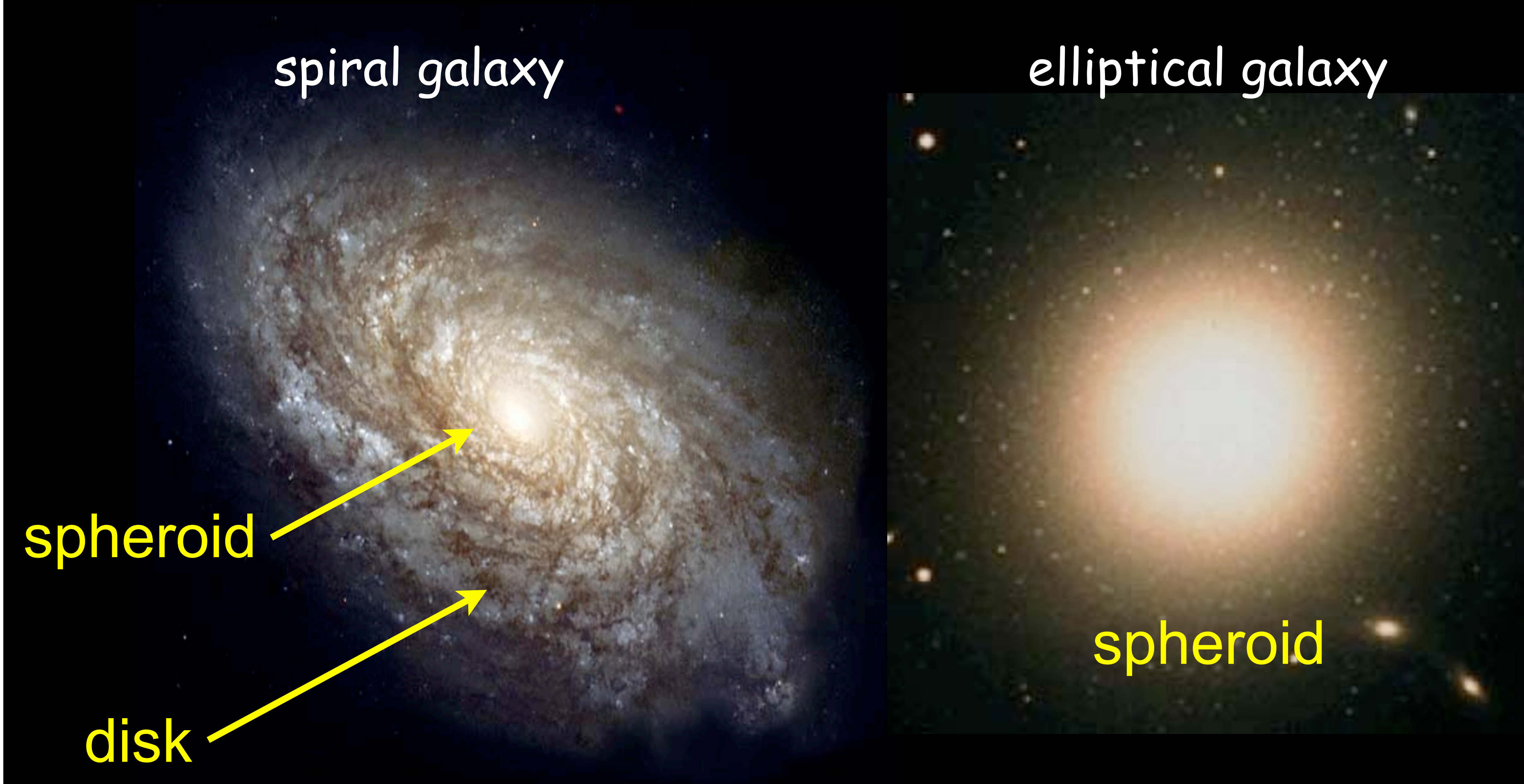

stellar mass is mostly in galactic spheroids

spheroid:disk = 0.74:0.26   Fukugita & Peebles 2004

Stellar mass is mostly in galactic spheroids

spheroid:disk = 0.74:0.26   Fukugita & Peebles 2004

Generalized Merger Hypothesis

Mergers of gas-rich disks are the dominant process for forming spheroid and SMBH populations (following Toomre 1977)

This implies that mergers are the main mechanism for

- most intense starbursts (ULIRGs)
- bright quasar activity

Columbia
Super-
Computer

FORMATION OF THE DARK MATTER HALO OF A BIG GALAXY LIKE THE MILKY WAY

Zoom-In
of
Dark
Matter
Simulation:

Columbia
Super-
Computer

NASA
Ames
Laboratory

Goals of Galaxy Interaction Simulations

- Understand the amount of star formation due to galaxy mergers TJ Cox PhD thesis 04, Cox+05,06,07,...

- Study properties of merger remnants

  DM/stellar/gas distributions Matt Covington+07,+08

  Angular momenta and kinematics Greg Novak+06...

- Predict appearance of interacting galaxies throughout merger, including dust scattering, absorption, and reradiation, and AGN P Jonsson PhD thesis 04, 06, Jonsson+06, Rocha+08, ...

- Statistically compare to observations (DEEP2 and GOODS: ACS, Chandra, Spitzer, etc.) Jennifer Lotz, Piero Madau, and Primack 04; Lotz+05, 06; Pierce +07, Nandra+07, Georgakakis+08; Lotz+08, ...

Galaxy Collision Simulations

T.J. Cox
PhD Dissertation
UC Santa Cruz
http://physics.ucsc.edu/~tj/work/thesis/

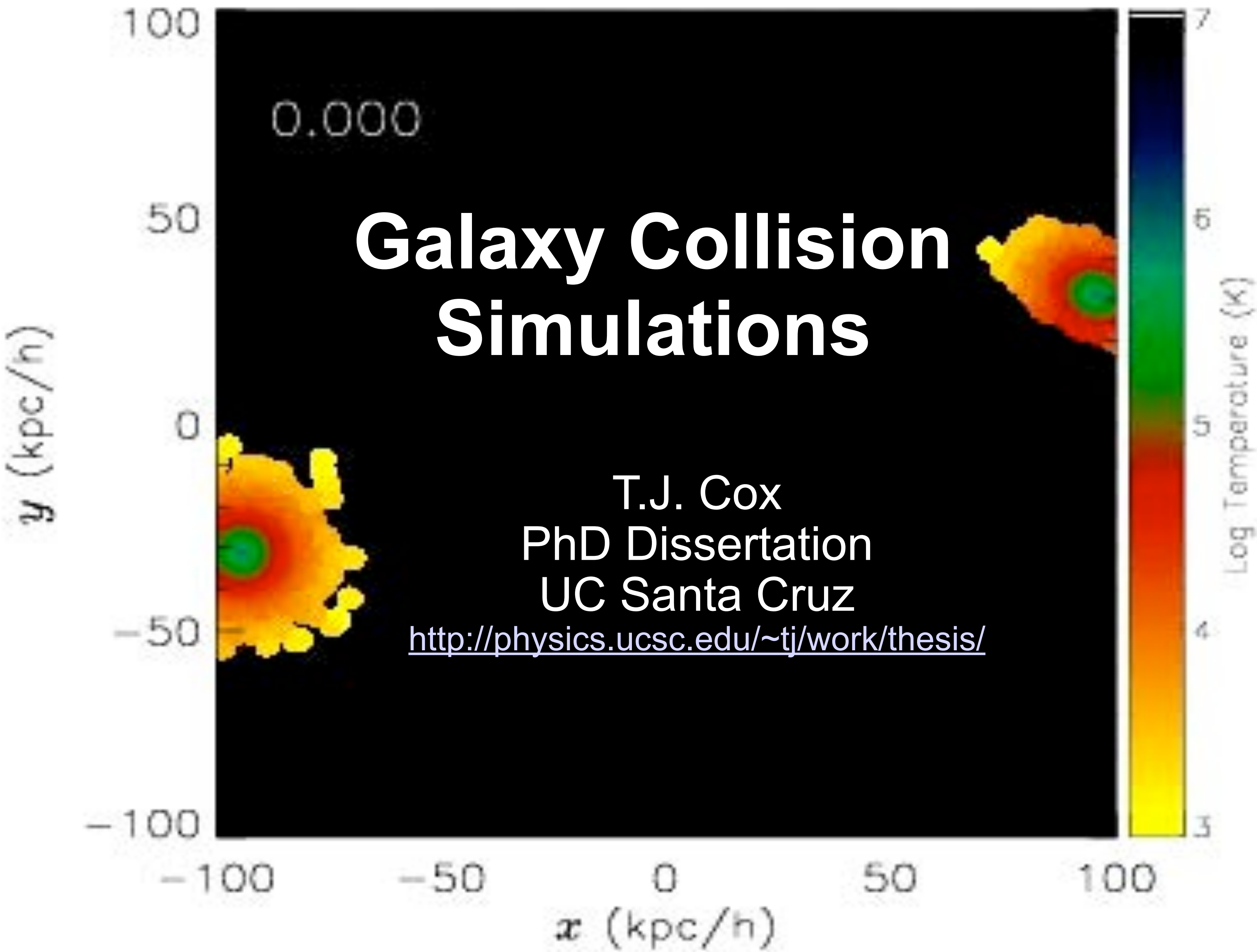

Numerical Simulations of Star Formation in Colliding Disk Galaxies: Earlier Work

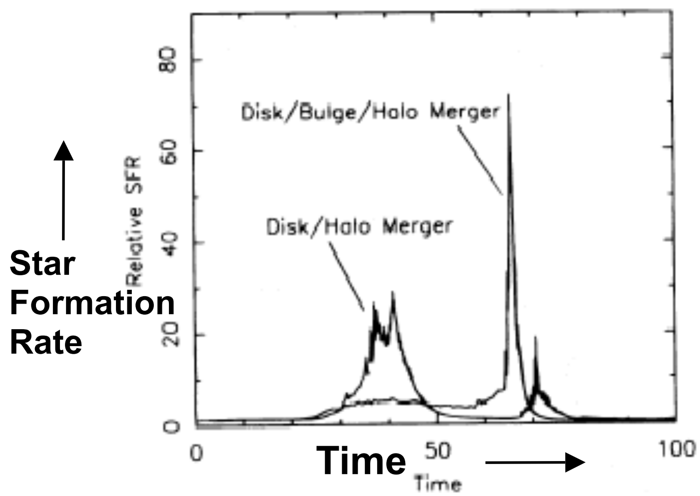

• **Major mergers** (Mihos & Hernquist 1996, Springel 2000) (original disks are identical) generate significant bursts of star formation consuming ~80% of the original gas mass.

• **Internal structure of progenitor disk galaxy (i.e. the presence of a bulge or not) dictates when the gas is funneled to the center and turned into stars.**

• **Minor mergers** (Mihos & Hernquist 1994) (satellite galaxy is 10% of the original disk mass) generate significant bursts of star formation only when there is no bulge in progenitor disk galaxy.

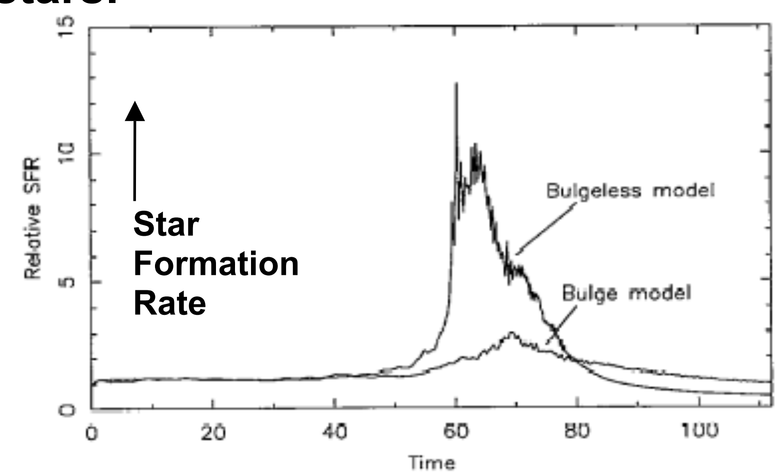

→ **NOTE: These simulations used a version of SPH which has been shown not to conserve entropy (Springel & Hernquist 2002).**

Parameterizing Starbursts

Based upon the results of Mihos & Hernquist (the 3 ‘data’ points), Somerville, Primack & Faber (2001, SPF01) estimated the burst efficiency (amount of gas converted to stars due to the galaxy merger) as a function of the merger mass ratio. A motivation of the present work is to improve the statistics and understanding of mergers.

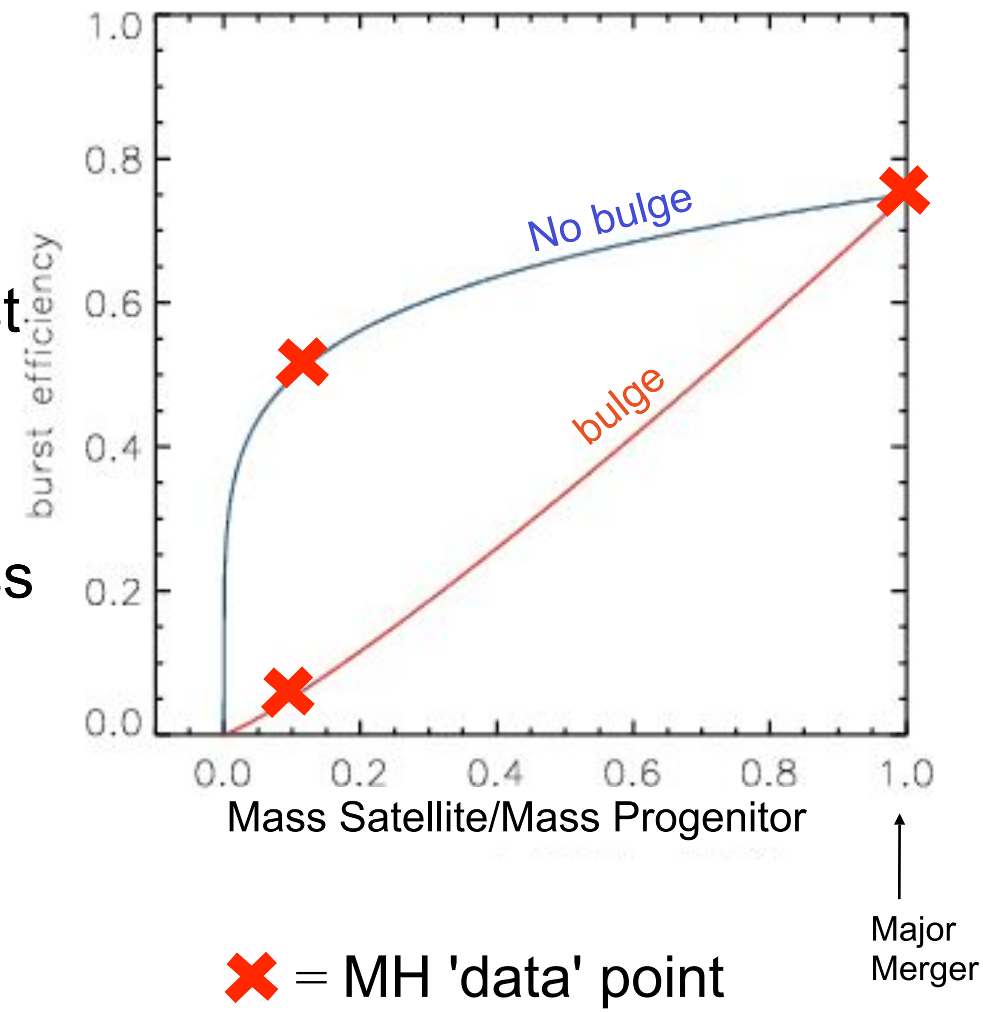

Our New Work

In order to investigate galaxy mergers (and interactions) we build observationally motivated N-body realizations of compound galaxies and simulate their merger using the SPH code GADGET (Springel, Yoshida & White 2000, Springel 2005). These simulations include:

- An improved version of smooth particle hydrodynamics (SPH) which explicitly conserves both energy and entropy (Springel & Hernquist 2002).
- The radiative cooling of gas
- Star formation: $\rho_{sfr} \sim \rho_{gas}/\tau_{dyn}$ for ($\rho_{gas} > \rho_{threshold}$)
- Metal Enrichment
- Stellar Feedback

* Our simulations contain ≥ 170,000 particles / big galaxy and the resolution is typically ~100 pc. (Tested up to 1.7×10^6 particles.)

Initial Conditions

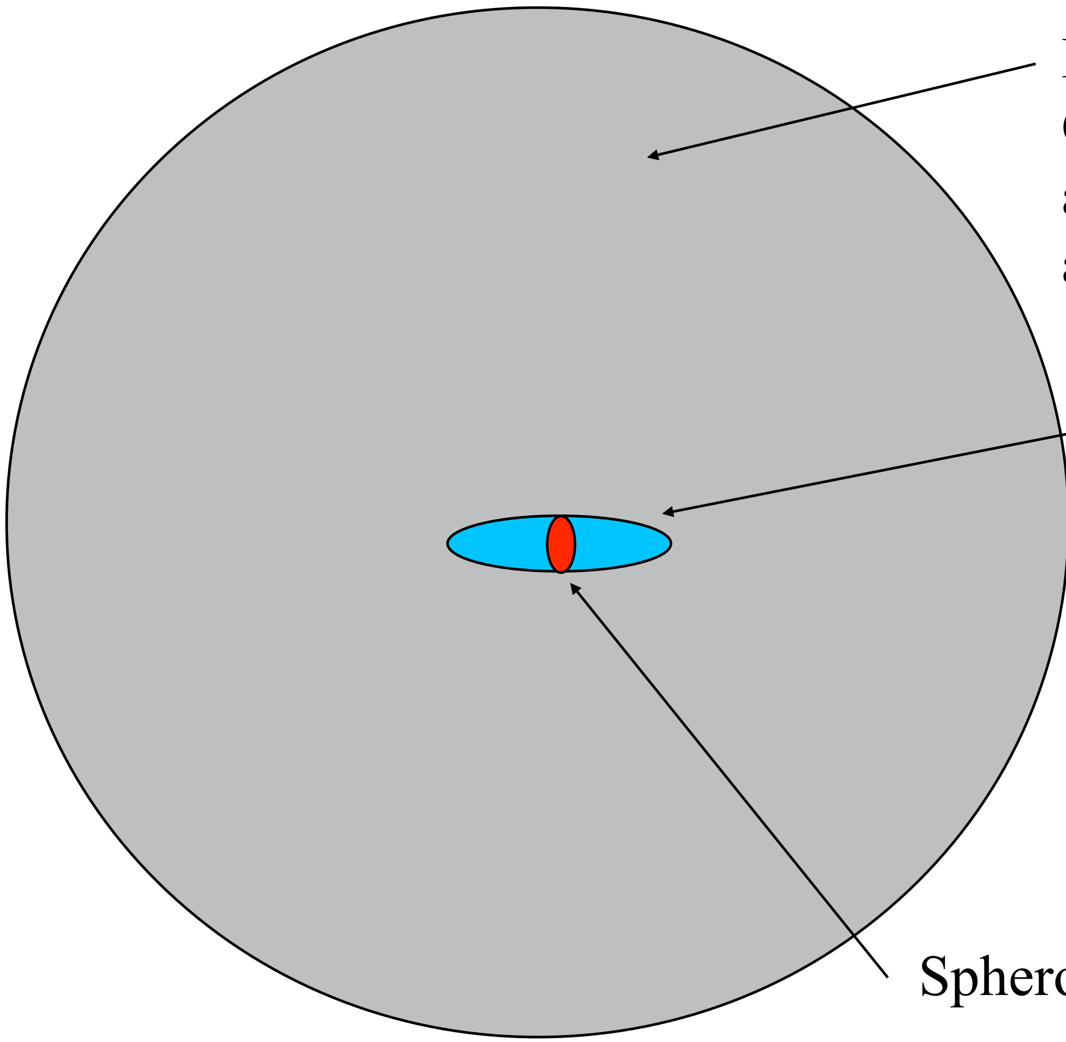

Dark Matter Halo: standard CDM NFW profile defined by a mass (>90% of the total) and a concentration.

Rotating exponential disk comprised of both stars and gas (the fuel for future star formation).

Spheroidal bulge (in some models)

Stable Disk

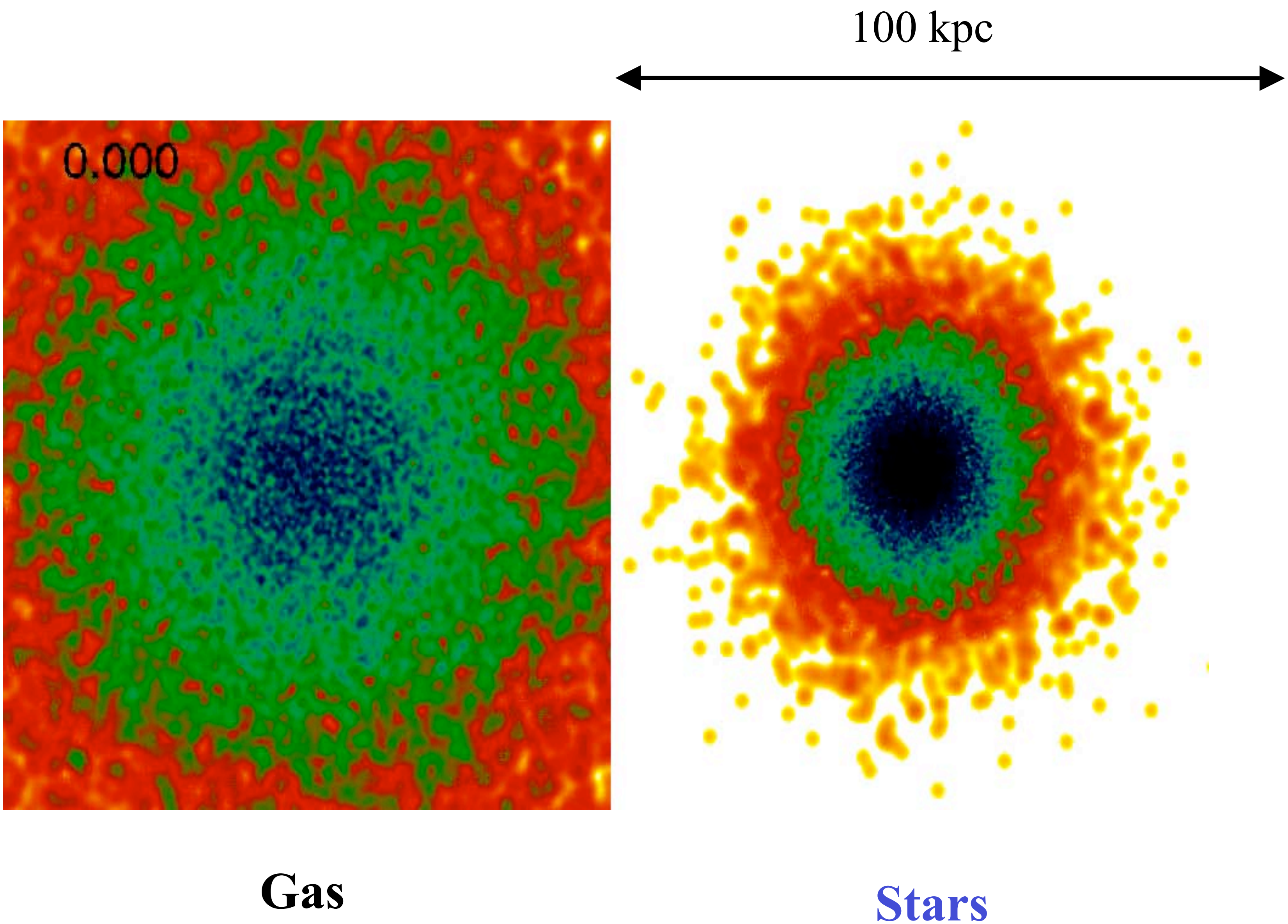

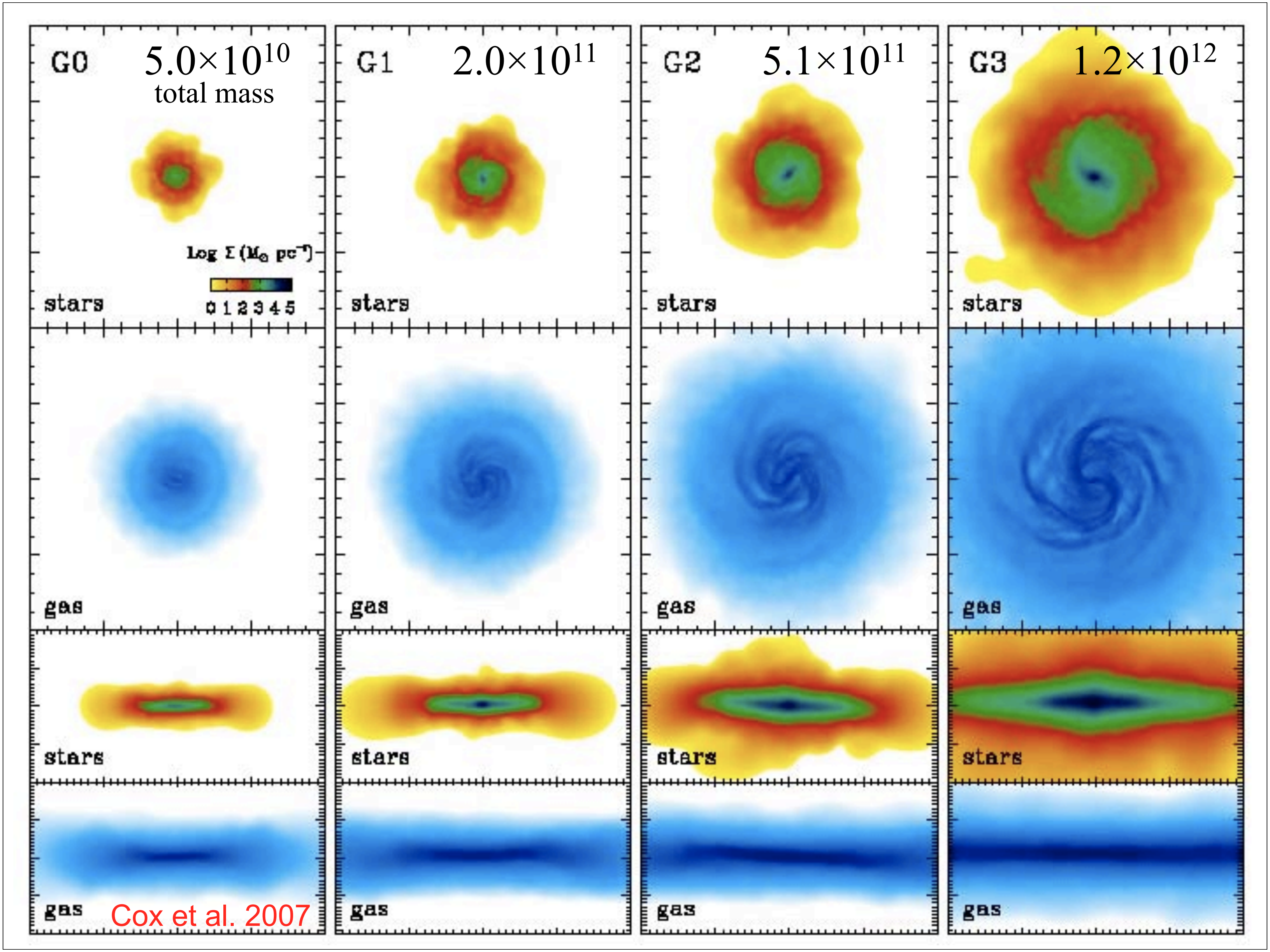
G0
5.0×10^{10}
total mass
Log Σ (M☉ pc⁻²)
0 1 2 3 4 5
stars
G1
2.0×10^{11}
G2
5.1×10^{11}
G3
1.2×10^{12}
stars
gas
stars
gas
Cox et al. 2007

Now Let's Merge Two Disks

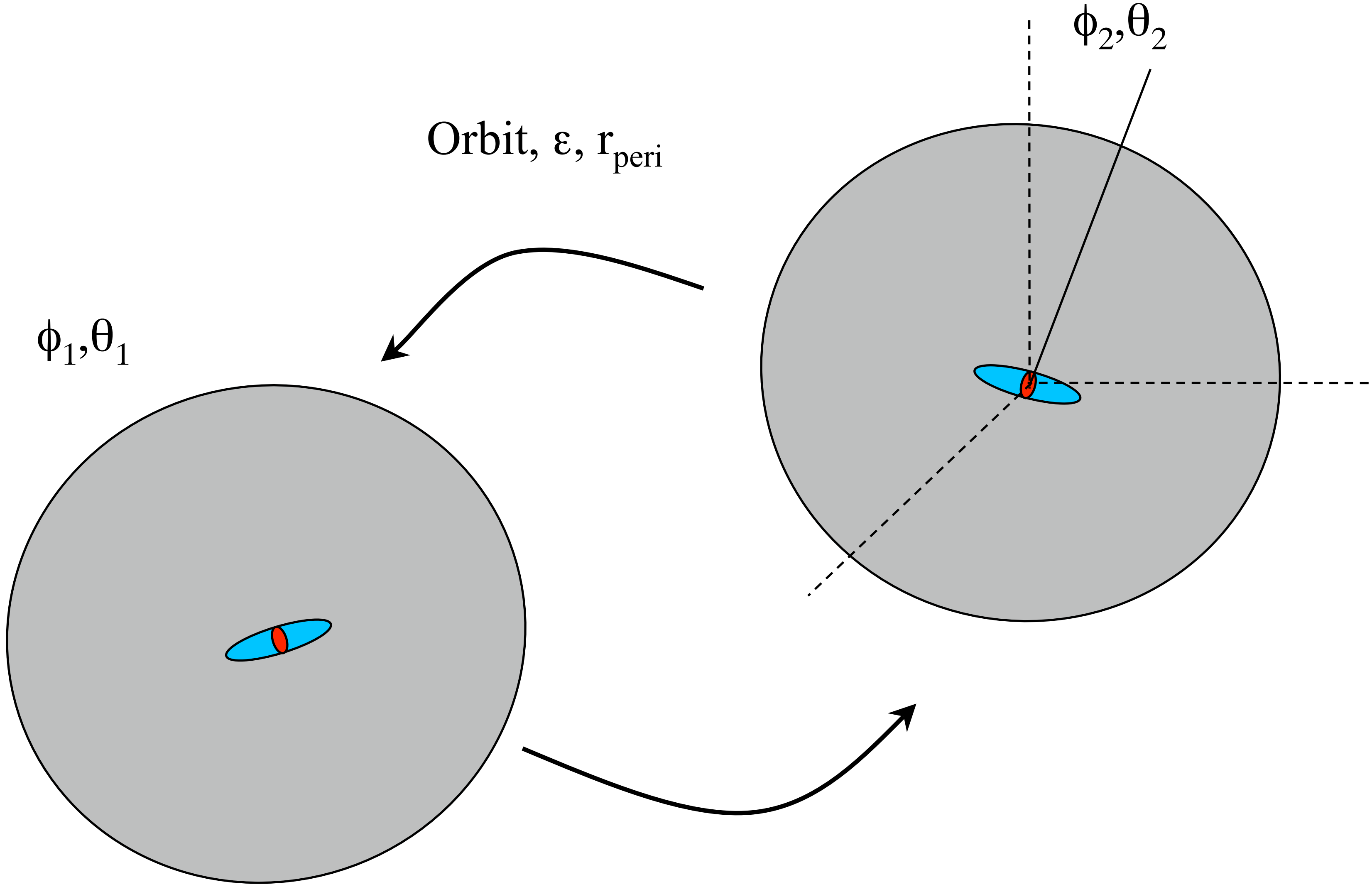

Gas Particles color-coded by density

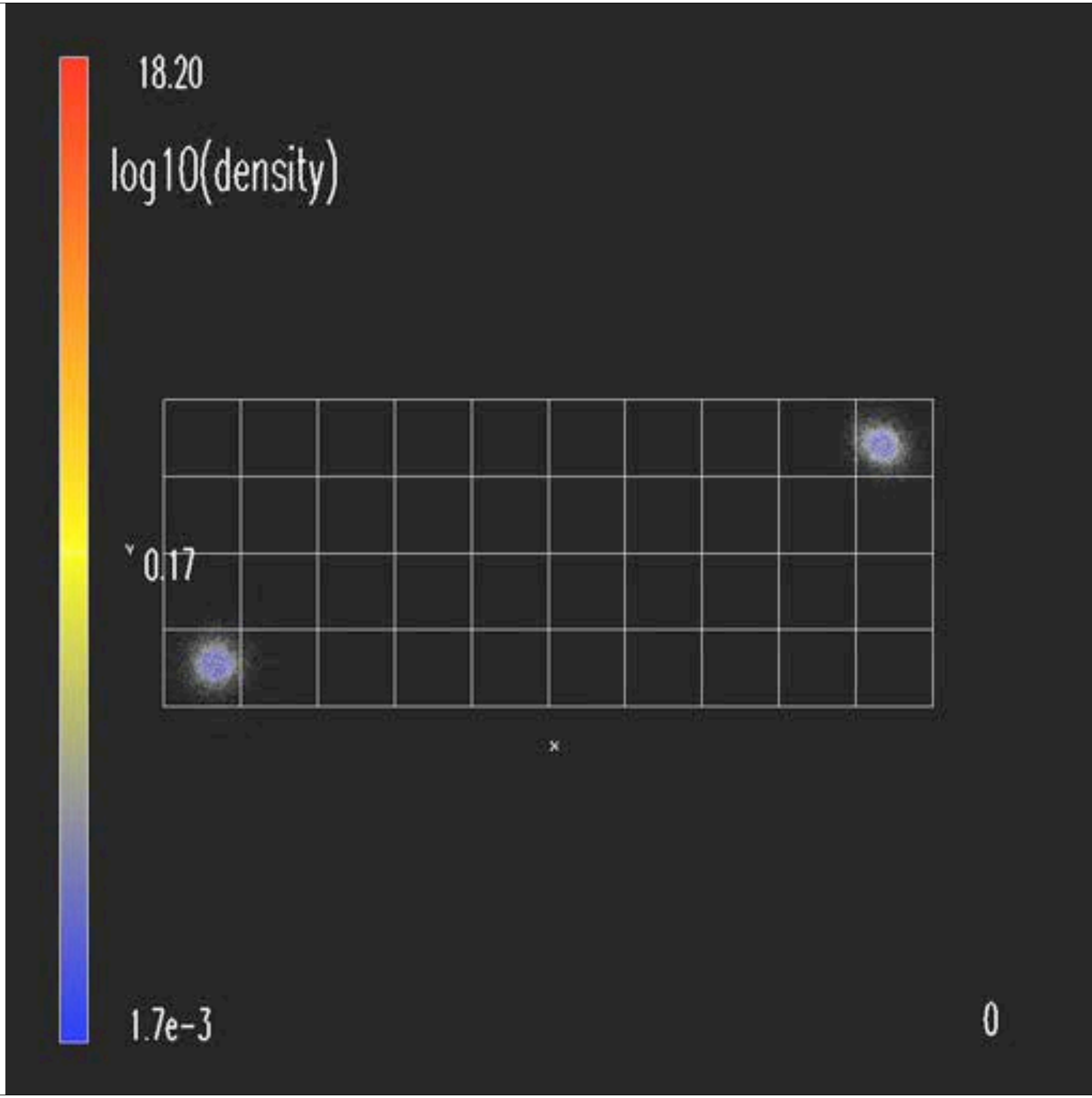

Major Merger Morphology and Resulting Star Formation

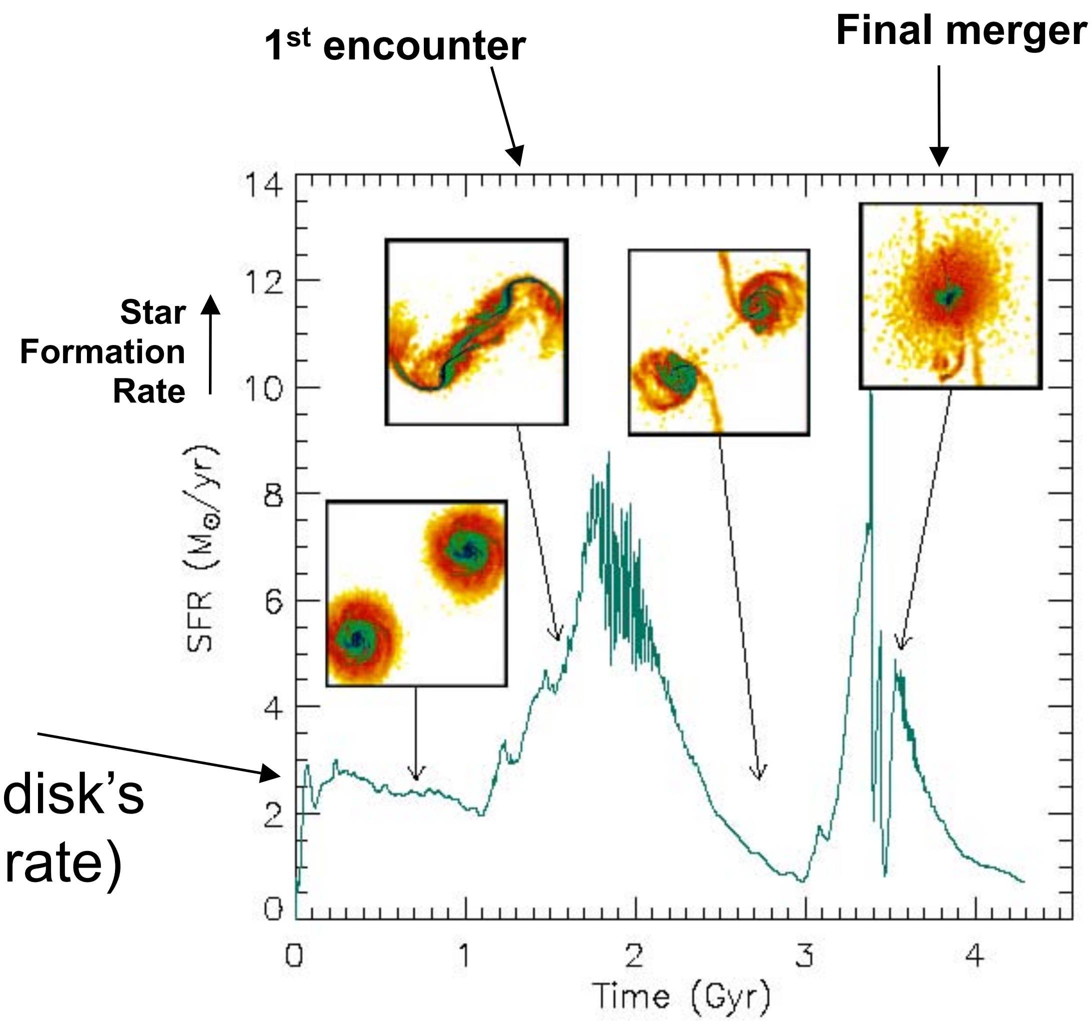

Initially, SFR ~ 2x(disk's quiescent rate)

Prograde parabolic orbit, initial separation 250 kpc, pericentric distance 7 kpc

Projected Gas Density
in the orbital plane

Projected Stellar Density
in the orbital plane

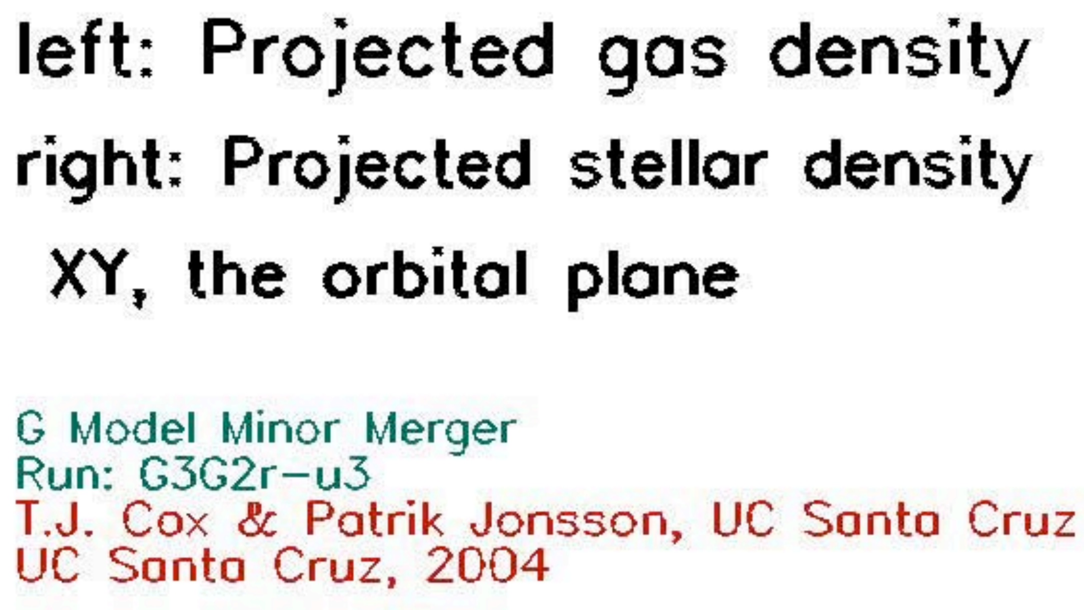

G3G2r: 1:3 retrograde merger

Movie at:
http://physics.ucsc.edu/~tj/work/movies/

SFR vs. Free Parameters

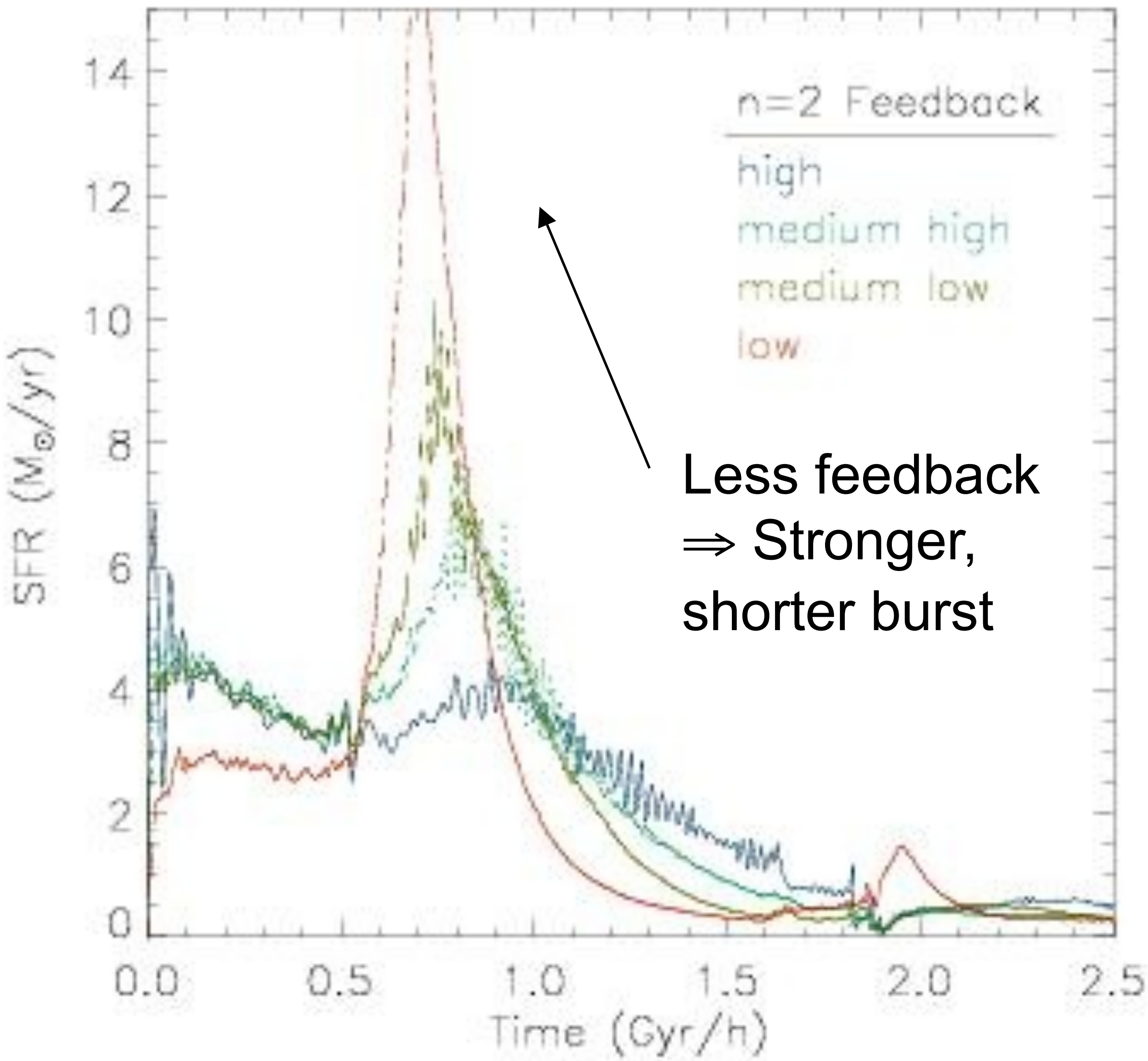

While SF/Fb parameters are fixed to make star formation fall on Kennicutt (1998), we can still get a range of burst strengths and durations.

Cox et al. 2006

Star Formation in G Mergers

- Due to the small bulge in G3 there is a small increase in star formation during the first encounter (between t=1-2 Gyr).
- Large (in some models) burst (>10x quiescent) of star formation follows final merger.
- Max SFR decreases with mass
- The burst strength increases with merger mass ratio, with rough dividing line at 1:5 for generating a burst at all.
- Large mass ratios are tricky!

Cox et al. 2007

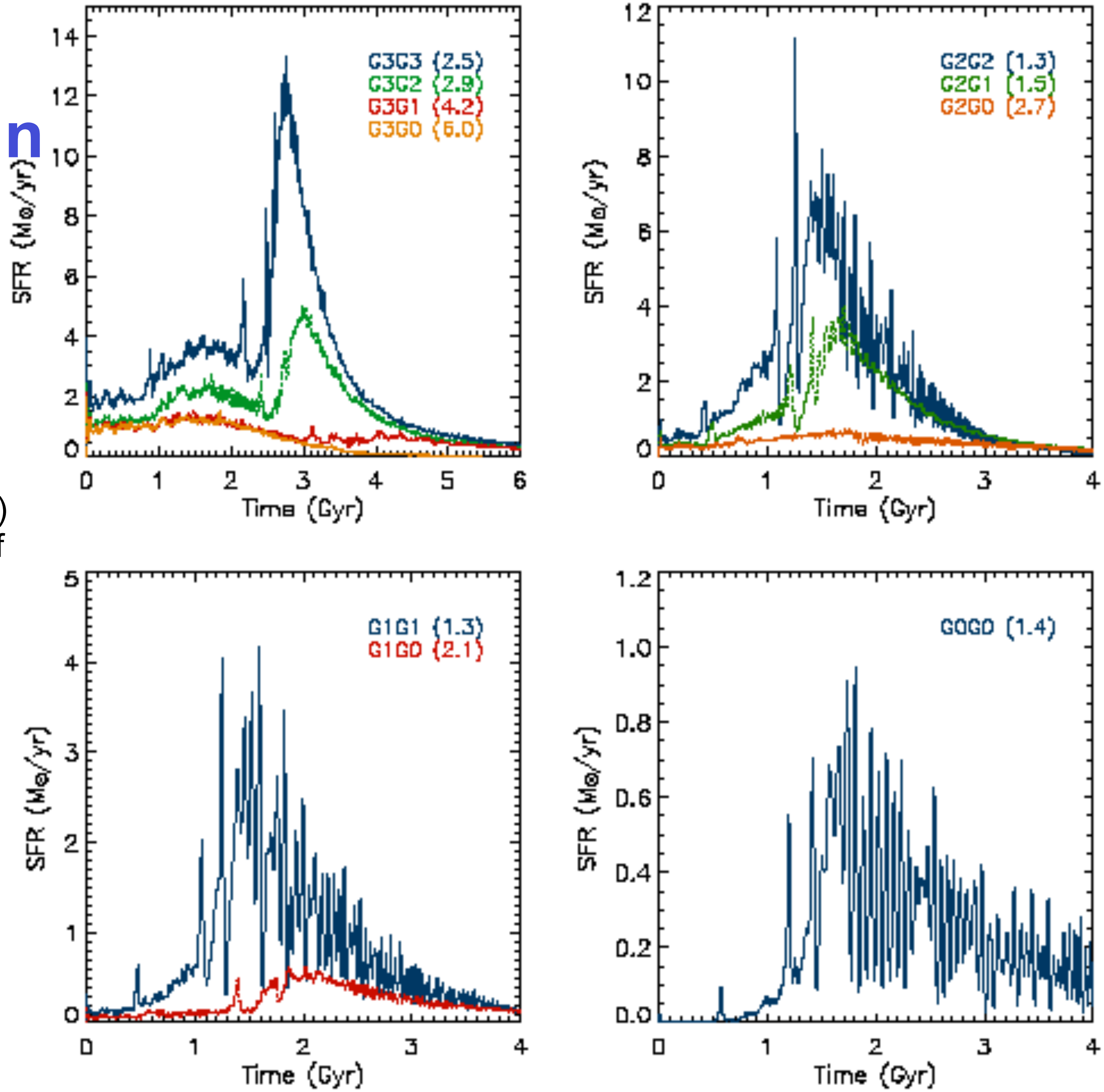

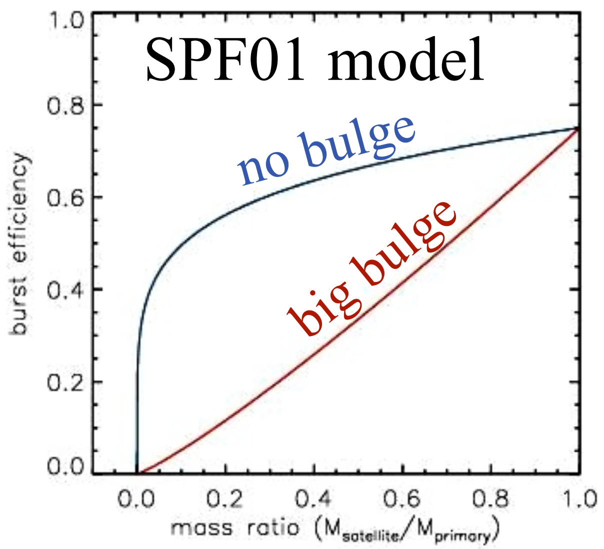

The quiescent star formation has been subtracted.

$$e = e_{1:1} \left(\frac{\mathrm{M_{sat}}}{\mathrm{M_{primary}}} \right)^{\gamma}$$

$$e_{1:1} = 0.56$$

$$\gamma = 0.7$$

Burst Efficiency

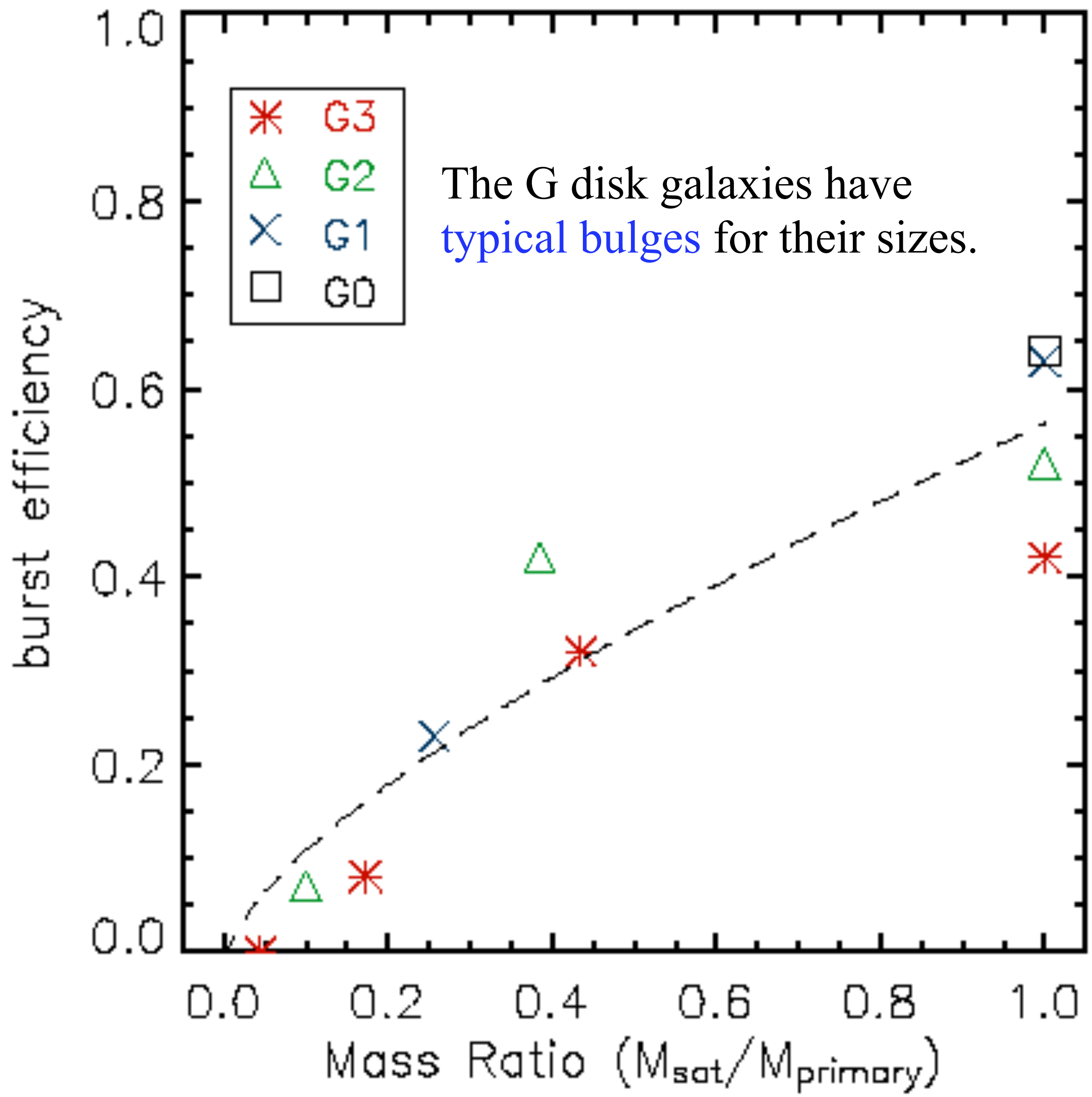

The G disk galaxies have typical bulges for their sizes.

Gas Temperature during Major Merger

7 kpc slice through orbital plane

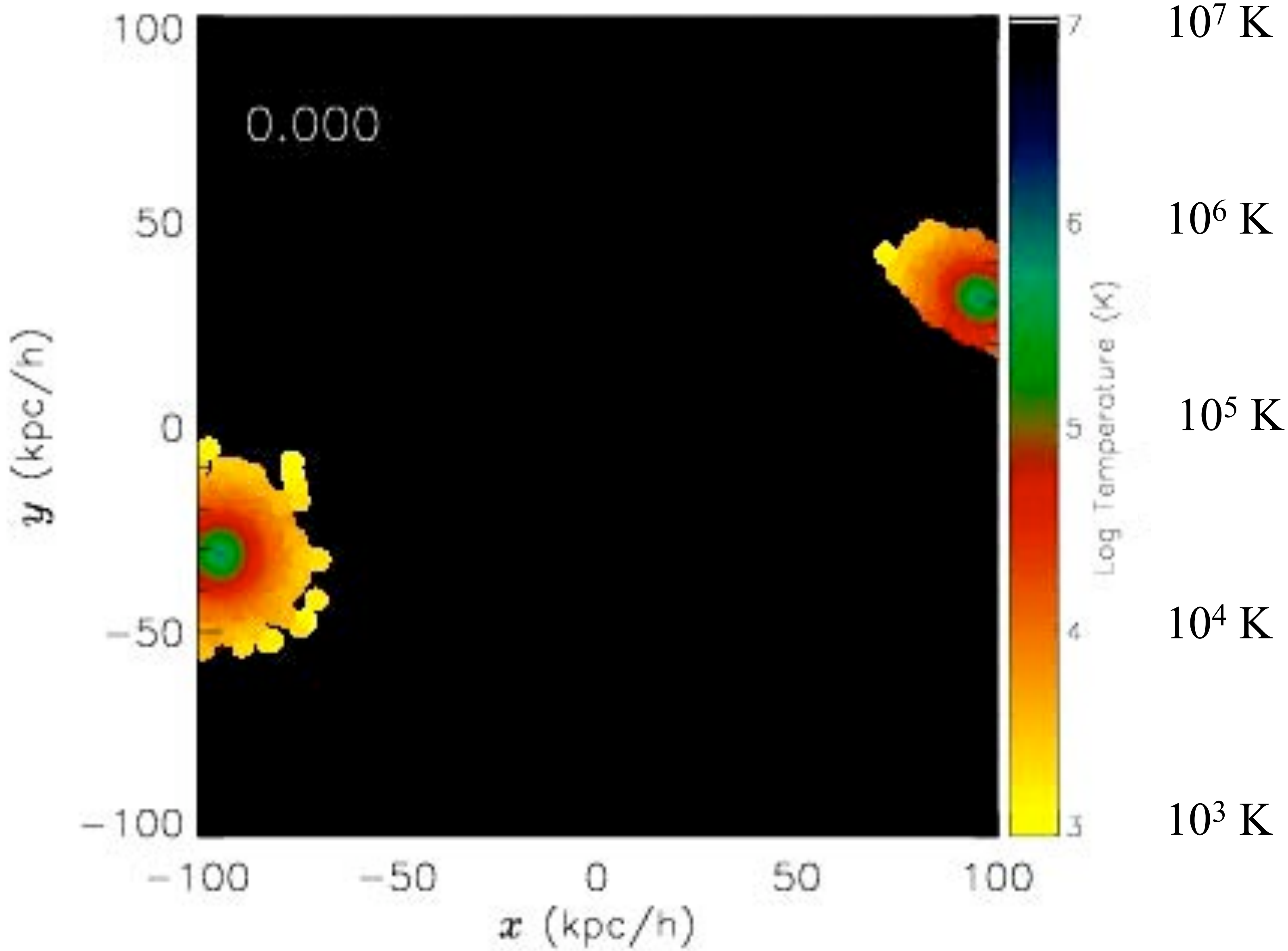

Gas velocity field on color gas density map

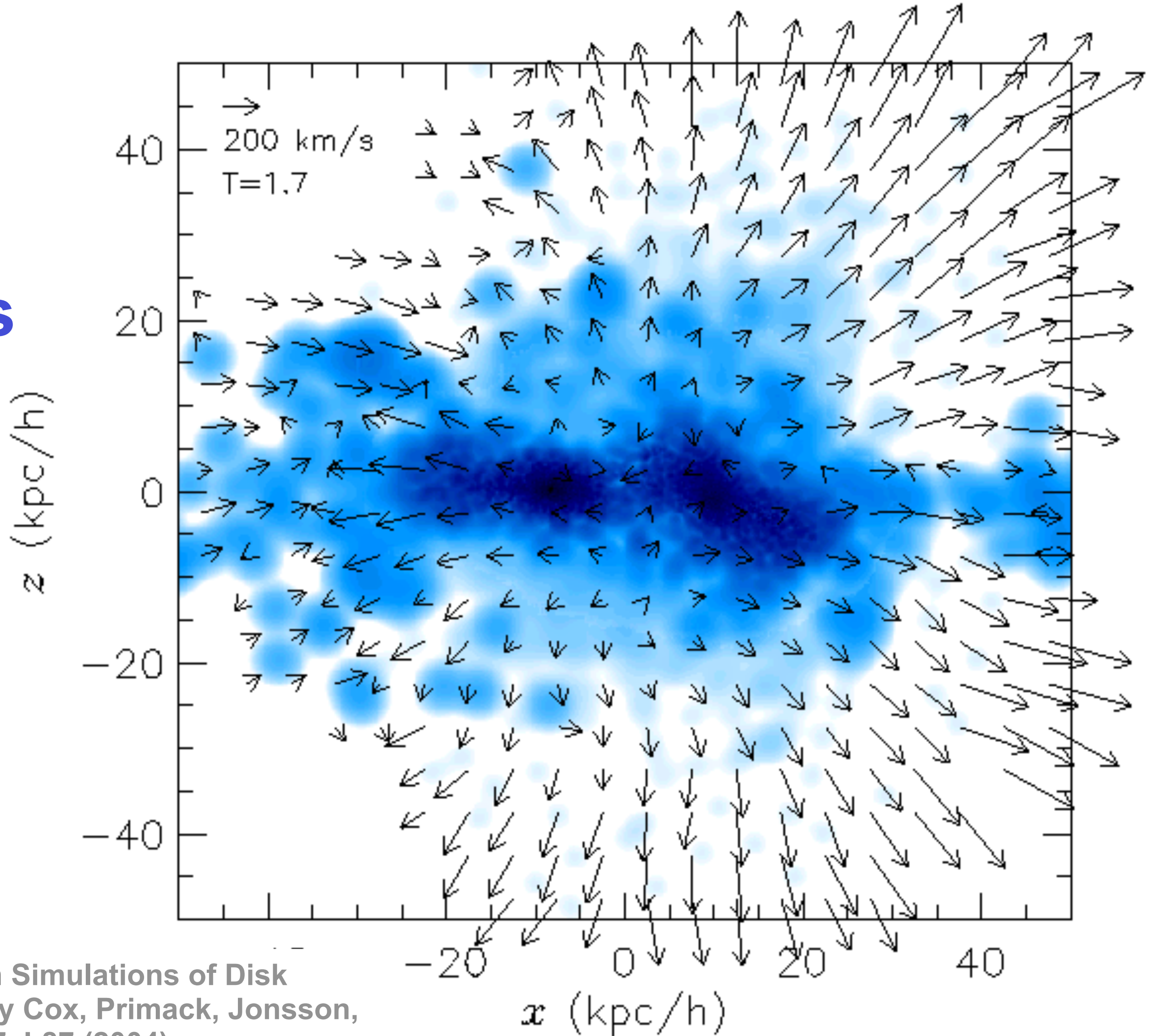

7 kpc slice through plane perpendicular to orbital plane

Generating Hot Gas in Simulations of Disk Galaxy Interactions, by Cox, Primack, Jonsson, & Somerville, ApJ, 607, L87 (2004).

Spatial, velocity, and angular momentum distribution of dark matter, stars, and gas in merger remnants:

Comparison with Planetary Nebulae and Globular Clusters – "Dark-Matter Haloes in Elliptical Galaxies: Lost and Found" Avishai Dekel et al., *Nature, 437,* 707 (2005)

Semi-analytic models of merger remnant properties (e.g., M*, $r_{1/2}$, σ_v, gas) – in progress by UCSC grad student Matt Covington working with Dekel and Primack. Radius and velocity dispersion predicted. Massive major mergers lie in fundamental plane, lower mass disky remnants do not.

Comparison with PNe and SAURON, and shapes of stellar spheroid and dark matter halos of merger remnants – in progress by UCSC grad student Greg Novak working with Dekel, Faber, and Primack.

Comparison with Planetary Nebulae and Globular Clusters "Dark-Matter Haloes in Elliptical Galaxies: Lost and Found" -- Dekel et al., *Nature, 437,* 707 (2005)

We show what's wrong with the conclusions drawn by

Romanowsky, Douglas, Arnaboldi, Kuijken, Merrifield, Napolitano, Capaccio li, & Freeman, "**A Dearth of Dark Matter in Ordinary Elliptical Galaxies**" *Science* **301**, 1696 (2003)

Abstract: The kinematics of the outer parts of three intermediate-luminosity elliptical galaxies were studied with the Planetary Nebula Spectrograph. The **galaxies' velocity-dispersion profiles were found to decline with the radius, and dynamical modeling of the data indicates the presence of little if any dark matter in these galaxies' halos.** This unexpected result conflicts with findings in other galaxy types and poses a challenge to current galaxy formation theories.

Note that more recent X-ray and Globular Cluster data imply massive dark matter halos in at least two of these galaxies. They thus conflict with this claim and and are consistent with our simulations.

Comparison with Planetary Nebulae and Globular Clusters – "Dark-Matter Haloes in Elliptical Galaxies: Lost and Found"

Dekel et al., *Nature, 707,* 437 (2005) astro-ph/0501622

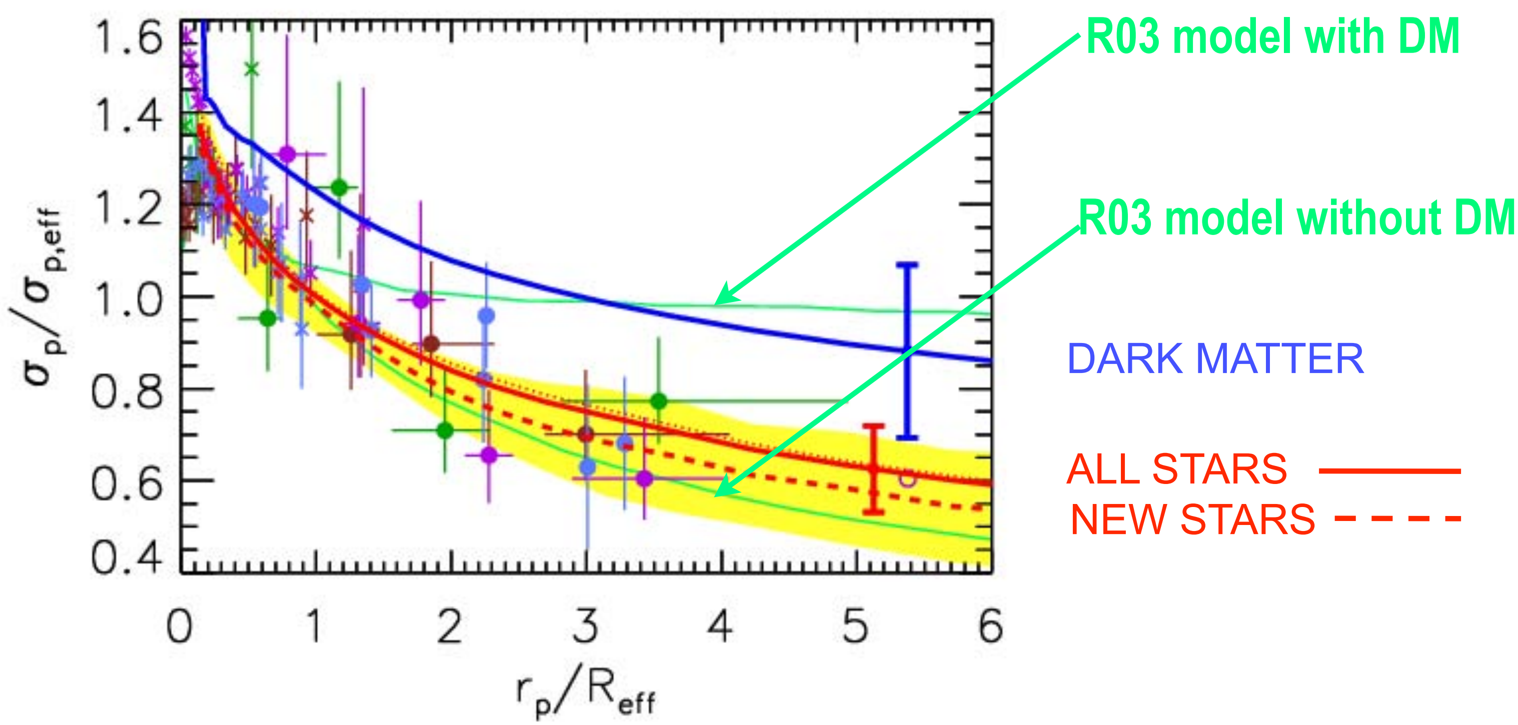

Projected velocity dispersion profiles: simulated galaxies versus observations. Ten major merger remnants are viewed from three orthogonal directions and the 60 profiles are stacked such that the stellar curves ("old"+"new") match at Reff. Dark matter (blue) versus stars (red), divided into "old" (dotted) and "new" (dashed). The < 3 Gyr "new" stars mimic the observed PNs. The shaded areas and thick bars mark 1σ scatter, partly due to triaxiality. The Romanowsky galaxies are marked green (821), violet (3379), brown (4494) and blue (4697). The surface densities shown for NGC 3379 and 4697 almost coincide with the simulated profile. Green lines refer to the R03 models with (upper) and without (lower) dark matter.

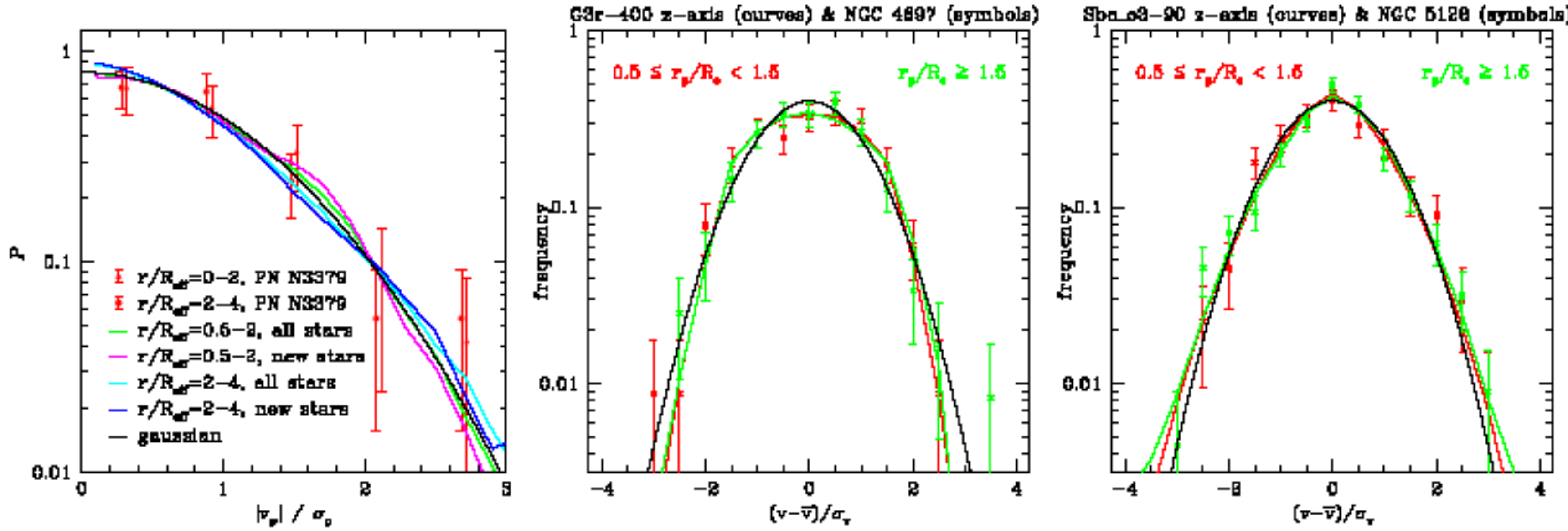

Figure 9. Line-of-sight velocity distribution $P(|v_{\rm p}|/\sigma_{\rm p})$ (LOSVD) of simulation versus data. The black curve marks a Gaussian distribution. The LOSVD is computed in two radial bins, as marked, within which the variation of $\sigma_{\rm p}$ is limited. The data is for N3379, N4697 and N5128 from left to right respectively. The deviations from Gaussian are small, with a tendency for negative and positive kurtosis in N4697 and N5128 respectively. The curves are LOSVD from three simulations. Left: the fiducial Sbc merger, stacked views from three orthogonal directions at the final time, with a near Gaussian LOSVD. Middle: a face-on view of a retrograde merger remnant (G3r) showing a negative kurtosis. Right: a face on view of another Sbc merger remnant showing a positive kurtosis. We learn that a high anisotropy, $\beta \sim 0.5$ beyond $R_{\rm eff}$, does not necessarily imply strong deviations from a Gaussian distribution.

From Supplementary Information online with Dekel et al. 2005 Nature article.

MERGER REMNANTS LIE IN THE FUNDAMENTAL PLANE

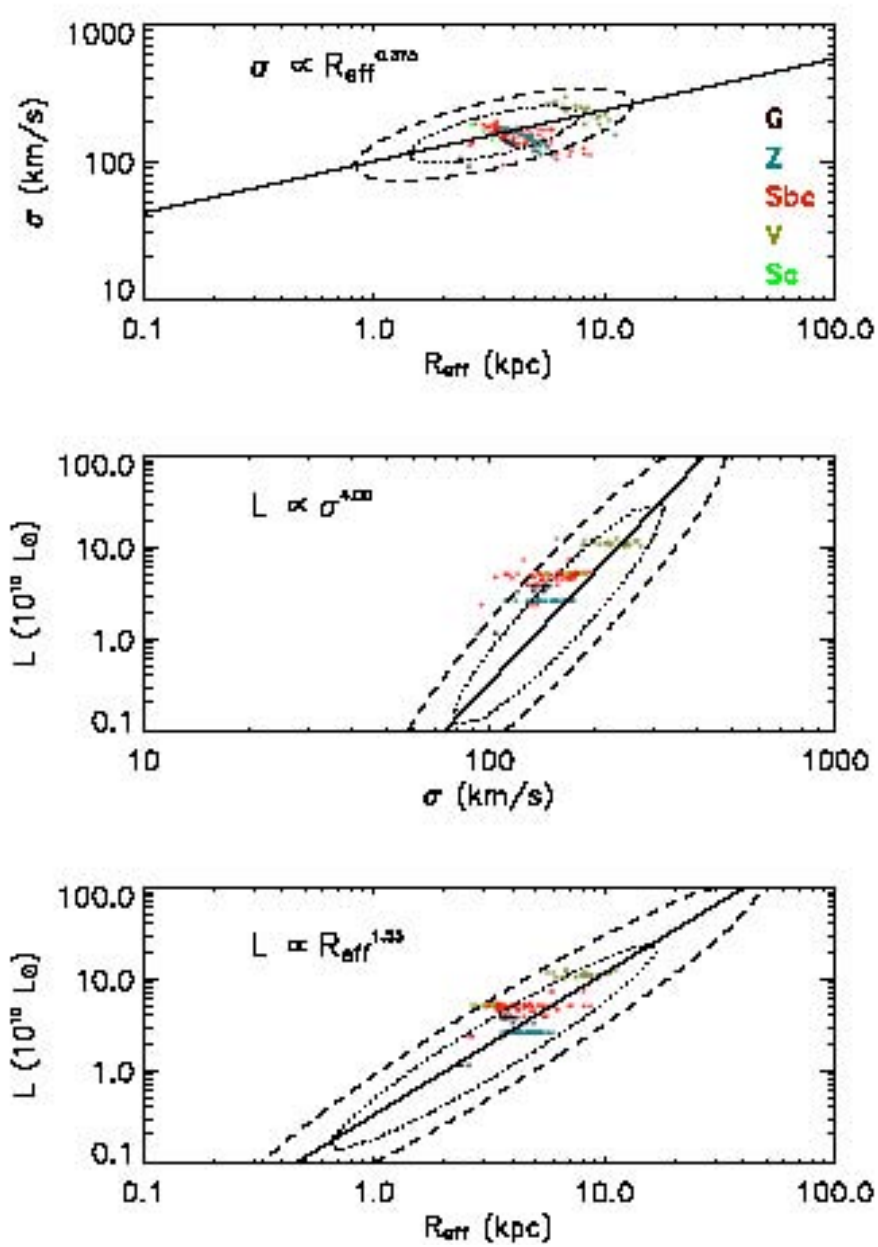

Figure 11. The global structure properties of the simulated merger remnants (symbols, colored by the merger type) in comparison with the Fundamental Plane distribution of elliptical galaxies in SDSS (1 and 2 contours). The dispersion velocity is measured in the central regions. The luminosity is derived from the stellar mass assuming an effective M/L = 3.

From Supplementary Information online with Nature article, also at astro-ph/0501622. Based on work by Matt Covington with Avishai Dekel and Joel Primack. See also Robertson et al. 2005.

A Physical Model for Predicting the Properties of Merger Remnants

We might expect that a more energetic encounter will cause increased tidal stripping and puff up the remnant.

NO! For our simulations, more energetic encounters create more compact remnants.

Why? Dissipative effects cause more energetic encounters to result in smaller remnants.

Impulse provides a measure of merger "violence." The greater the impulse, the more the gas is disturbed, therefore the more it can radiate and form stars.

A number of physical mechanisms conspire to make this so (e.g. greater tidal effects, lower angular momentum, and more gas disk overlap).

Matt Covington, Cox, Dekel, & Primack 2007

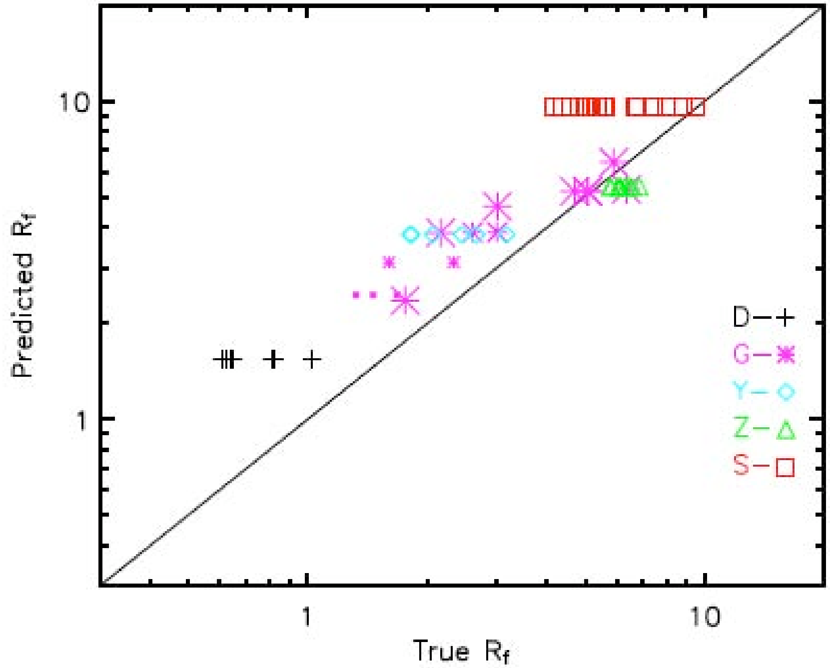

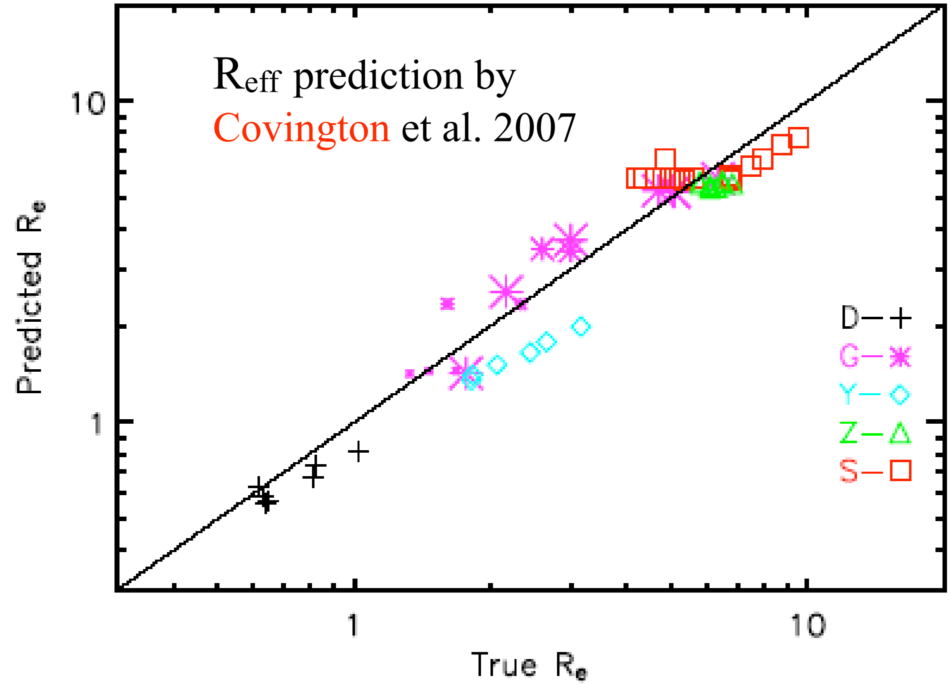

R_{eff} prediction by
Cole et al. 2000
dissipationless model

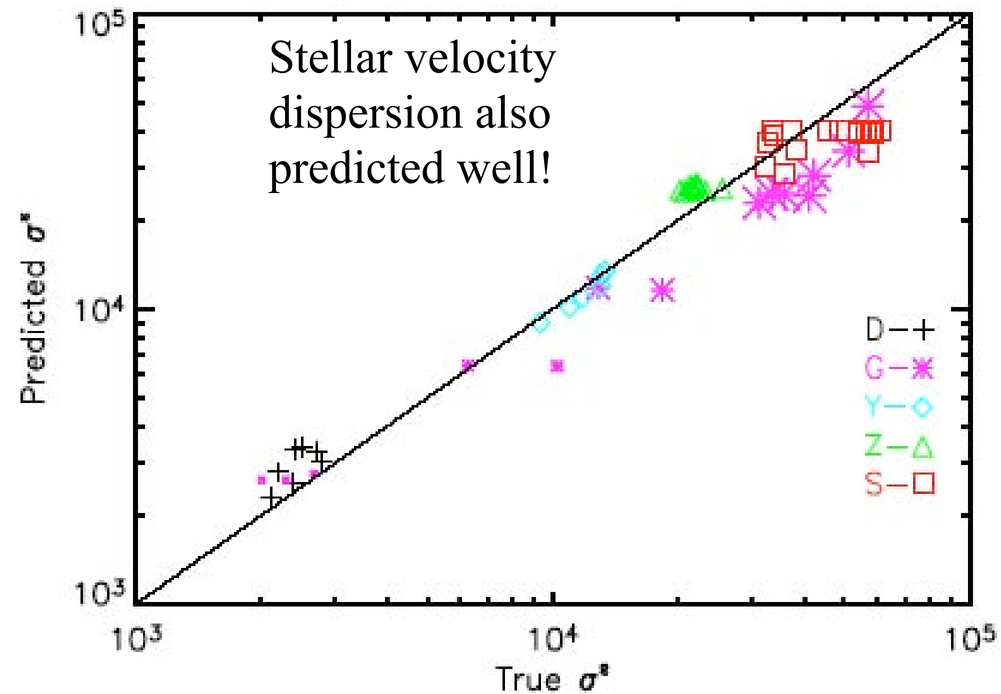

Covington et al. 2007 model also works well for non-equal mass mergers, including minor mergers!

Comparison with SAURON data in progress by UCSC grad student Greg Novak working with Cox, Jonsson, Faber, and Primack.

NGC 474

Views of G3G3 merger, plotted like SAURON data.

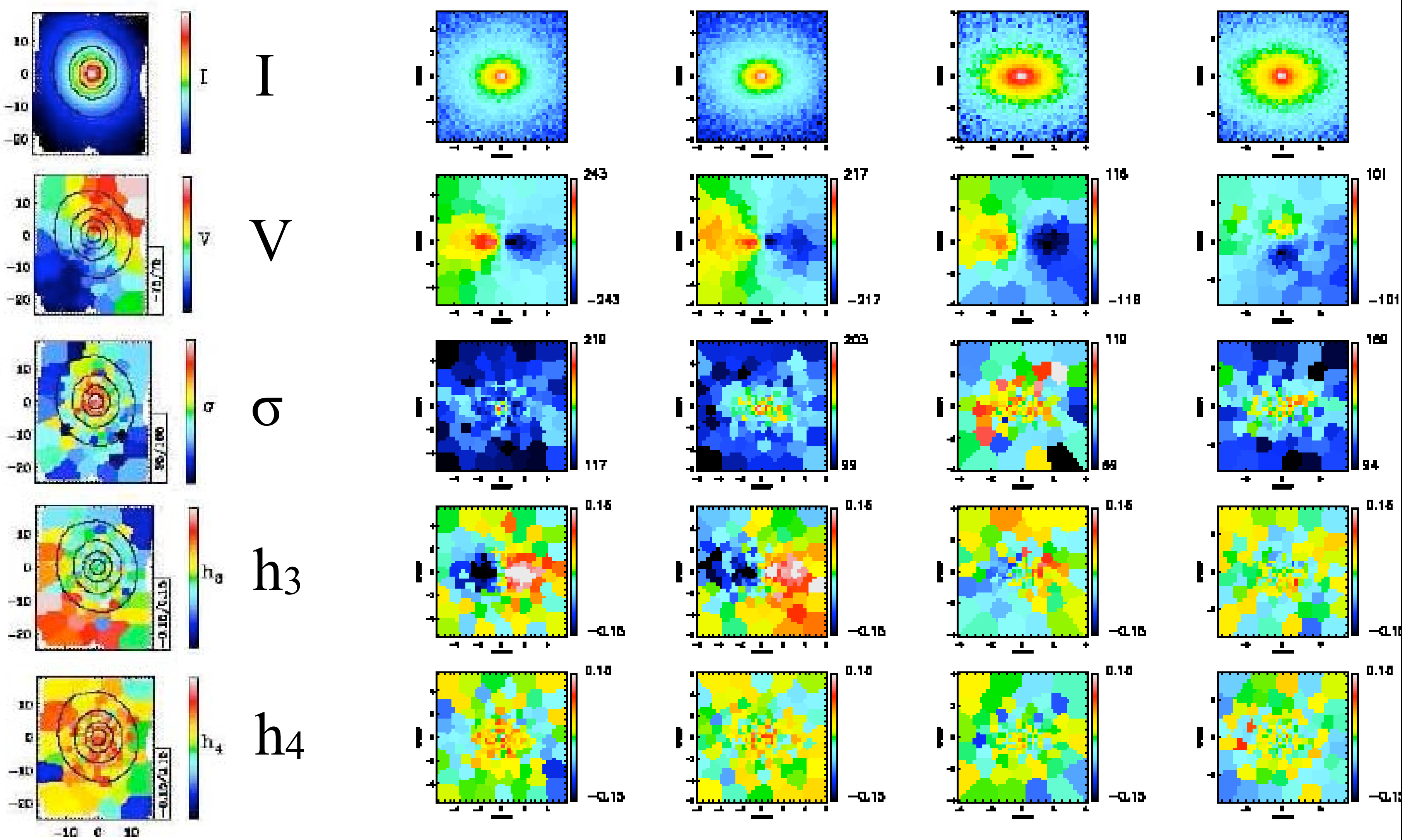

Greg Novak's conclusions so far regarding the SAURON comparison are:

1) Binary hydrodynamic major mergers form qualitatively similar replicas of the SAURON "fast rotator" early-type galaxies, about 2/3 of SAURON early-type galaxies.

2) Binary gas-poor major-mergers spiral galaxy and binary gas poor elliptical-elliptical mergers cannot form the SAURON "fast rotators." They have too little rotation and get the V-H3 correlation wrong.

3) Binary gas-poor major-mergers spiral galaxy and binary gas poor elliptical-elliptical mergers may be able to form the SAURON slow rotators, if slow rotators are significantly more elliptical on average than is indicated by the SAURON survey.

Greg Novak is now running various types of multiple mergers to try to form galaxies like the SAURON slow rotators.

The short (rotation) axis of the visible elliptical galaxy is perpendicular to the long axis of its dark matter halo. Why? The long axis of the halo is along the merger axis, while the angular momentum axis is perpendicular to that axis.

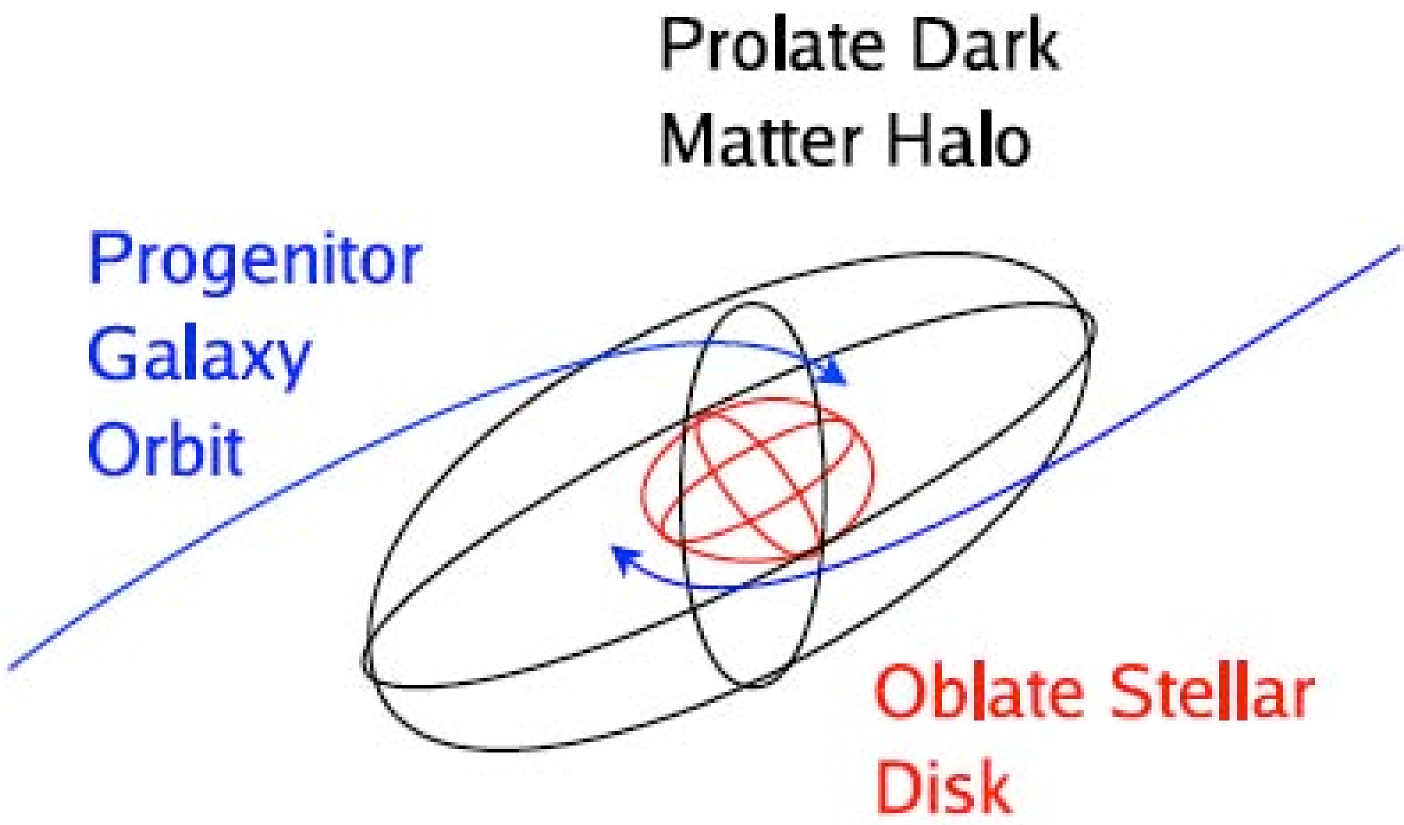

Novak, Cox, Primack, Jonsson,
& Dekel, ApJ Letters 2006

Shapes of Stellar Ellipsoids and Dark Halos of Major Merger Remnants

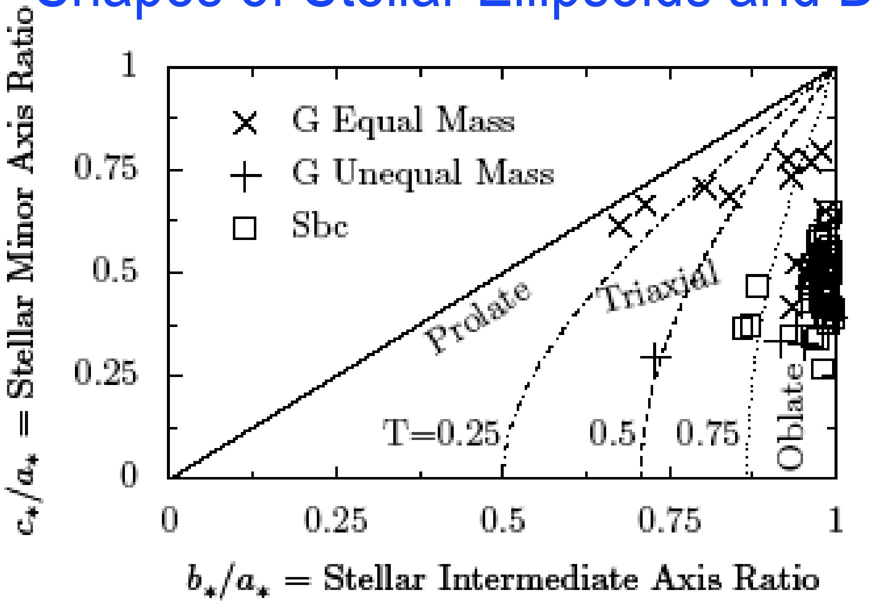

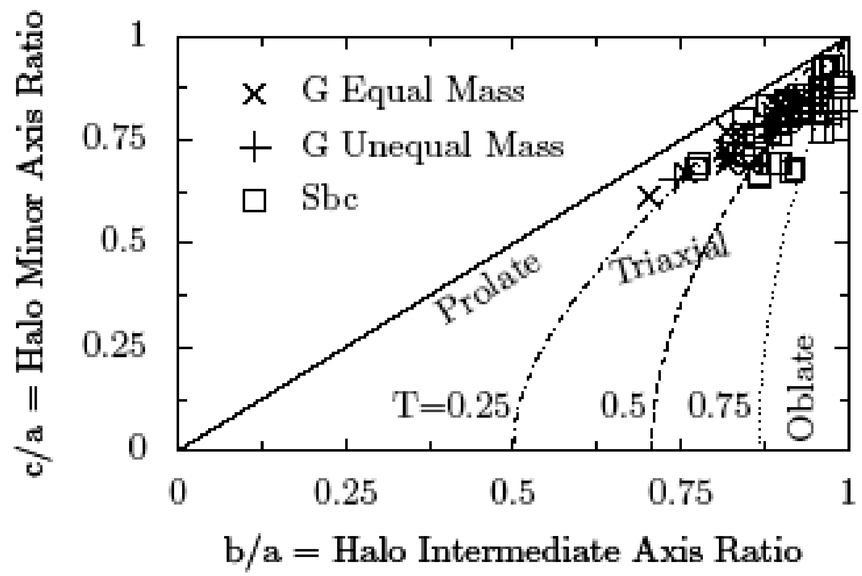

The stellar ellipsoids are mostly oblate but the dark matter halo is usually triaxial or prolate.

The stellar minor axis usually aligns with the angular momentum axis, which aligns with the dark matter smallest axis, perpendicular to the dark matter major axis.

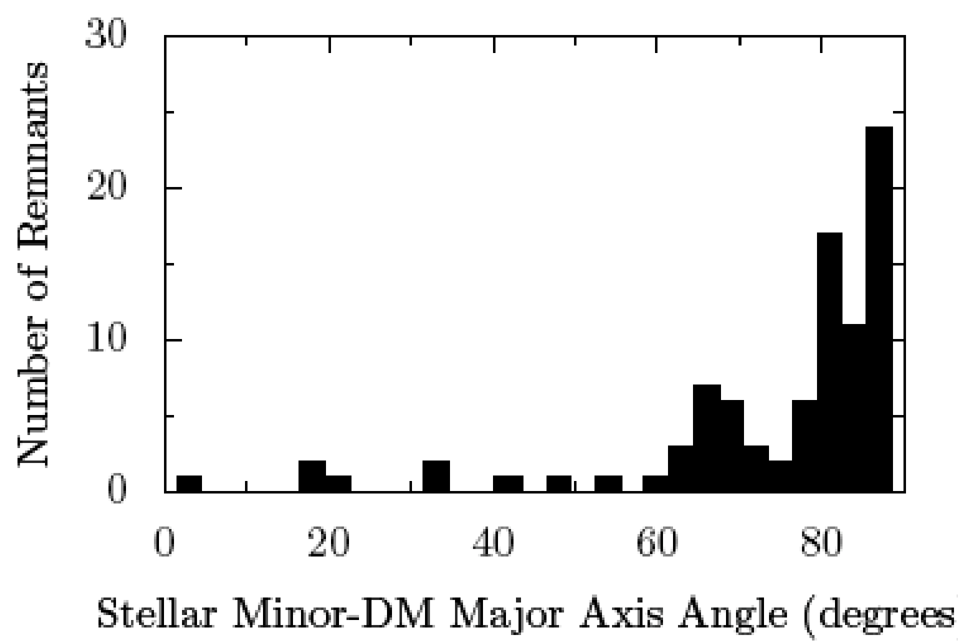

Novak, Cox, Primack, Jonsson, & Dekel, ApJ Letters 2006

Simulations of Dust in Interacting Galaxies

Patrik Jonsson

UCSC

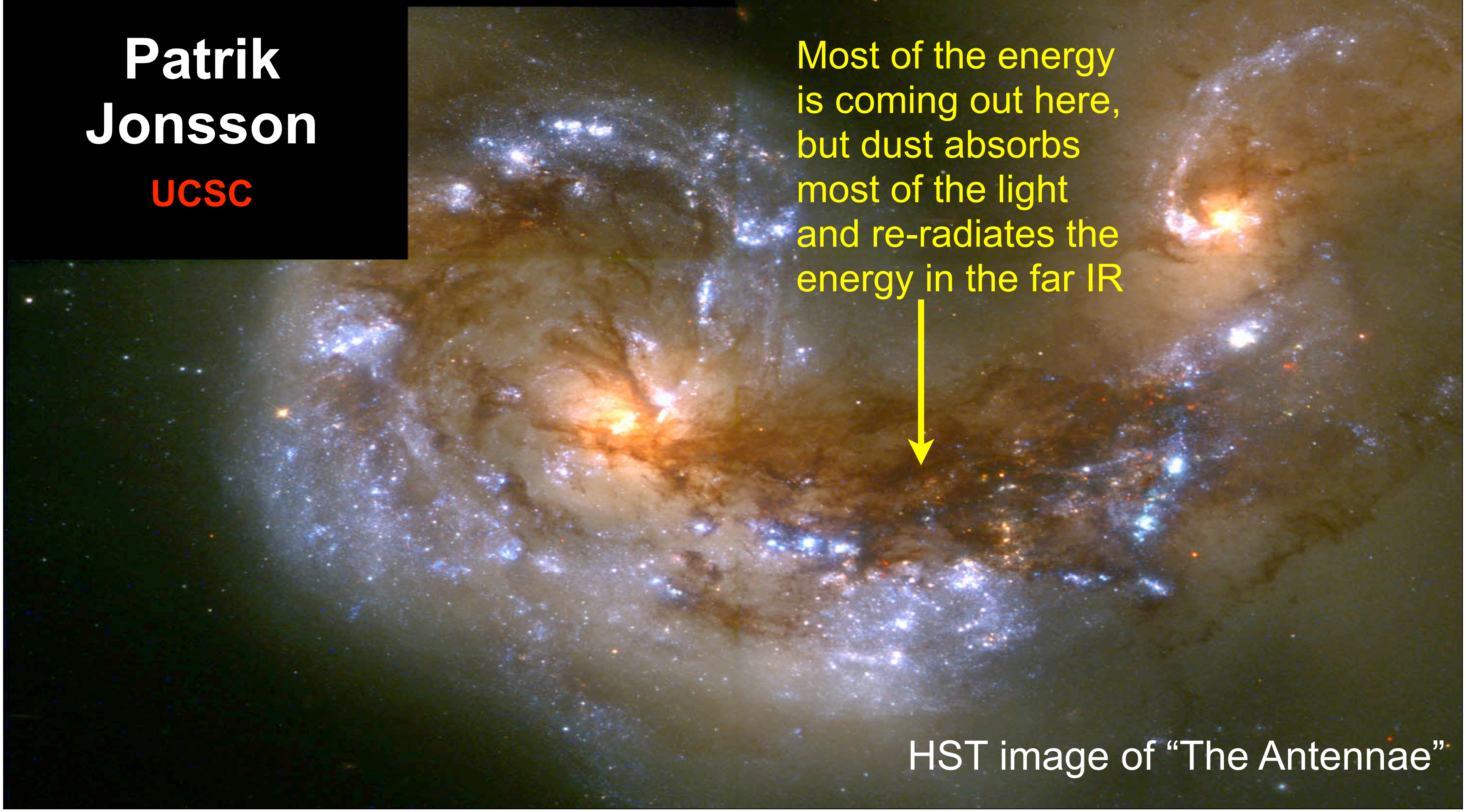

HST image of “The Antennae”

Introduction

- Dust in galaxies is important
  - Absorbs about 40% of the local bolometric luminosity
  - Makes brightness of spirals inclination-dependent
  - Completely hides the most spectacular bursts of star formation
  - Makes high-redshift SF history very uncertain
- Dust in galaxies is complicated
  - The mixed geometry of stars and dust makes dust effects geometry-dependent and nontrivial to deduce
  - Needs full radiative transfer model to calculate realistically
- Previous efforts have used 2 strategies
  - Assume a simple, schematic geometry like exponential disks, or
  - Simulate star-forming regions in some detail, assuming the galaxy is made up of such independent regions
  - (Have not used information from N-body simulations)

Our Approach

For every simulation snapshot:

- SED calculation
- Adaptive grid construction
- Monte Carlo radiative transfer

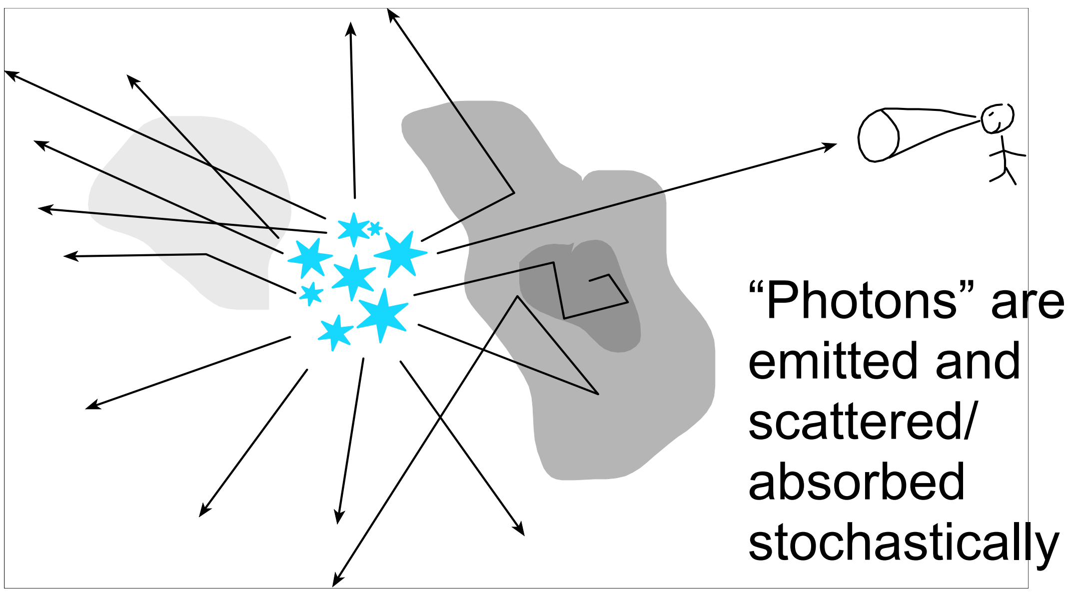

Sunrise Radiative Transfer Code

- Run entire SED at once without scattering -- determines unabsorbed SED
- Run with scattering for a single wavelength; repeat for all wavelengths desired - code includes Ly alpha, beta; interpolate SED to full resolution
- New “polychromatic” method does wide range of wavelengths simultaneously, saves factor of ~100 computer time!
- Now incorporating “Mappings” to model HII regions in starbursts

Spectral Energy Distribution

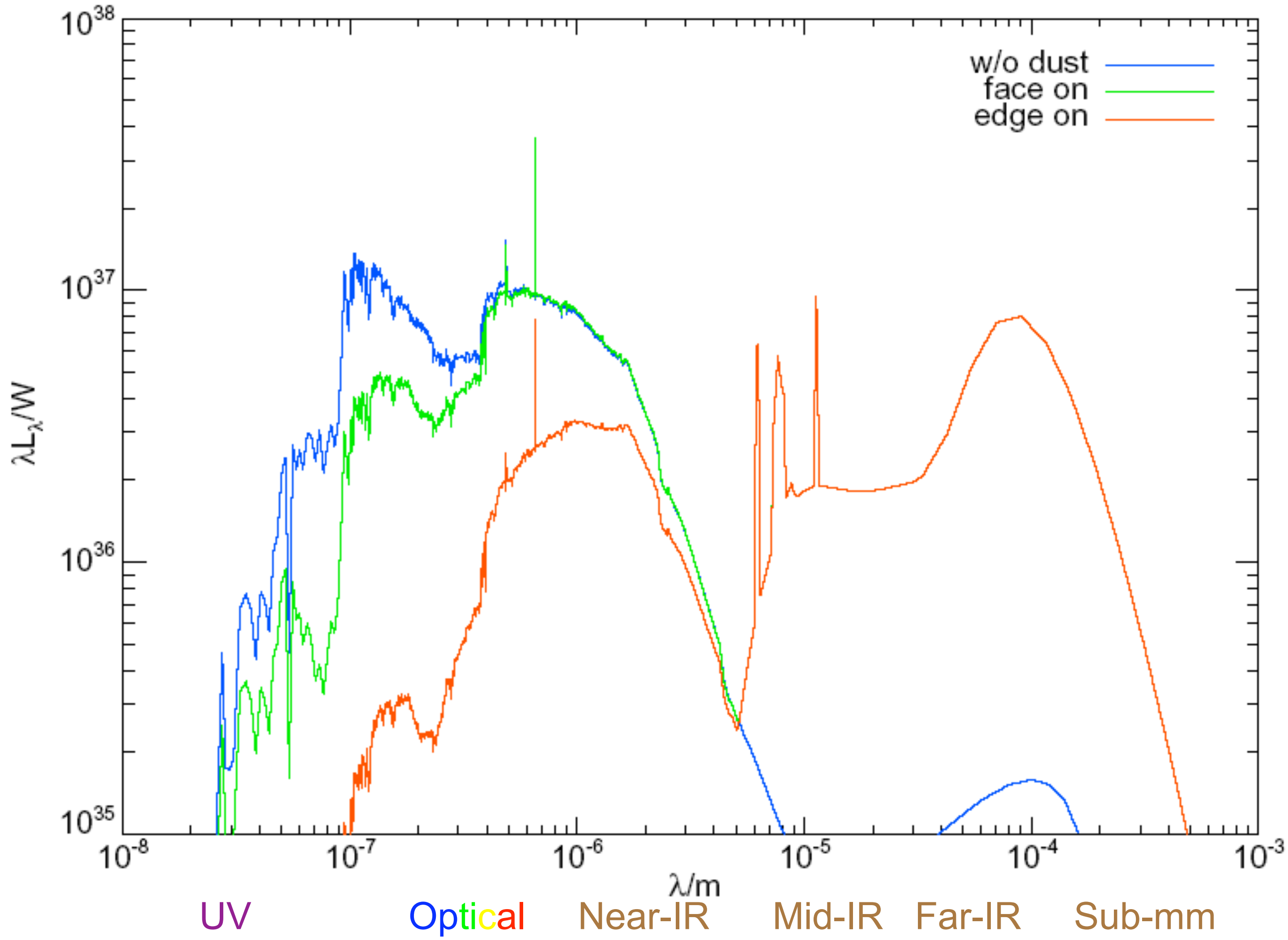

Monochromatic vs. Polychromatic Radiative Transfer Models

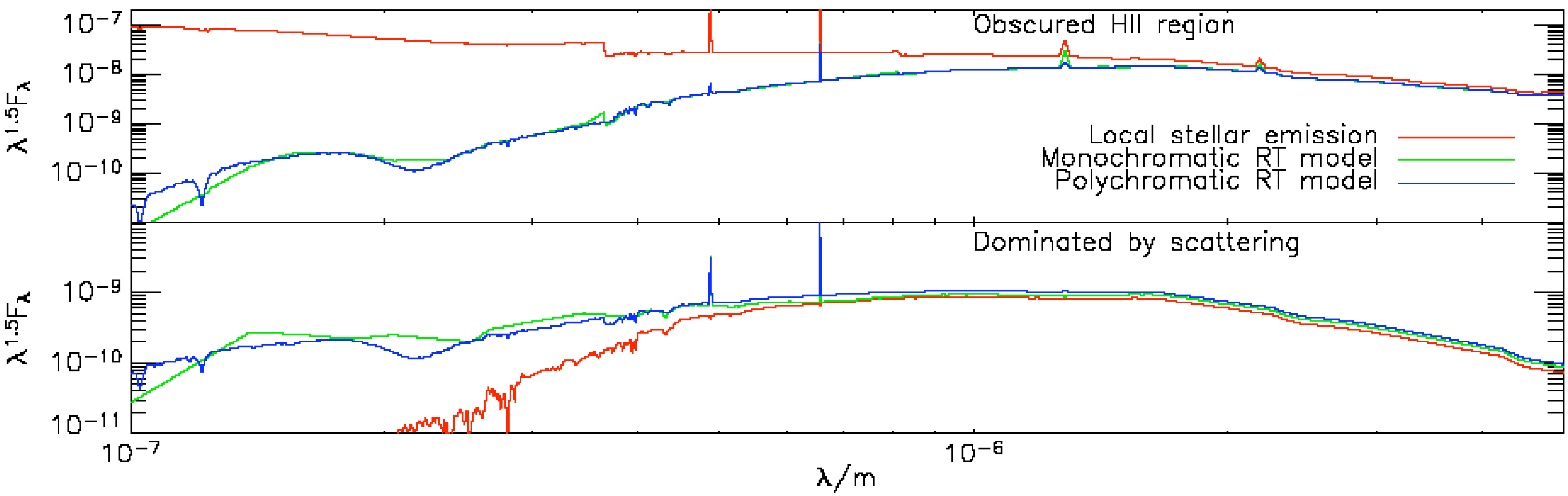

Figure 8. Spectra from the galaxy merger simulations, exemplifying the effects of the new polychromatic algorithm. In both images, the red line shows the intrinsic emission in the pixel, neglecting radiative-transfer effects. The green line shows the old algorithm, where the spectrum is interpolated between 20 discrete wavelengths, and the blue line is the result from the polychromatic radiative transfer. The top plot shows a pixel containing an obscured H II region, the bottom plot a pixel near an H II region where the UV flux is dominated by scattered light. While the results agree well on the overall spectral shape, the new method gives significantly more realistic results especially for the small-scale spectral features, at a fraction of the runtime. Note in particular how the polychromatic algorithm predicts the appearance of the Ly α absorption line, the disappearance of the nebular Balmer continuum edge, and the increased attenuation of the Paschen β line at 1.3 μm in the spectrum of the H II region. The polychromatic calculation, including 500 wavelengths, used about 8 times the CPU time required for one monochromatic calculation. With monochromatic ray tracing, 500 separate wavelengths would have to be used to predict the same amount of detail, which would require a factor of 50 more CPU time.

Patrik Jonsson, MN 2006

Images of quiescent disk galaxies with effects of dust from *Sunrise* Monte Carlo radiative transfer code

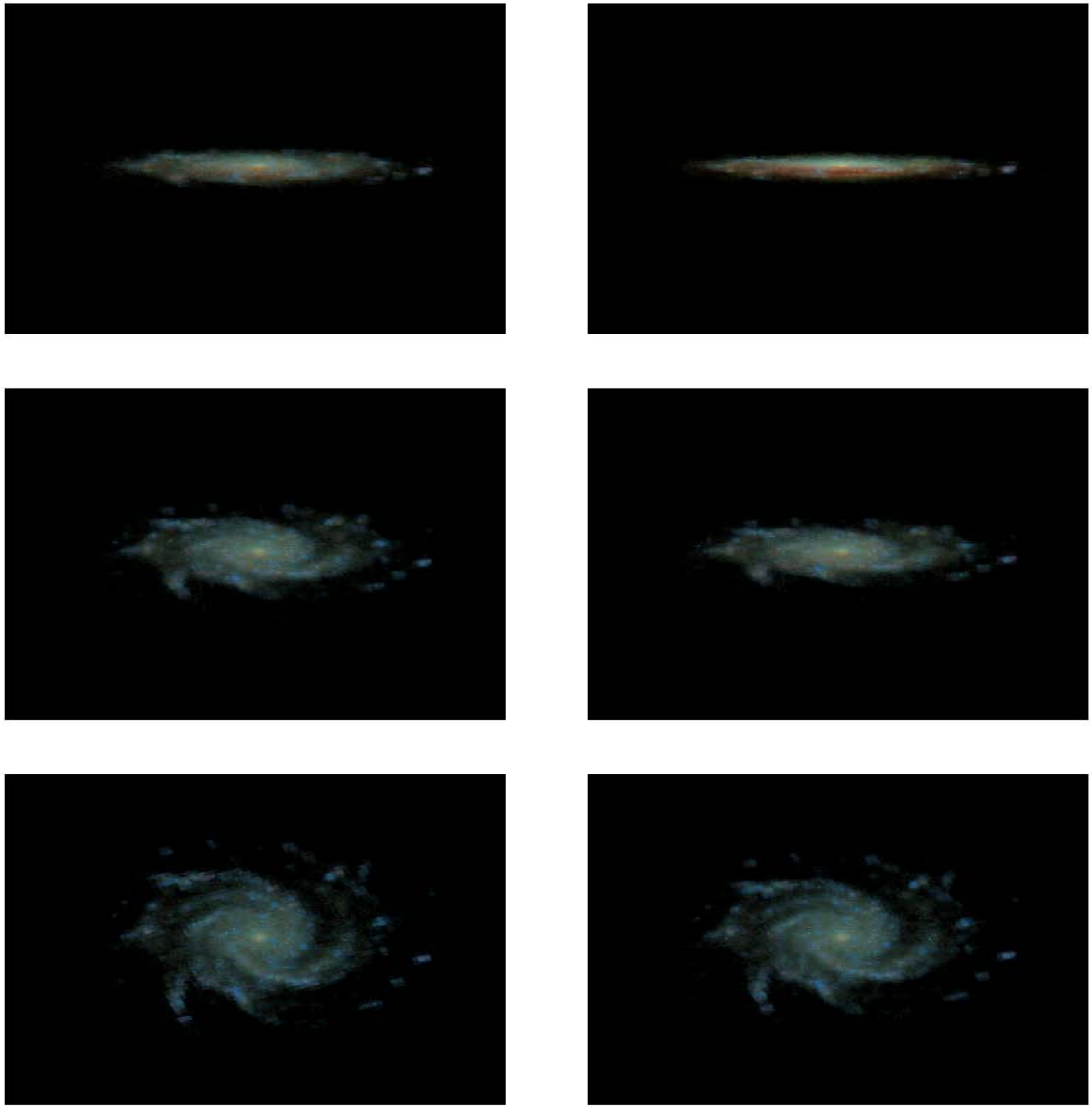

Near edge-on images (with dust) from *Sunrise* Monte Carlo radiative transfer code

These were run with no radial metallicity gradient, but our latest work shows that observed radial gradients predict attenuation vs. inclination in agreement with observations -- Miguel Rocha's senior thesis, supervised by P Jonsson & Primack

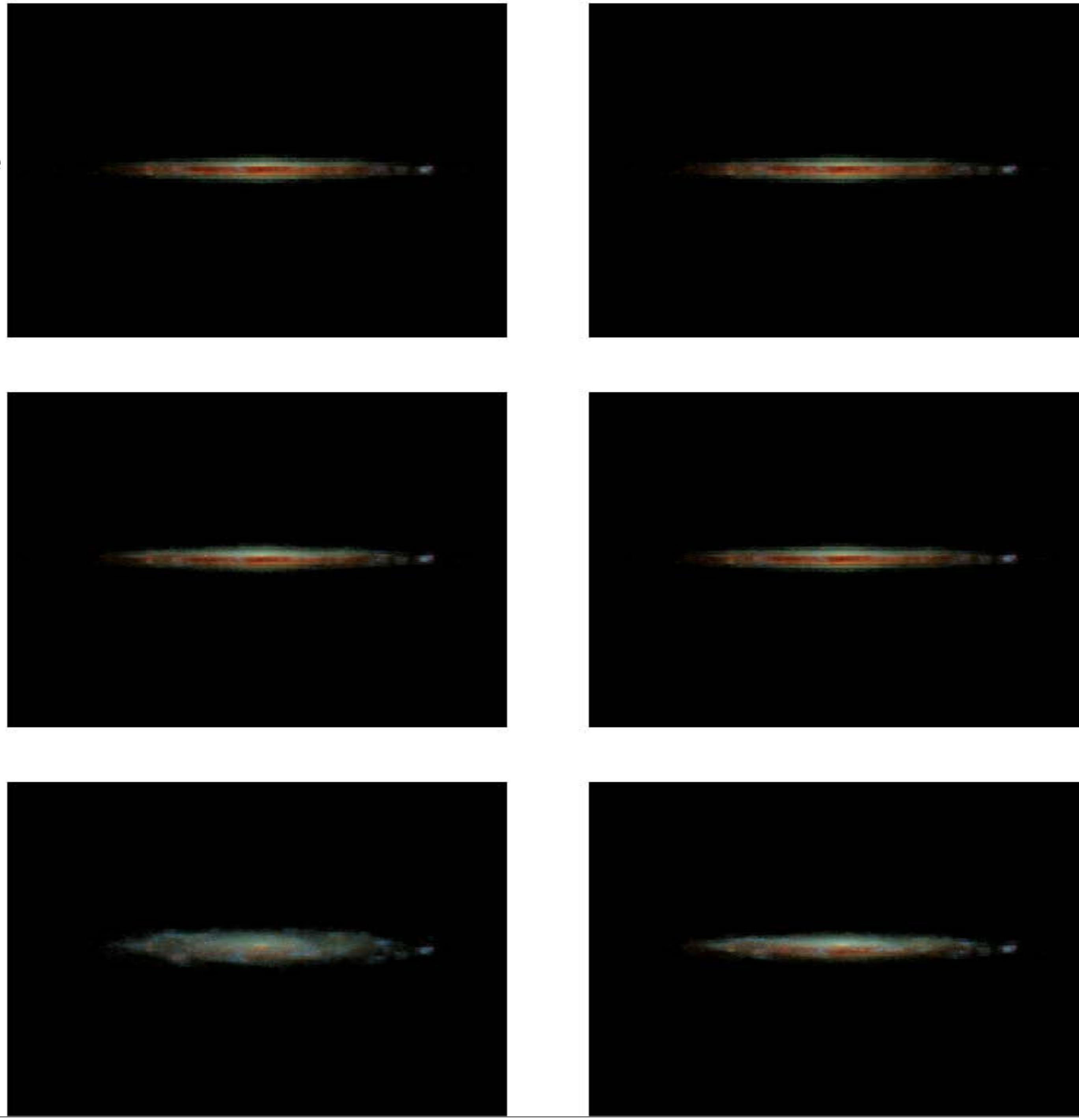

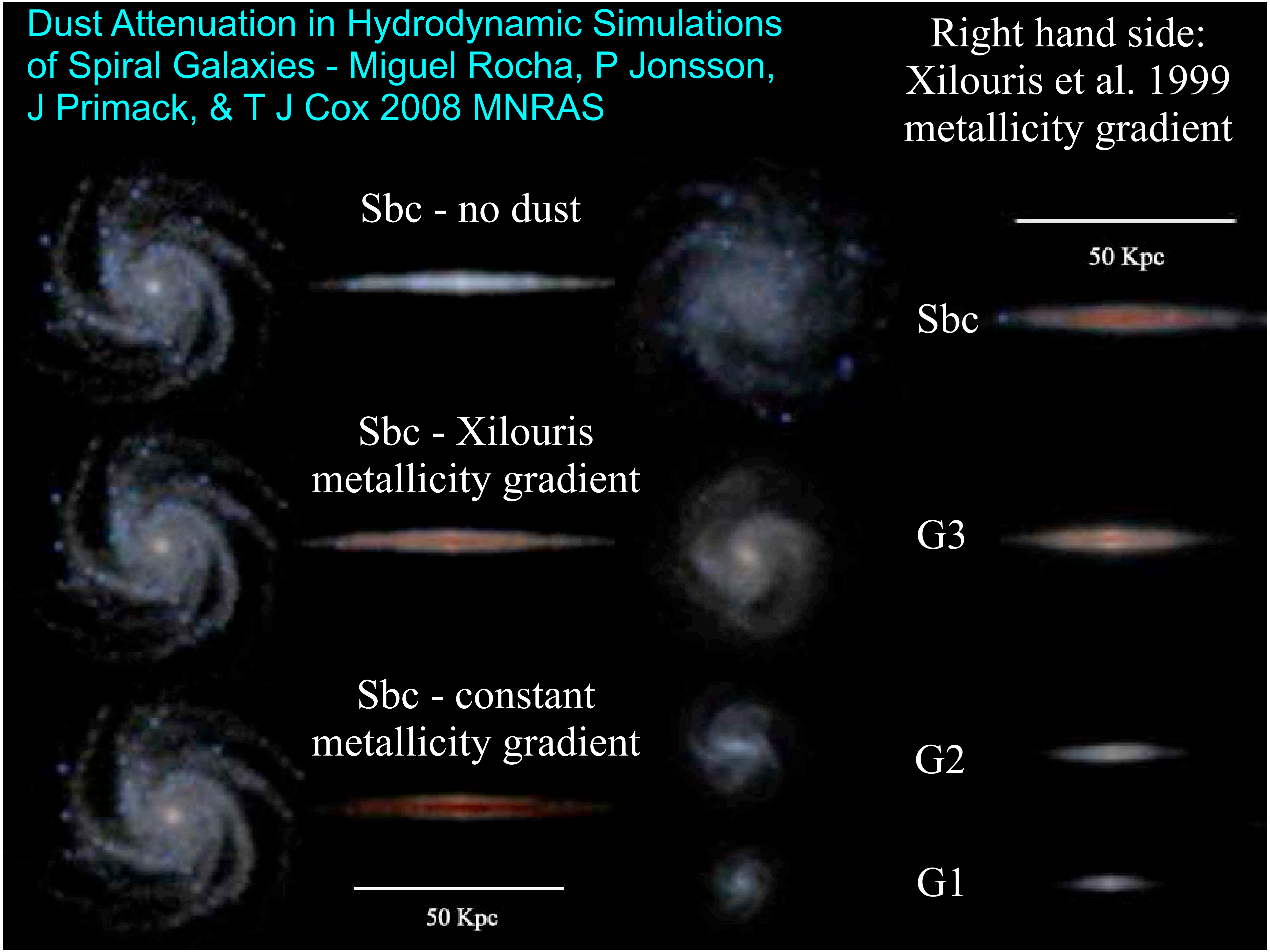
Dust Attenuation in Hydrodynamic Simulations of Spiral Galaxies - Miguel Rocha, P Jonsson, J Primack, & T J Cox 2008 MNRAS
Right hand side: Xilouris et al. 1999 metallicity gradient
Sbc - no dust
Sbc - Xilouris metallicity gradient
Sbc - constant metallicity gradient
50 Kpc
50 Kpc
Sbc
G3
G2
G1

Galaxy Merger Simulation

run on the Columbia Supercomputer

by Greg Novak and Patrik Jonsson

This and the following images show a merger between two Sbc galaxies, each simulated with 1.7 million particles (10x more than the previous images), and with dust absorption computed with ~10^6 rays per image. The images are realistic color composites of u, r, and z-band images.

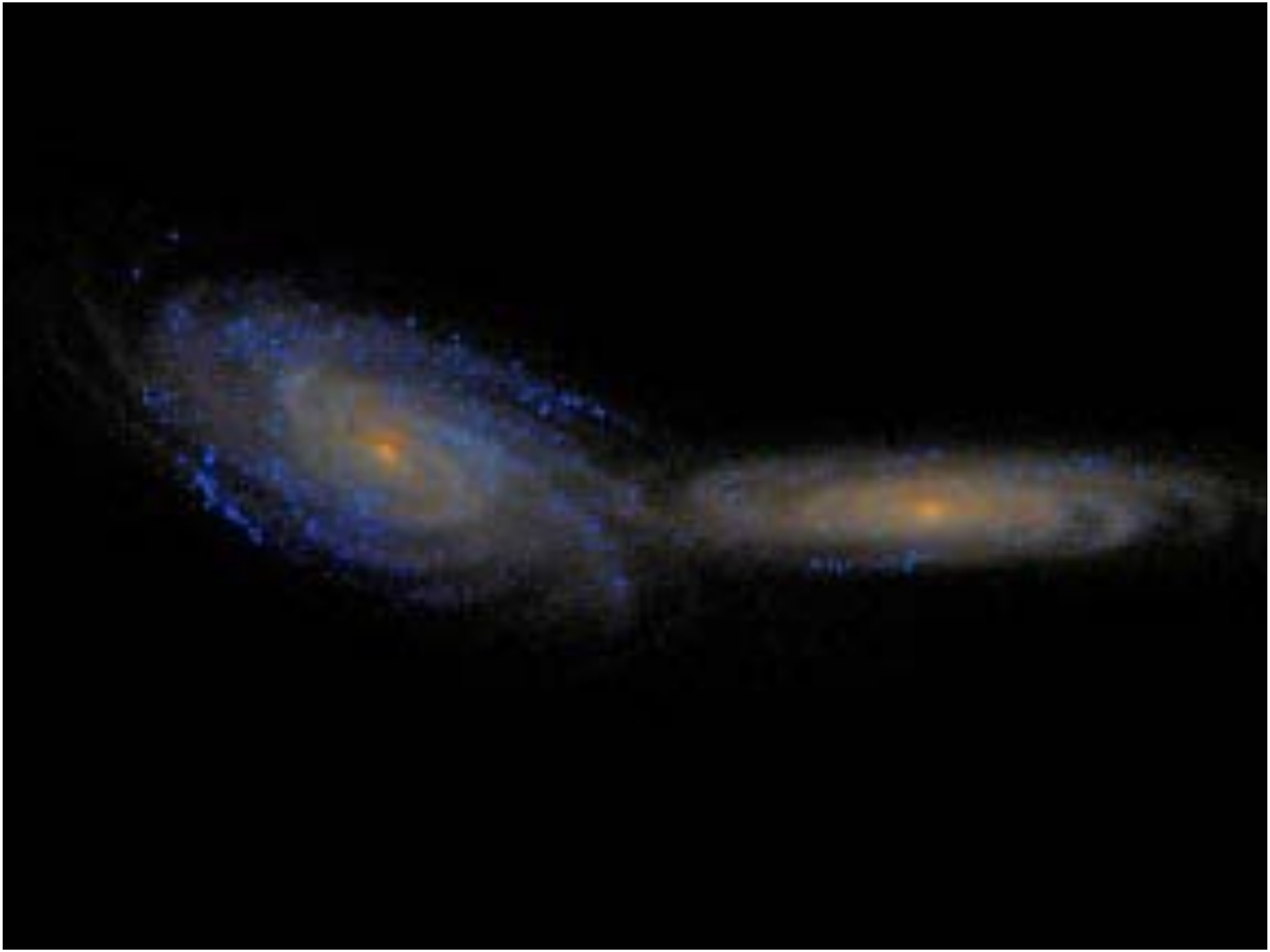

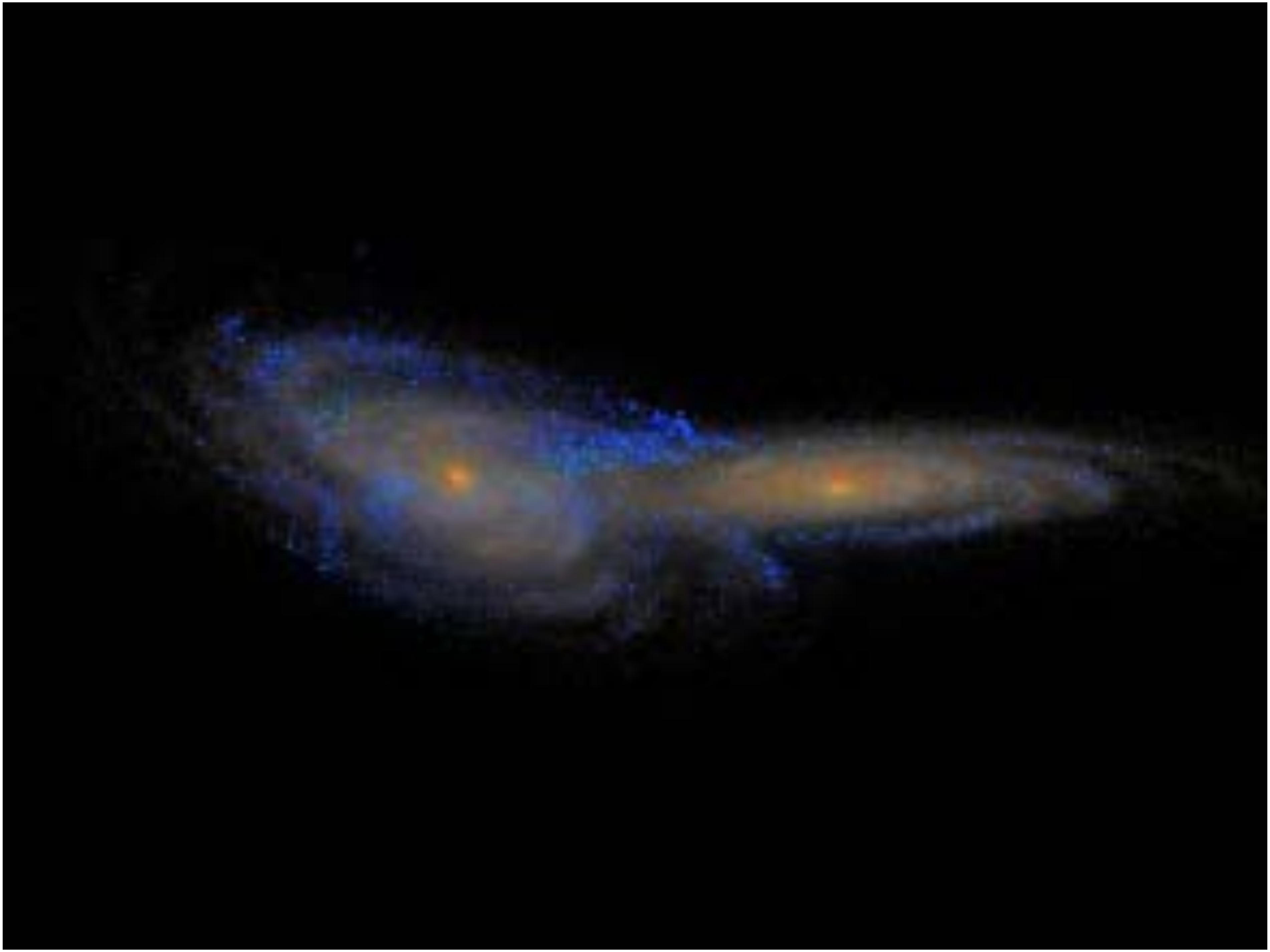

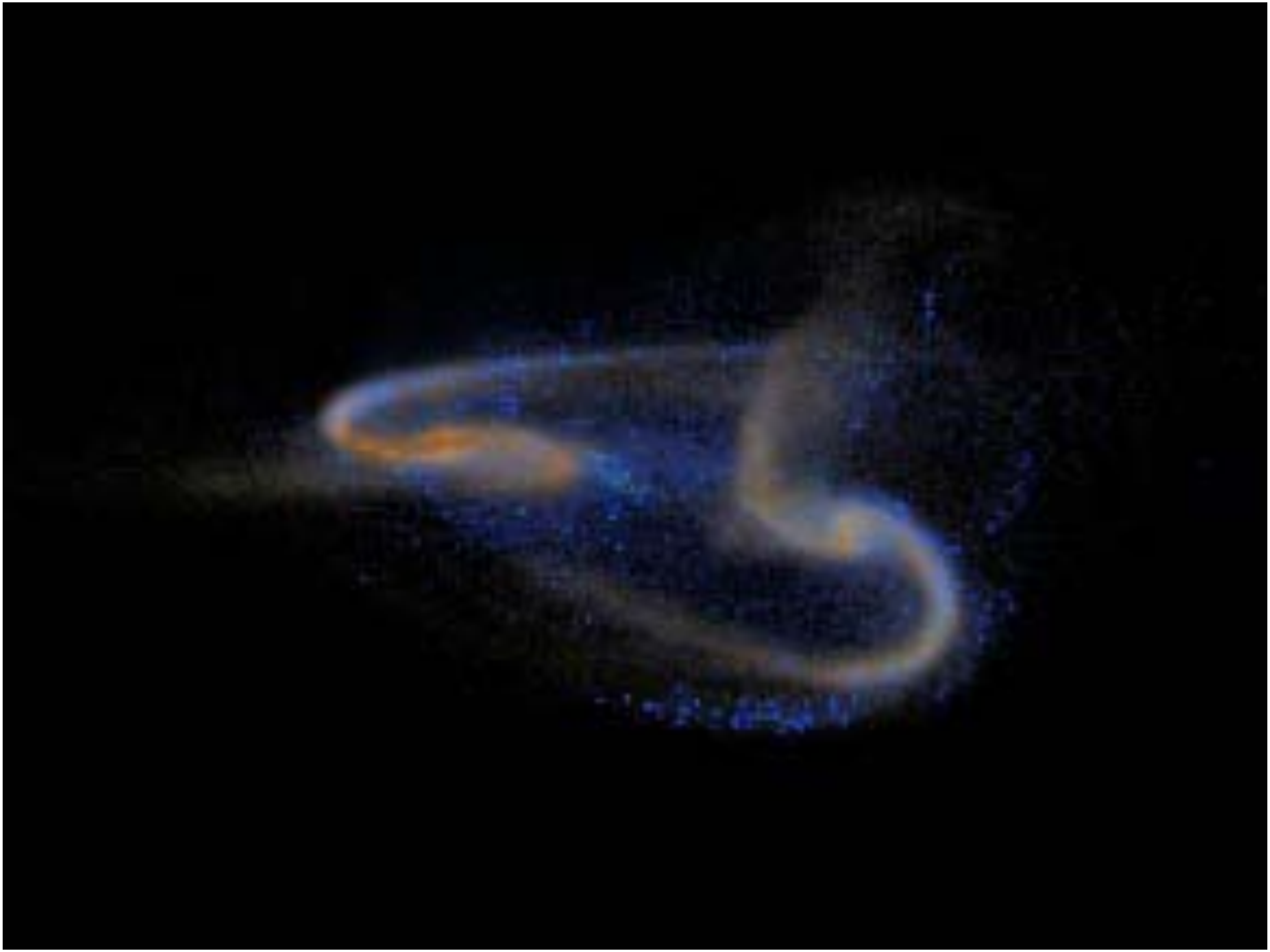

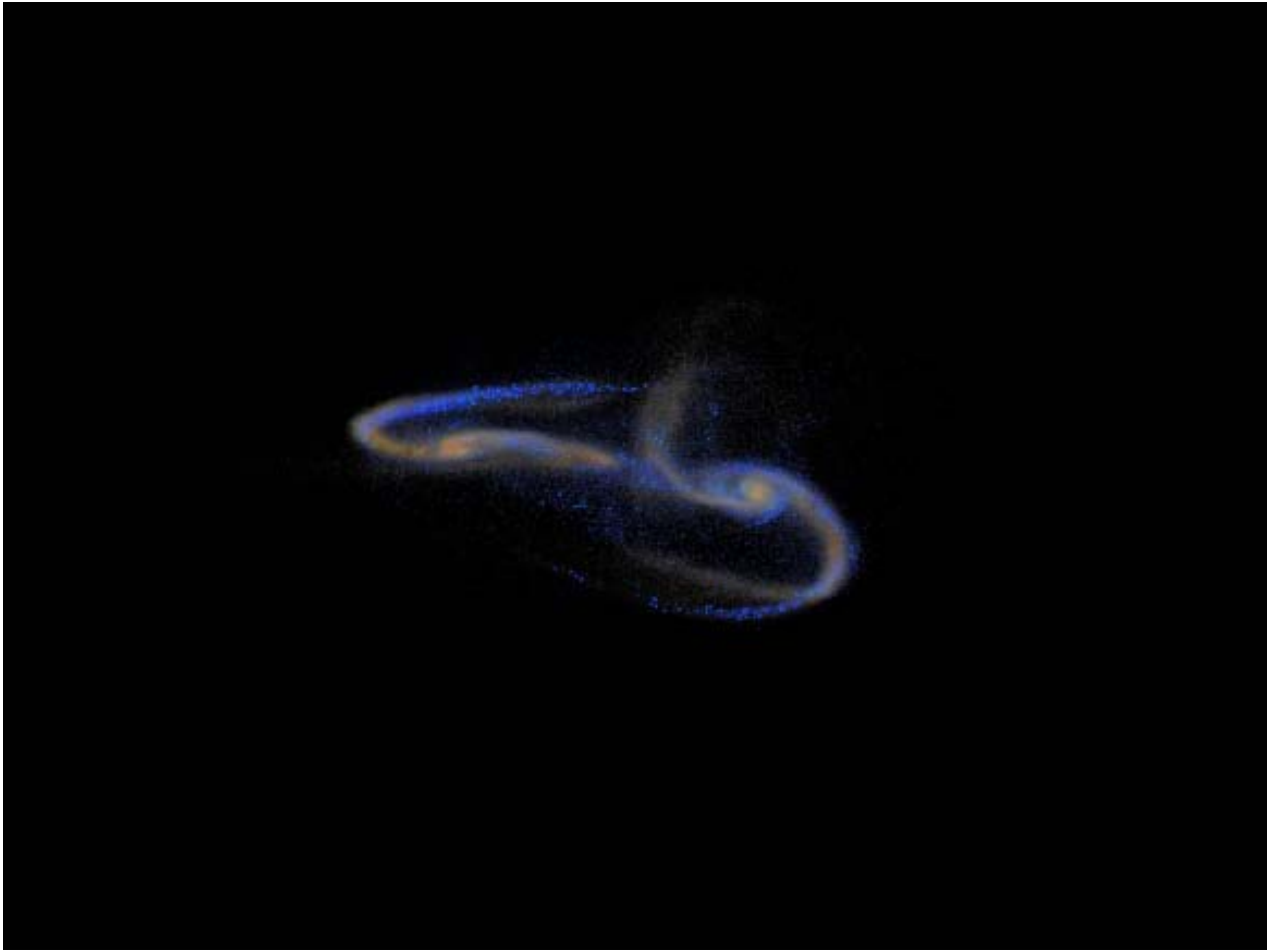

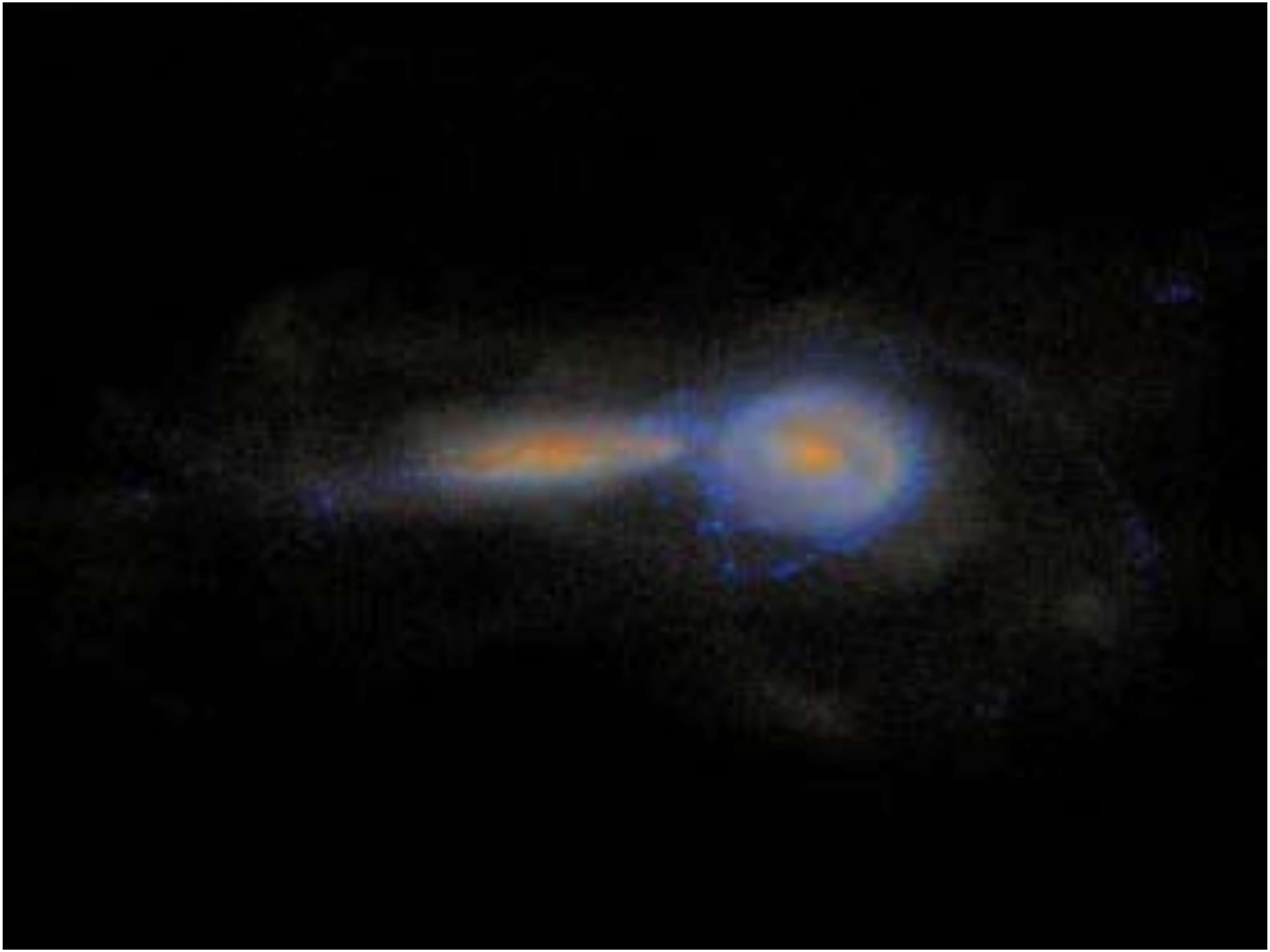

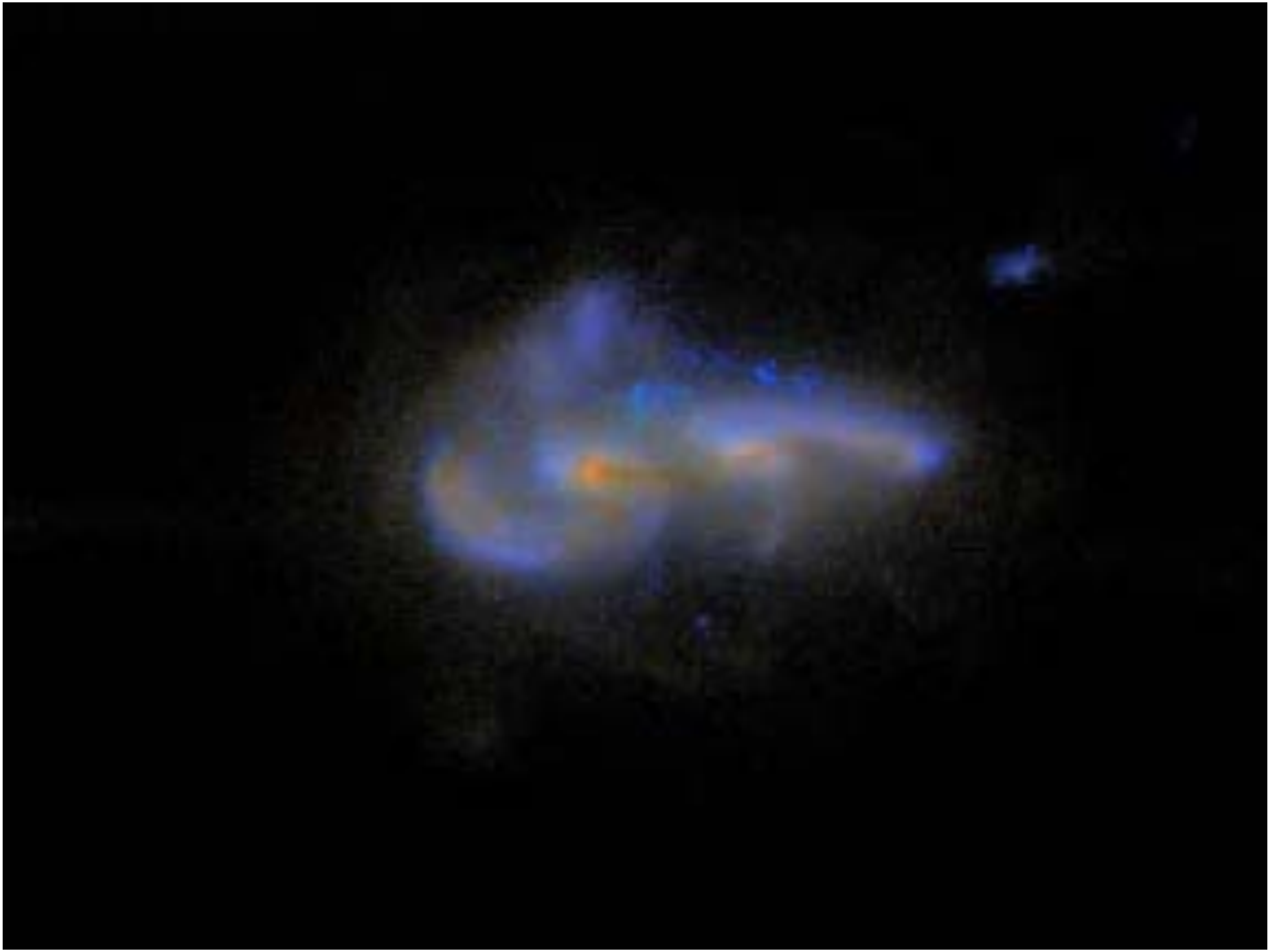

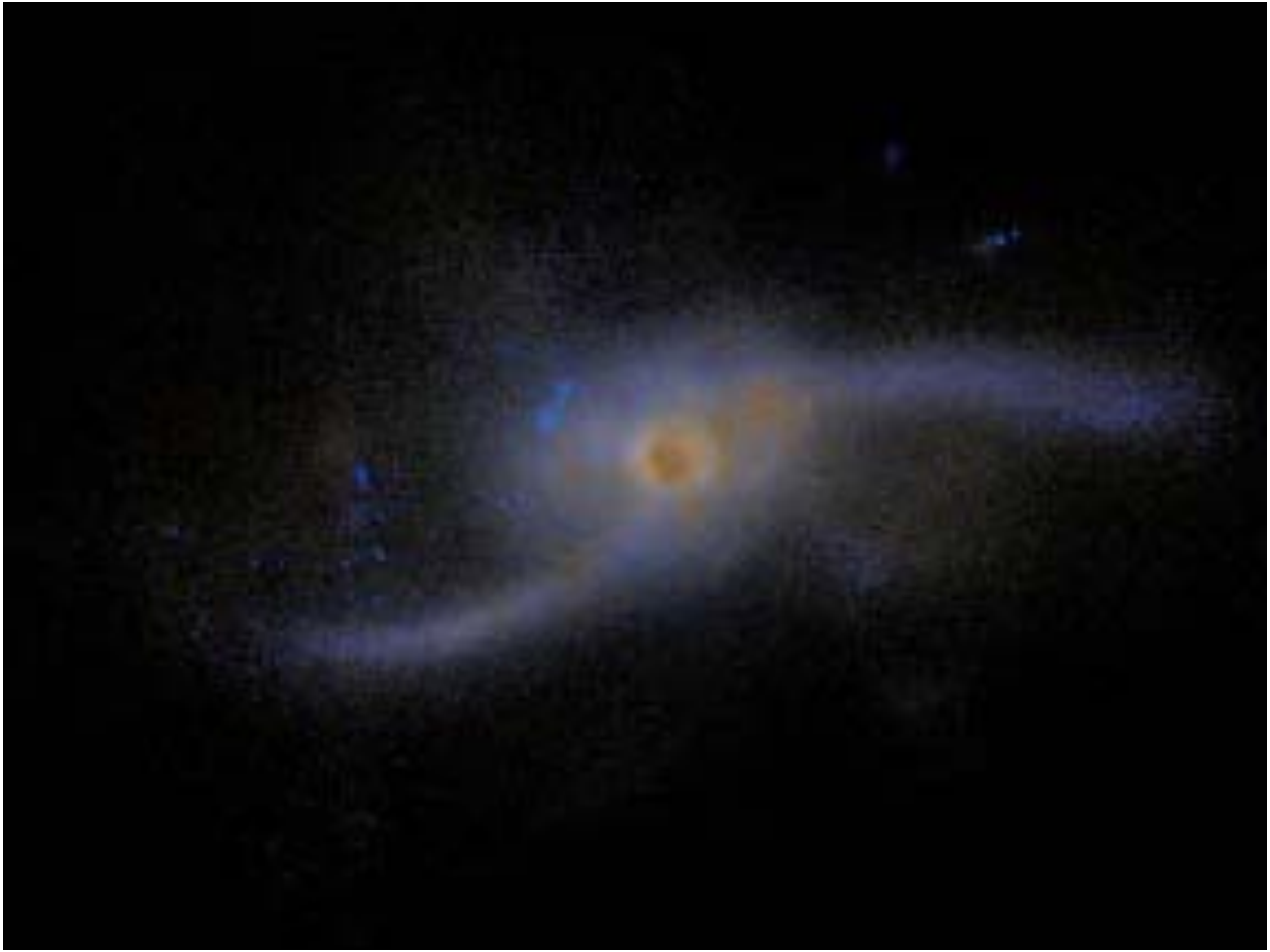

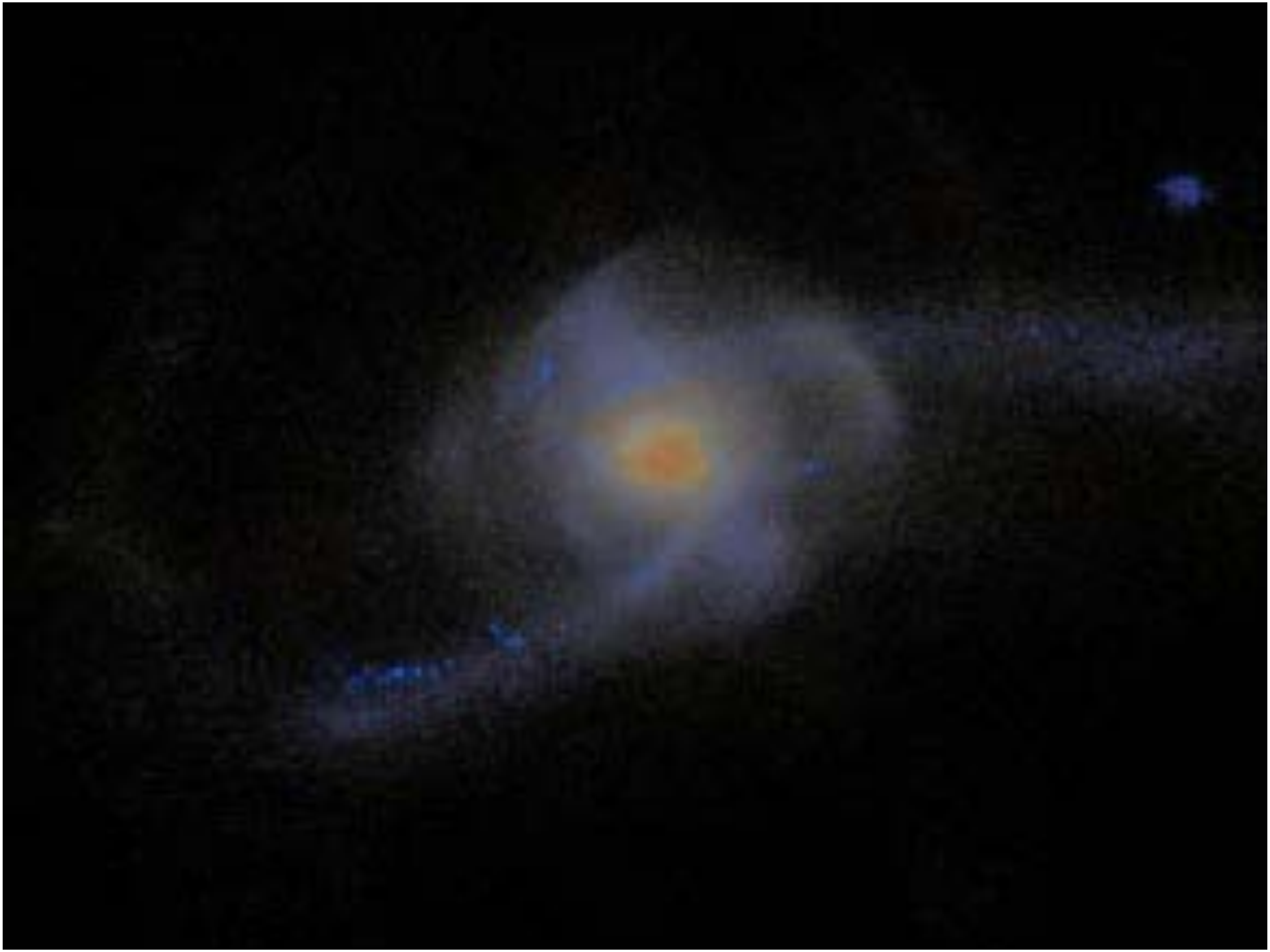

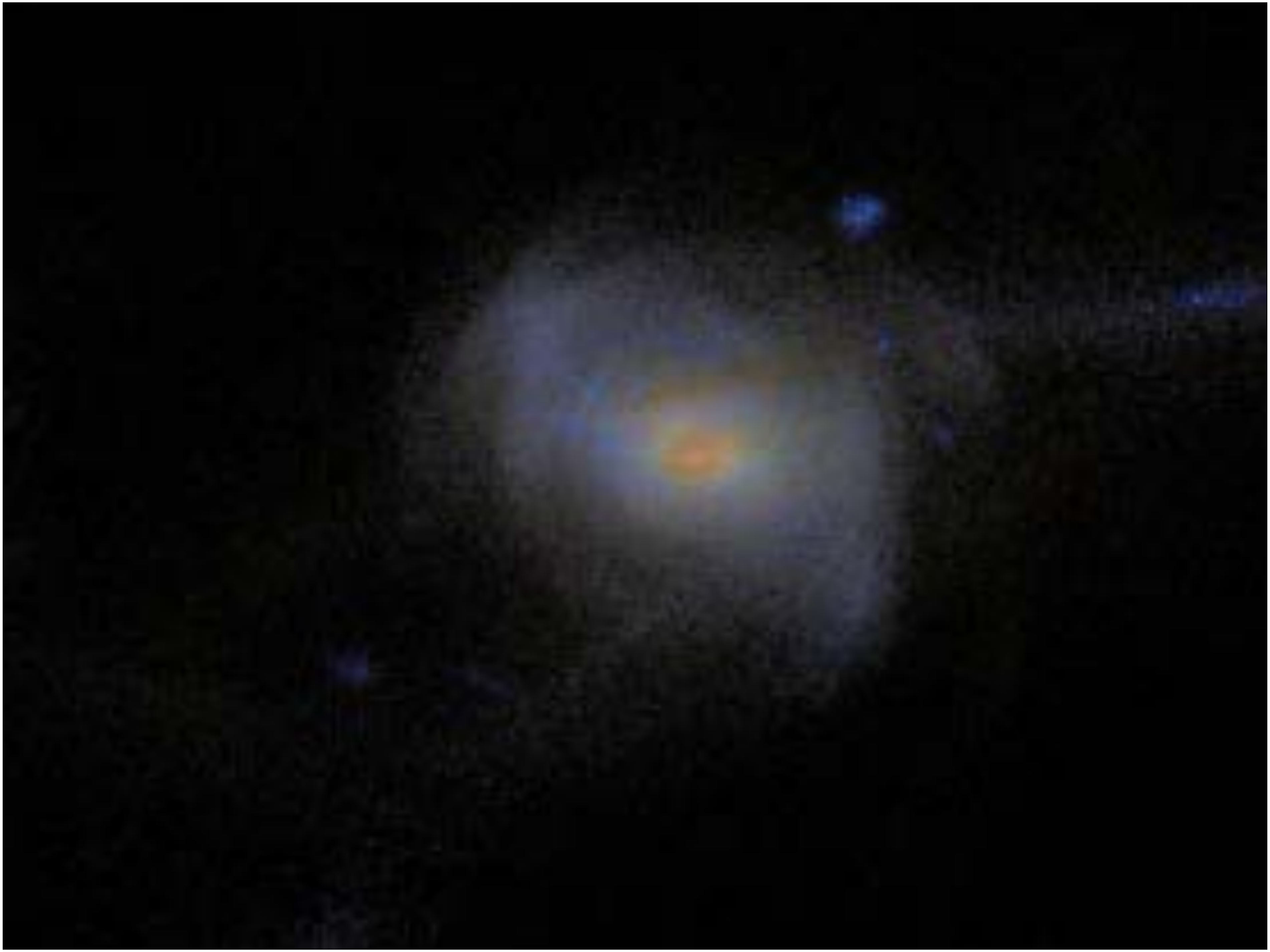

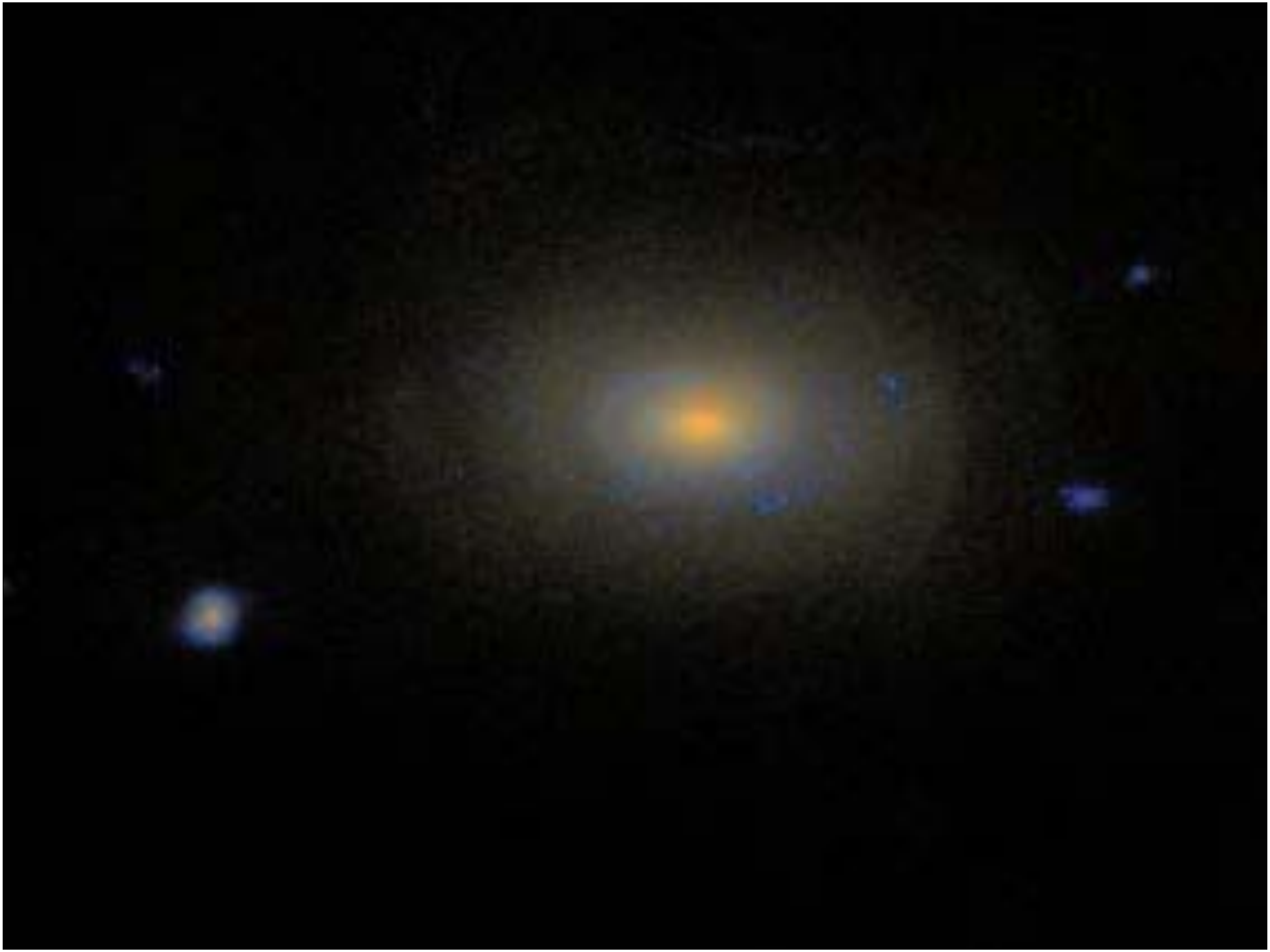

Galaxy Merger Simulation

run on the Columbia Supercomputer

(music by Nancy Abrams)

Multiple Merger Simulations

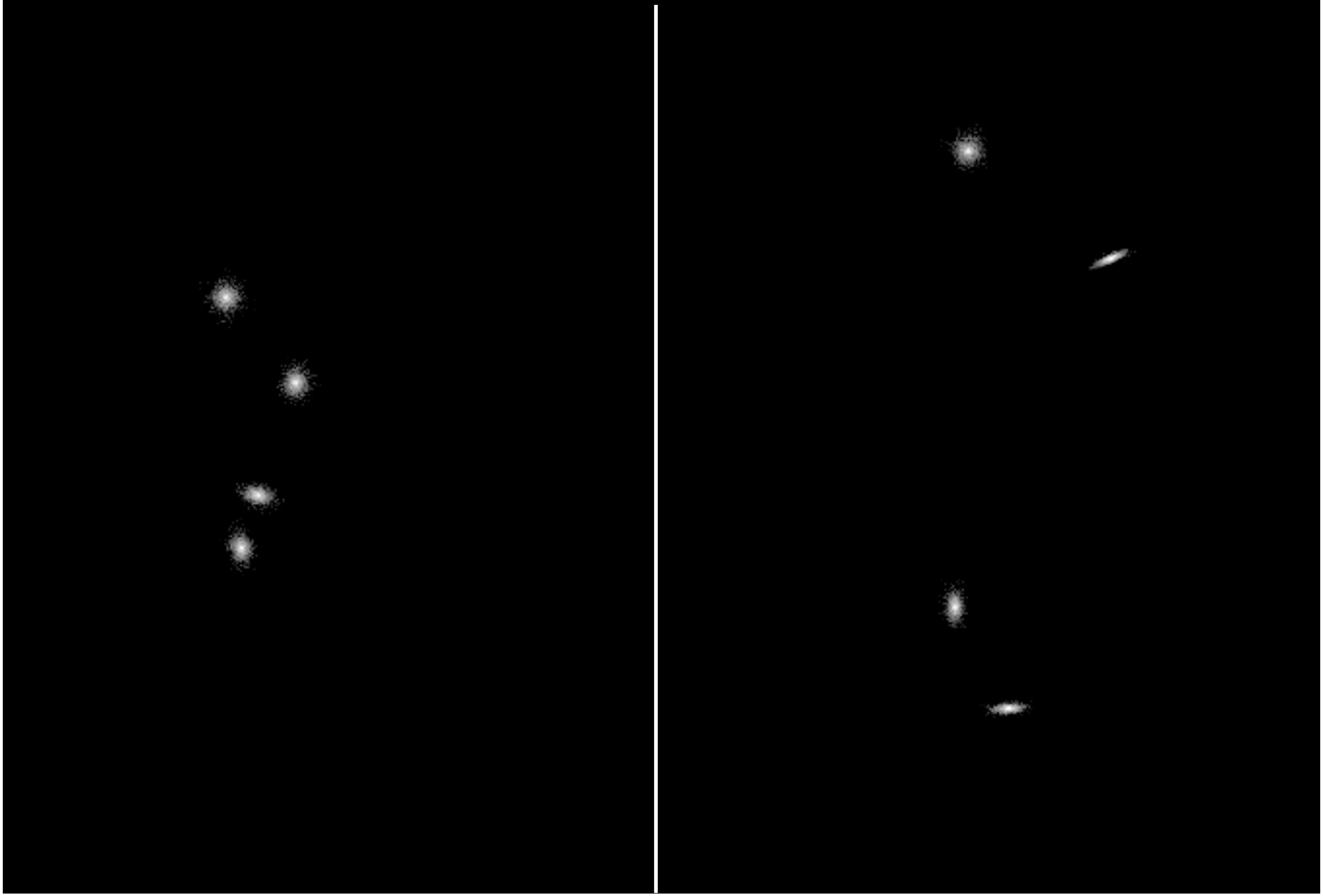

[redacted]

Predictions from Galaxy Modeling:

Quantifying Galaxy Morphology and Identifying Mergers

see Lotz, Primack & Madau 2004, AJ, 128, 163; ApJ 2008; and papers in prep.

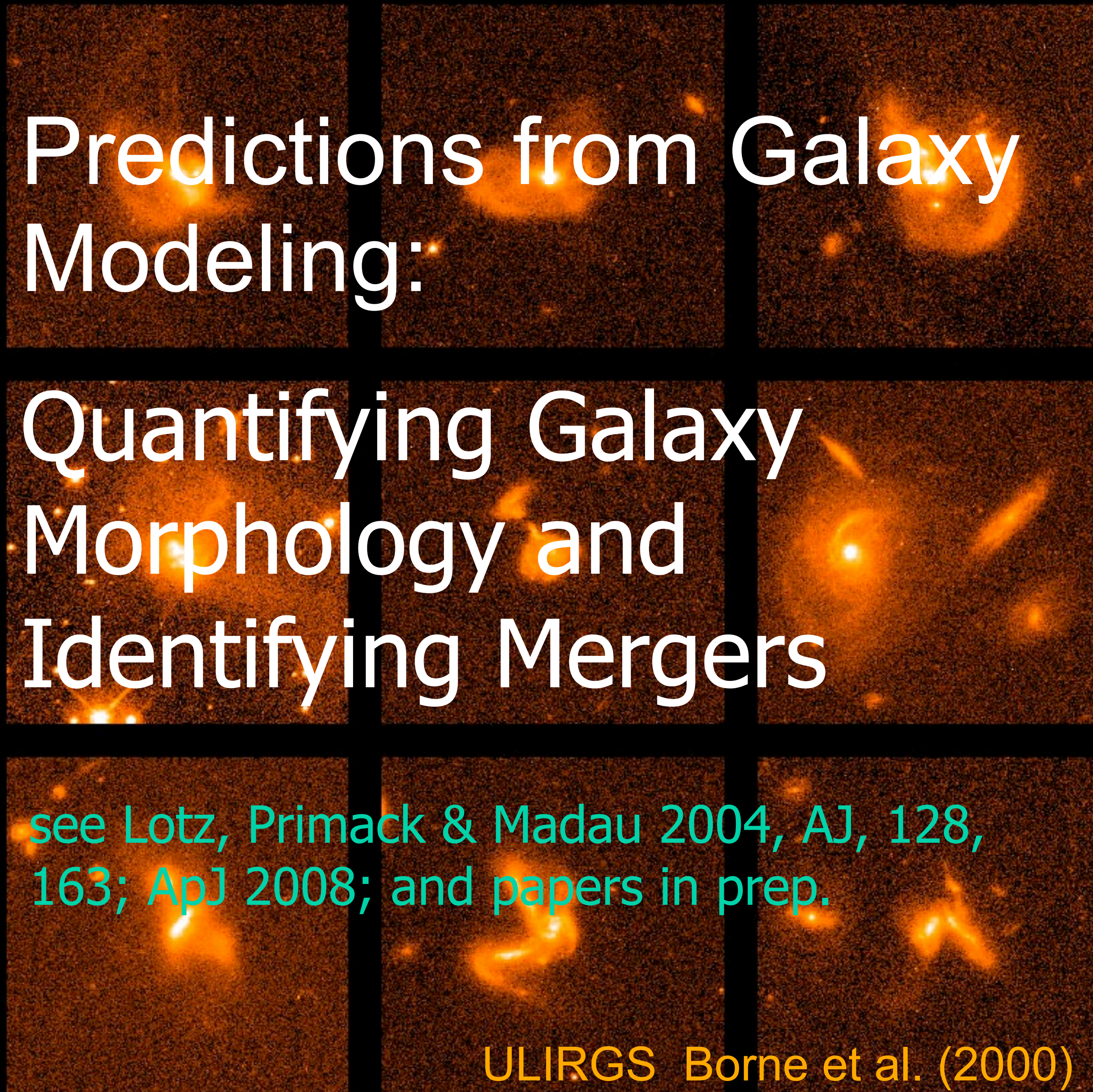

ULIRGS Borne et al. (2000)

Measuring Galaxy Morphology

- by "eye" - Hubble tuning fork E-Sa-Sb-Sc-Sd-(Irr)

- parametric
  1-D profile fit ($r^{1/4}$, exponential, Sersic)
  2-D profile fit (bulge+disk; GIM2D, GALFIT)
  → doesn't work for irregular/merging galaxies

- non-parametric
  "CAS" - concentration, asymmetry, clumpiness
  neural-net training
  shaplet decomposition

new: Gini Coefficient (Abraham et al. 2003)
M_{20} 2nd order moment of brightest regions

The Gini Coefficient

used in economics to measure distribution of wealth in population
→ distribution of flux in galaxy's pixels (Abraham et al. 2003)

G=0 for completely egalitarian society (uniform surf brightness)
G=1 for absolute monarchy (all flux in single pixel)
(G = 0.445 for US in 1999)

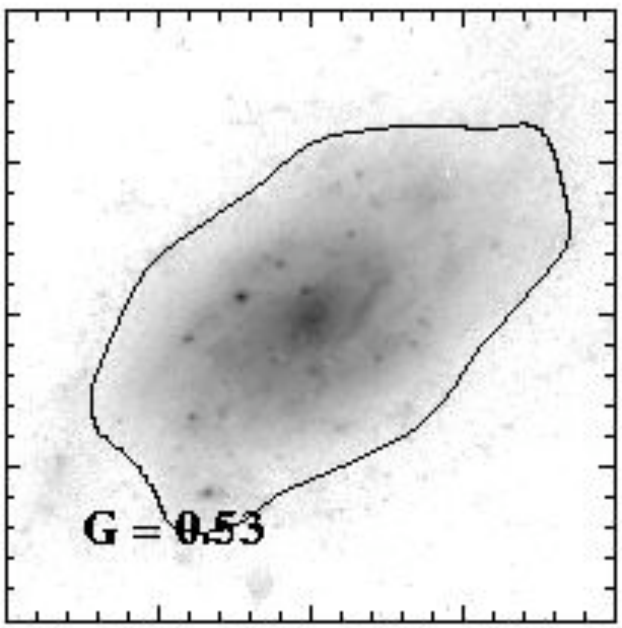

The Gini Coefficient

used in economics to measure distribution of wealth in population
→ distribution of flux in galaxy's pixels (Abraham et al. 2003)

G=0 for completely egalitarian society (uniform surf brightness)
G=1 for absolute monarchy (all flux in single pixel)
(G = 0.445 for US in 1999)

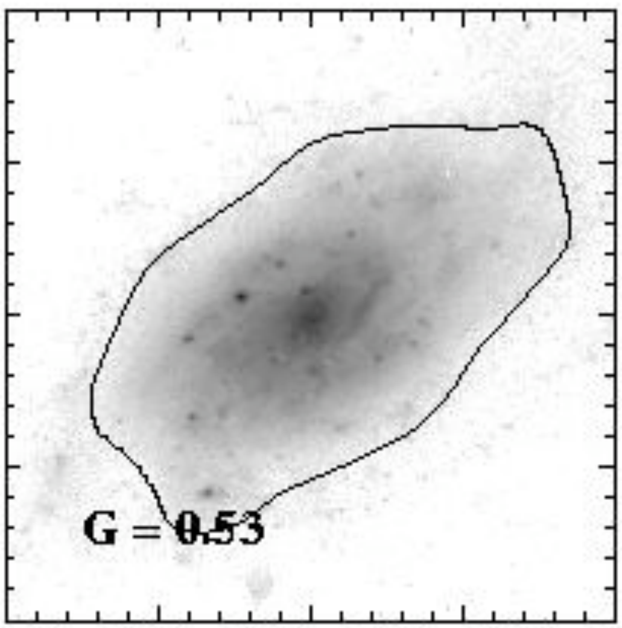

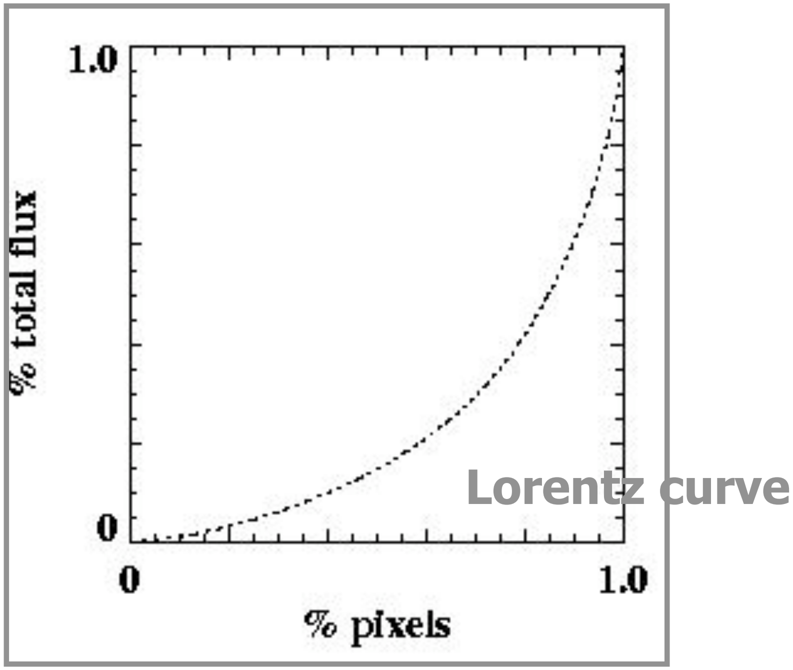

The Gini Coefficient

used in economics to measure distribution of wealth in population
→ distribution of flux in galaxy's pixels (Abraham et al. 2003)

G=0 for completely egalitarian society (uniform surf brightness)
G=1 for absolute monarchy (all flux in single pixel)
(G = 0.445 for US in 1999)

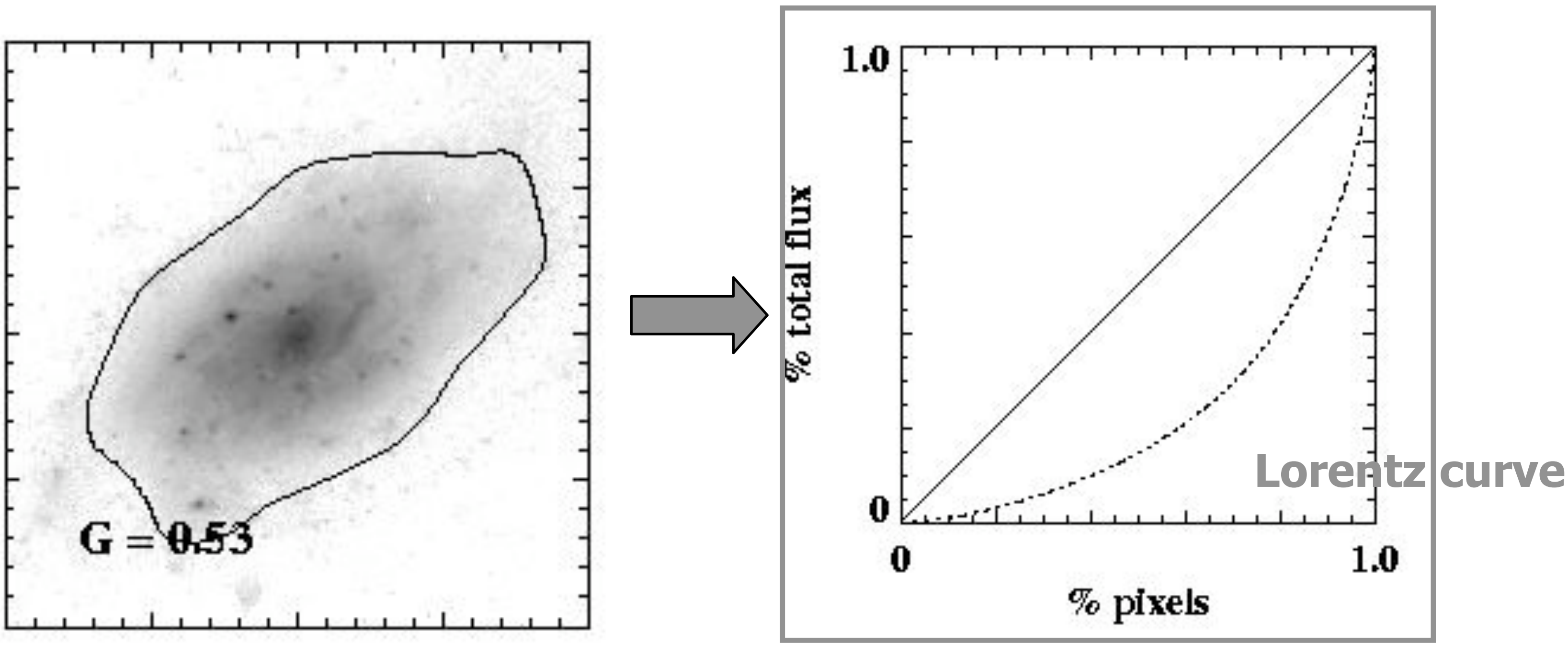

The Gini Coefficient

used in economics to measure distribution of wealth in population
→ distribution of flux in galaxy's pixels (Abraham et al. 2003)

G=0 for completely egalitarian society (uniform surf brightness)
G=1 for absolute monarchy (all flux in single pixel)
(G = 0.445 for US in 1999)

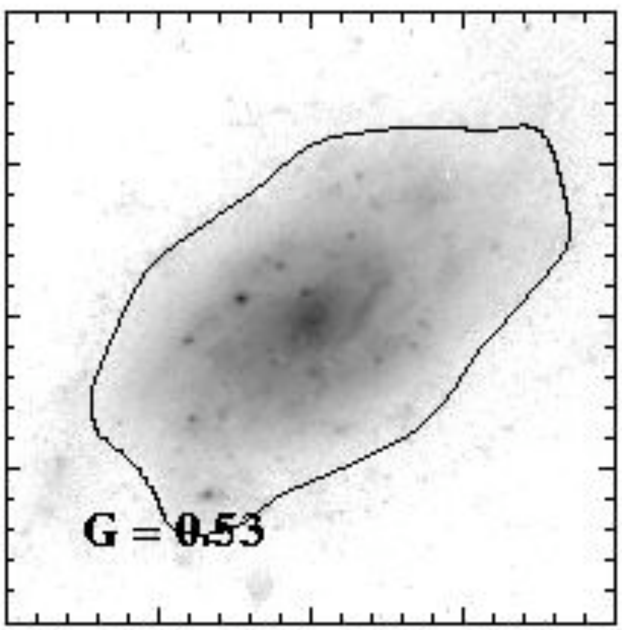

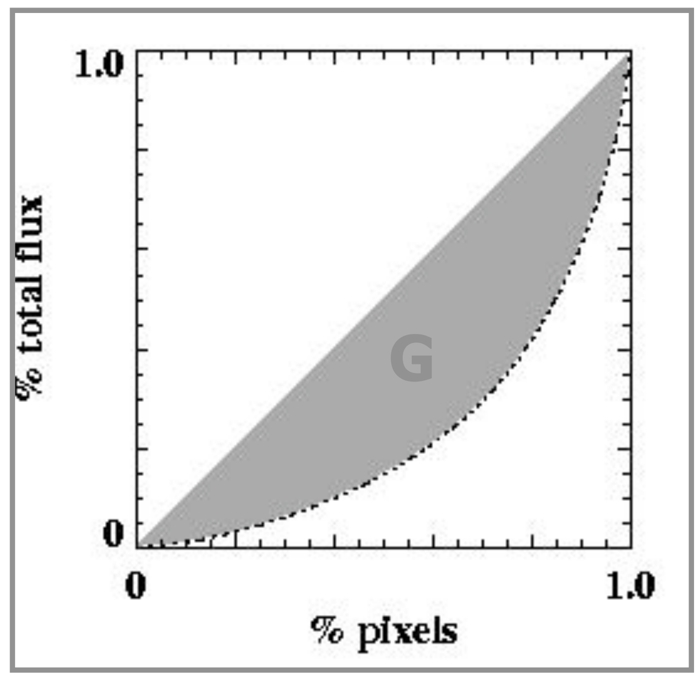

The Gini Coefficient

used in economics to measure distribution of wealth in population
→ distribution of flux in galaxy’s pixels (Abraham et al. 2003)

G=0 for completely egalitarian society (uniform surf brightness)
G=1 for absolute monarchy (all flux in single pixel)
(G = 0.445 for US in 1999)

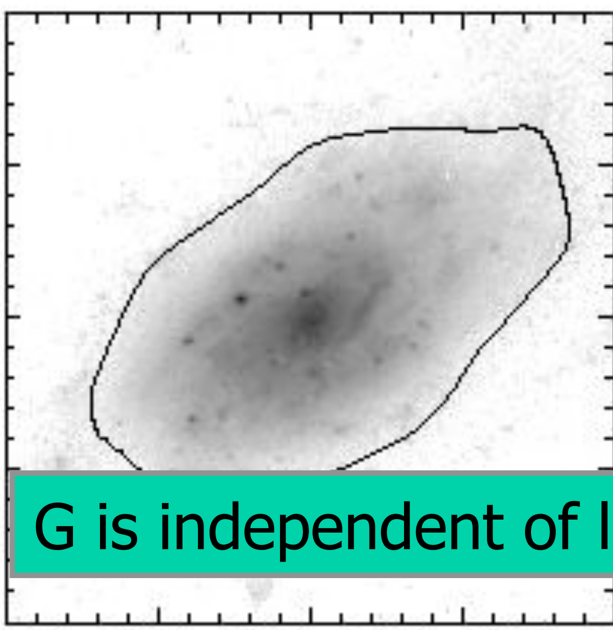

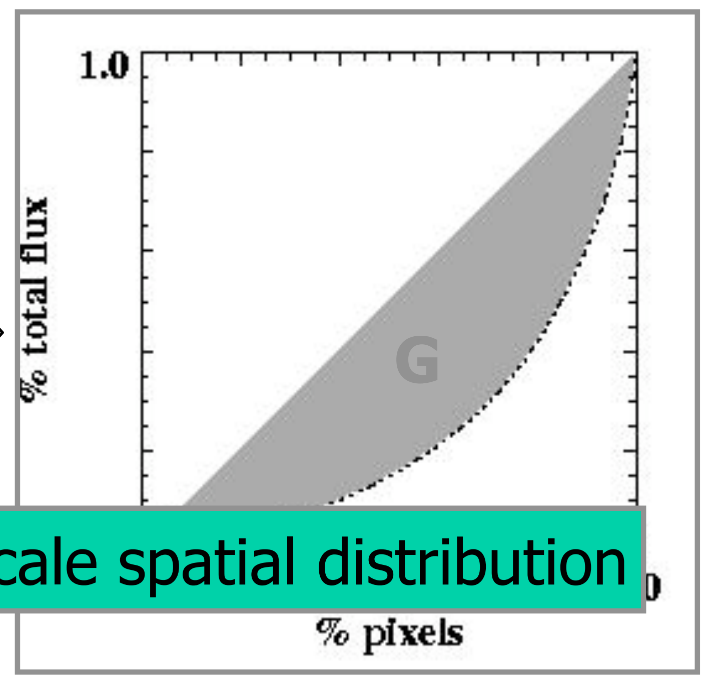

G is independent of large-scale spatial distribution

2^{nd} order moment of light

$M_{total} = \sum f_i r_i^2$ (minimize to find center of light)

this depends on size + luminosity
→ find relative moment of brightest regions

$$M_{20} = \log_{10} \frac{\sum_{1}^{n} f_i r_i^2}{M_{total}} \quad \text{where} \quad \sum_{1}^{n} f_i = 0.2 \sum f_i$$

- very similar to $C = \log (r_{80\%}/r_{20\%})$
  but does NOT assume particular geometry

- more sensitive to merger signatures (double nuclei)

Local Galaxy G-M20 relation

Frei et al 1996: ~100 bright local Hubble types
B/g (~4500 AA) + R/r (~6500 AA)

SDSS DR1: ~50 local bright (u<14) galaxies
u (~3600 AA), g (~4700 AA), r(~6200 AA)

Borne et al 2000: ~100 HST WFPC2 z < 0.2 ULIRGs
F814W (~ 6500 AA rest-frame)

Local Galaxy G-M20 relation

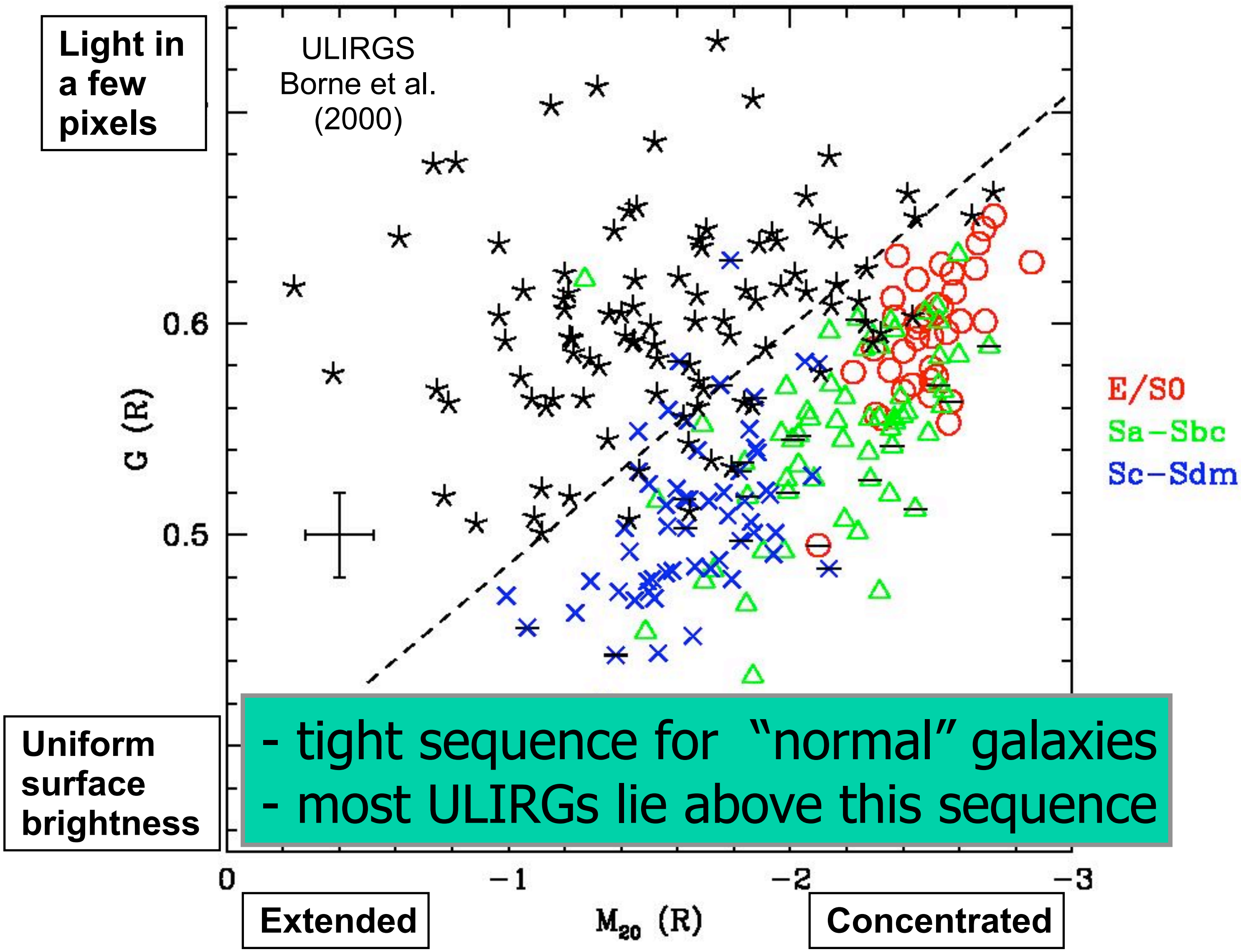

- tight sequence for "normal" galaxies
- most ULIRGs lie above this sequence

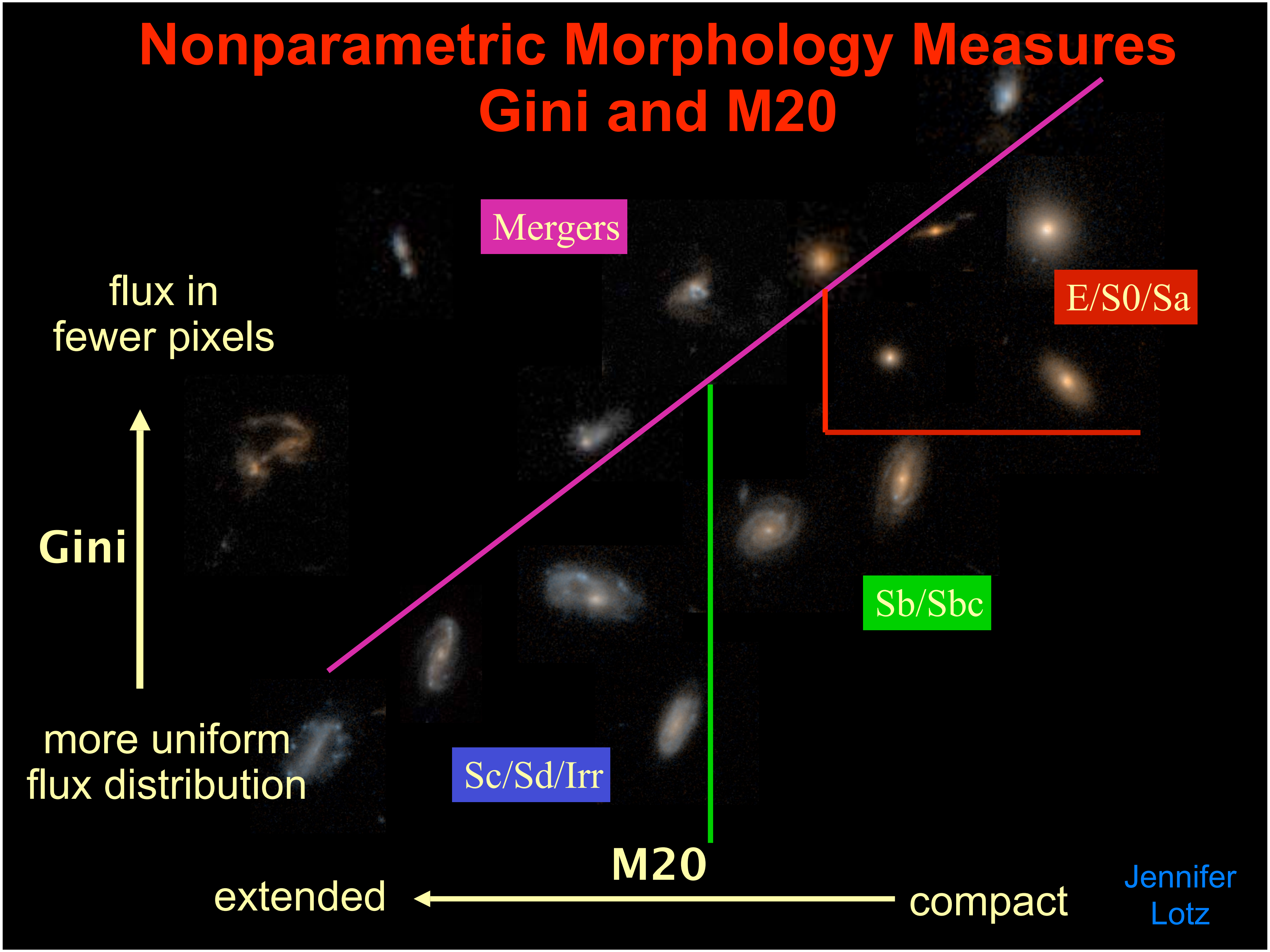
Nonparametric Morphology Measures
Gini and M20
Mergers
E/S0/Sa
flux in
fewer pixels
Gini
Sb/Sbc
more uniform
flux distribution
Sc/Sd/Irr
M20
extended
compact
Jennifer
Lotz

Modeling Merger Morphologies

Light in a few pixels

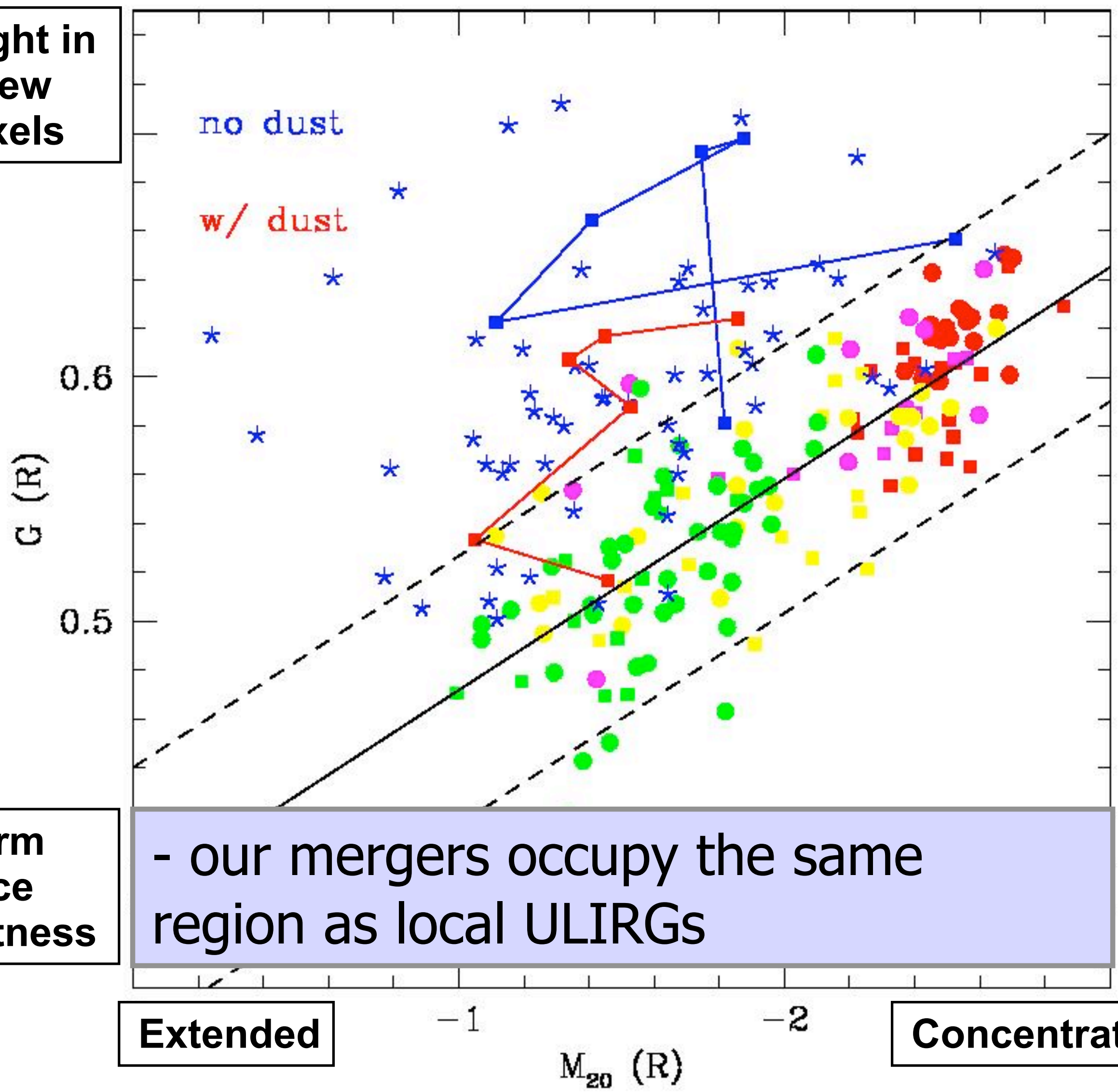

Uniform surface brightness

- our mergers occupy the same region as local ULIRGs

Extended

Concentrated

E/S0

Sa/Sab

Sb/Sbc

Sc/Scd

ULIRGs

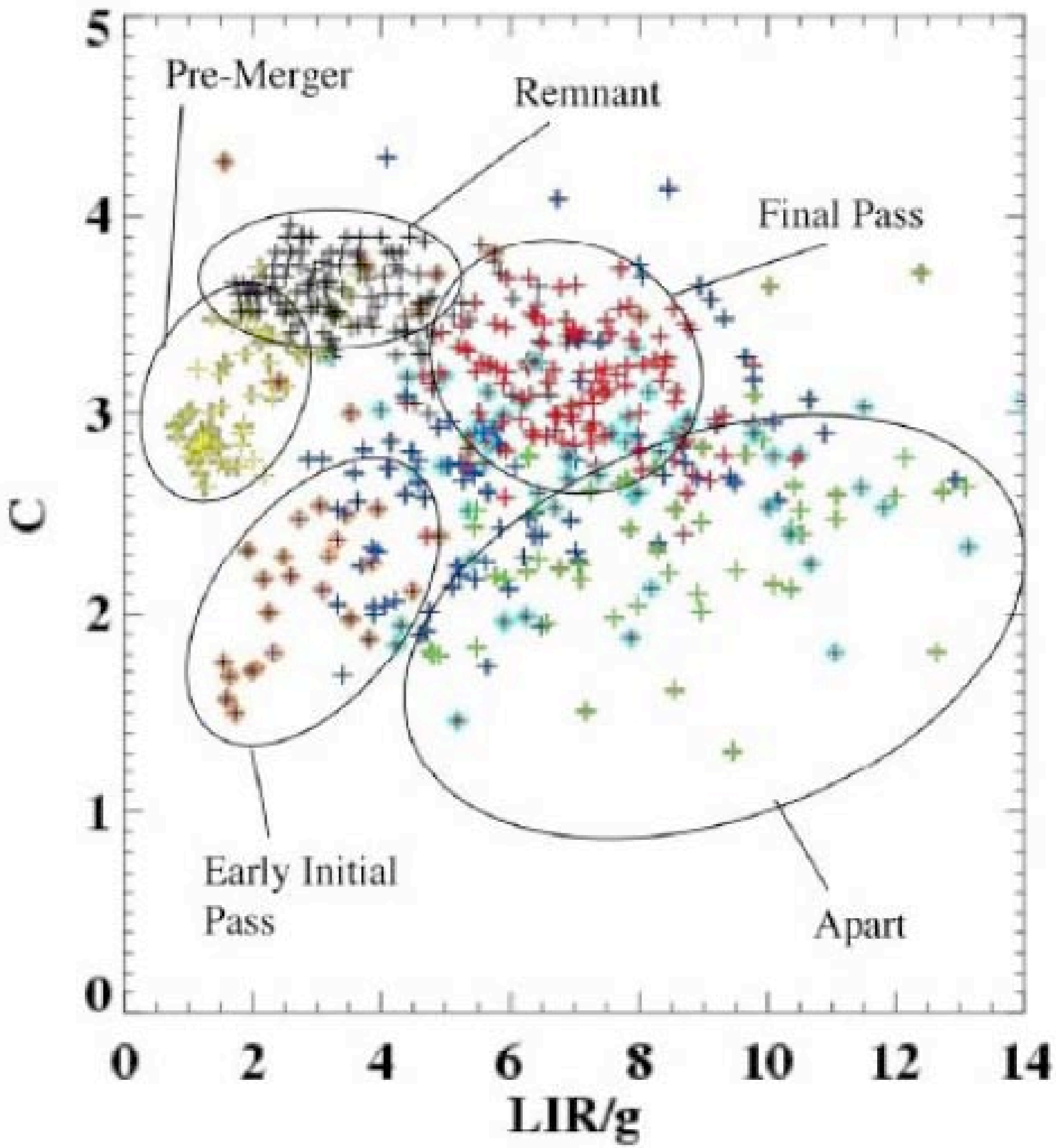

Using morphology and log L_{IR}/optical color, **it's possible to determine the merger stage of simulated galaxies** (senior thesis of Seth Cottrell, supervised by Lotz and Primack). We're now applying these techniques to a larger sample of simulations, and to observations. This will enable accurate measurement of merger rates. Related 08 sr thesis by Taylor Davalos.

Merger Simulations
with Supermassive Black Holes

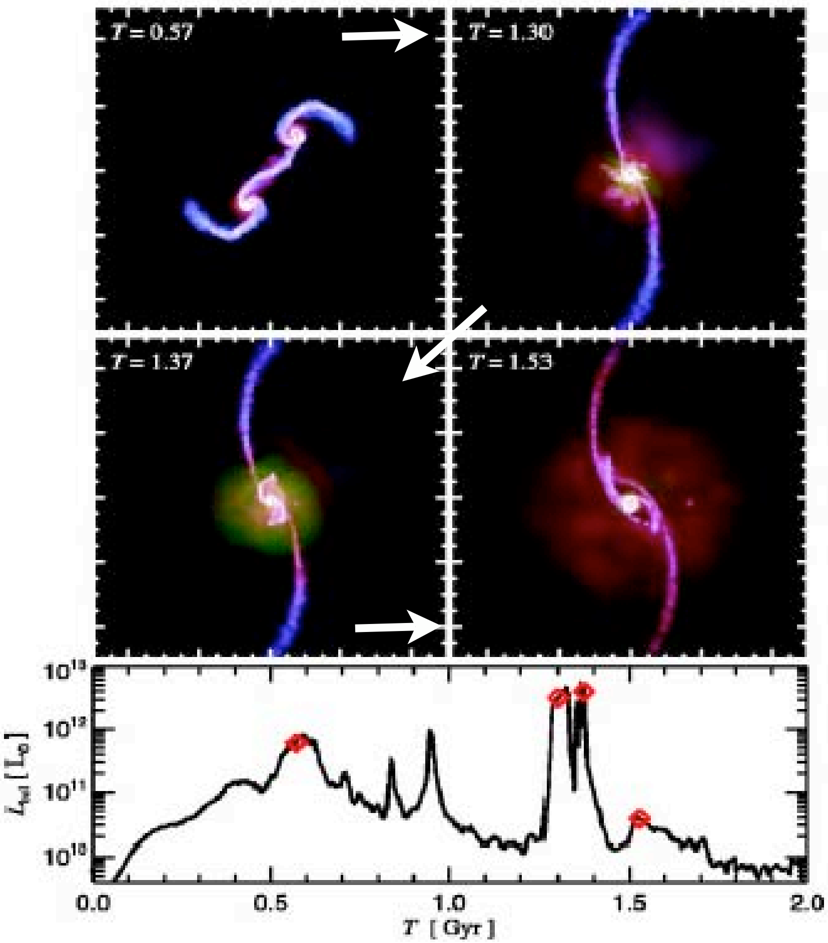

(Hopkins et al. 2005, ApJ, 625, L71)

- Mergers of gas-rich disk galaxies hosting SMBHs
- Snapshots: gas densities at time (T) since interaction began
- Plot: intrinsic bolometric luminosity (diamonds match snapshots)
- Morphology most disturbed at T~1.30-1.37 Gyrs.
- AGNs turn on at T~1.30 Gyr.

Proposed Co-Origin of Spheroids, SMBHs

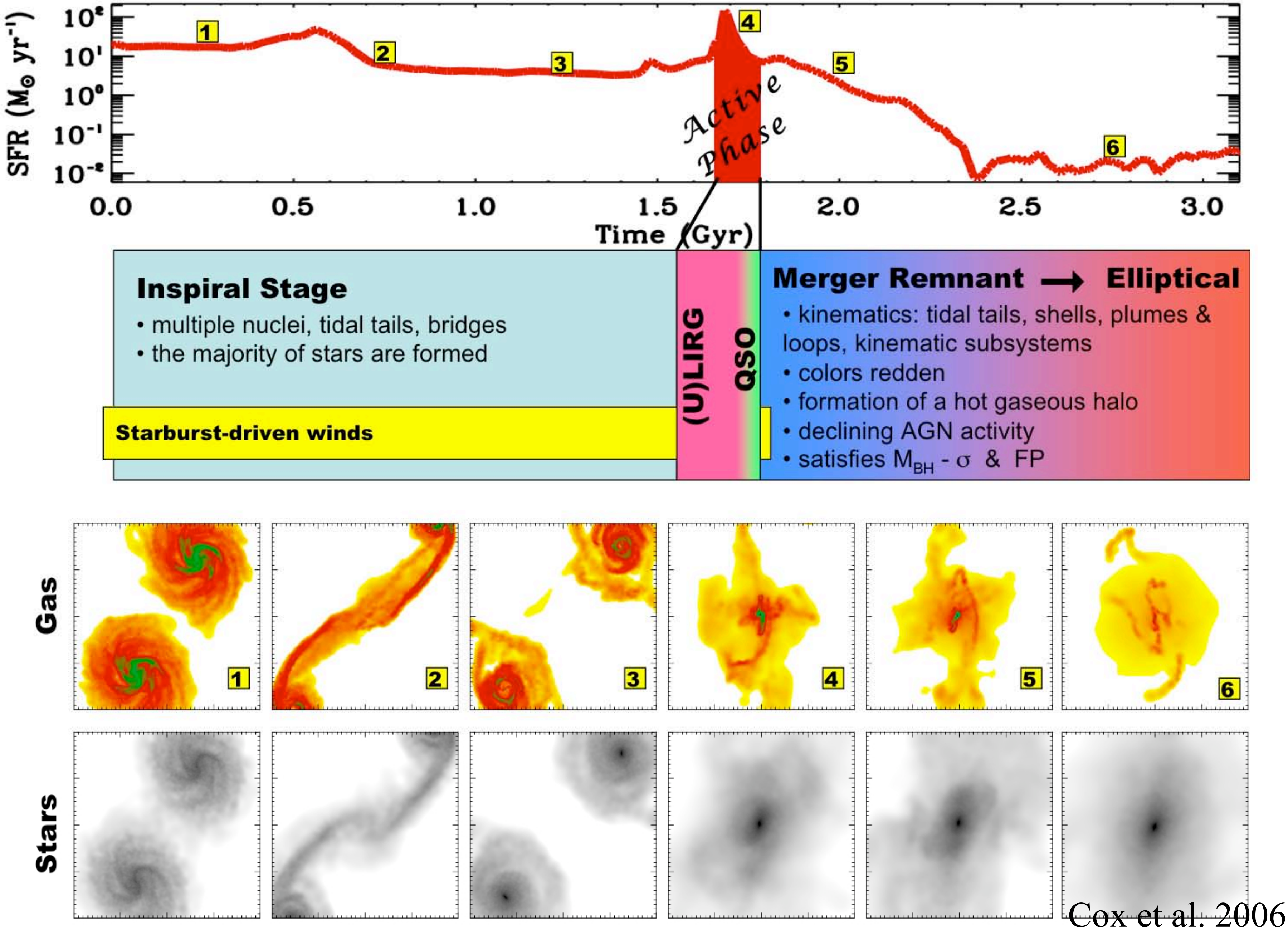

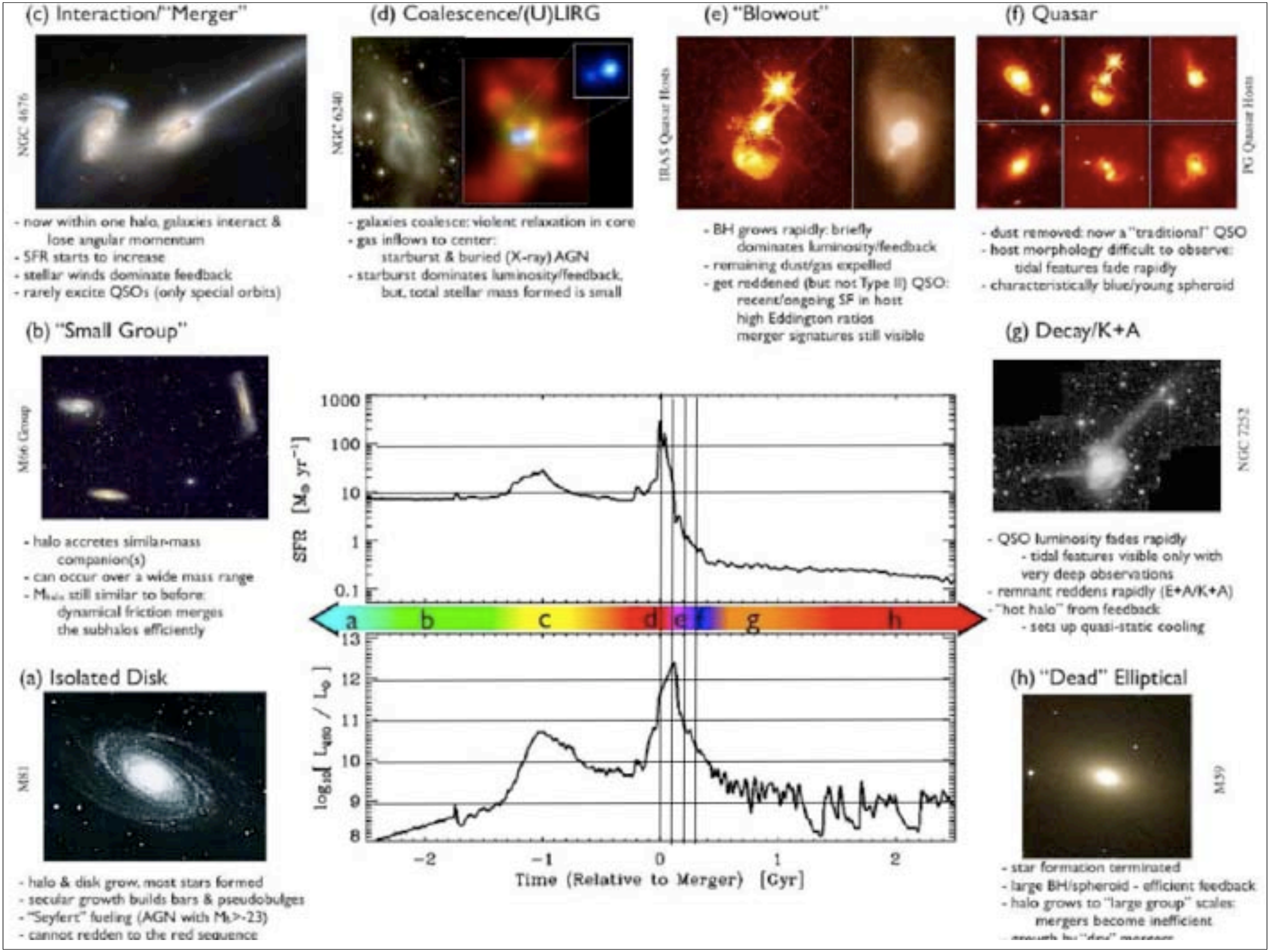

(c) Interaction/"Merger"
NGC 4676
- now within one halo, galaxies interact & lose angular momentum
- SFR starts to increase
- stellar winds dominate feedback
- rarely excite QSOs (only special orbits)
(d) Coalescence/(U)LIRG
NGC 6240
- galaxies coalesce: violent relaxation in core
- gas inflows to center: starburst & buried (X-ray) AGN
- starburst dominates luminosity/feedback, but, total stellar mass formed is small
(e) "Blowout"
IRAS Quasar Hosts
- BH grows rapidly: briefly dominates luminosity/feedback
- remaining dust/gas expelled
- get reddened (but not Type II) QSO: recent/ongoing SF in host high Eddington ratios merger signatures still visible
(f) Quasar
PG Quasar Hosts
- dust removed: now a "traditional" QSO
- host morphology difficult to observe: tidal features fade rapidly
- characteristically blue/young spheroid
(b) "Small Group"
M66 Group
- halo accretes similar-mass companion(s)
- can occur over a wide mass range
- M_{halo} still similar to before: dynamical friction merges the subhalos efficiently
(g) Decay/K+A
NGC 7252
- QSO luminosity fades rapidly
- tidal features visible only with very deep observations
- remnant reddens rapidly (E+A/K+A)
- "hot halo" from feedback
- sets up quasi-static cooling
(a) Isolated Disk
M81
- halo & disk grow, most stars formed
- secular growth builds bars & pseudobulges
- "Seyfert" fueling (AGN with M_B>-23)
- cannot redden to the red sequence
(h) "Dead" Elliptical
M59
- star formation terminated
- large BH/spheroid - efficient feedback
- halo grows to "large group" scales: mergers become inefficient
SFR [$M_\odot$ yr^{-1}]
1000
100
10
1
0.1
a b c d e f g h
$\log_{10}$ [L_{gal} / $L_\odot$]
13
12
11
10
9
8
-2
-1
0
1
2
Time (Relative to Merger) [Gyr]

Comparison with Observational Data

Extended Groth Strip (EGS)

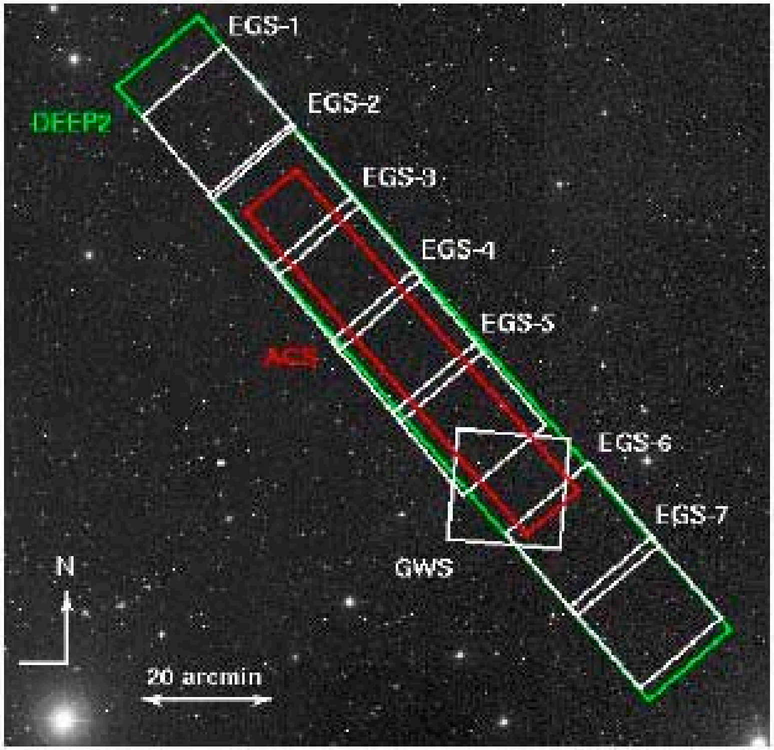

(http://astro.ic.ac.uk/Research/Xray/egs/
)

- EGS: ~0.5 deg^2 (green area)
- ACS: ~0.33 deg^2 (red area)
- IRAC: ~0.5 deg^2 (full EGS)
- Chandra: ~3.75 sq. arcmin. (Groth Westphal Strip; extra pointings now available)
- Canada-France-Hawaii Telescope Legacy Survey: photometric redshifts
- DEEP2 spectroscopic redshifts

Morphological distribution of EGS X-ray selected AGN

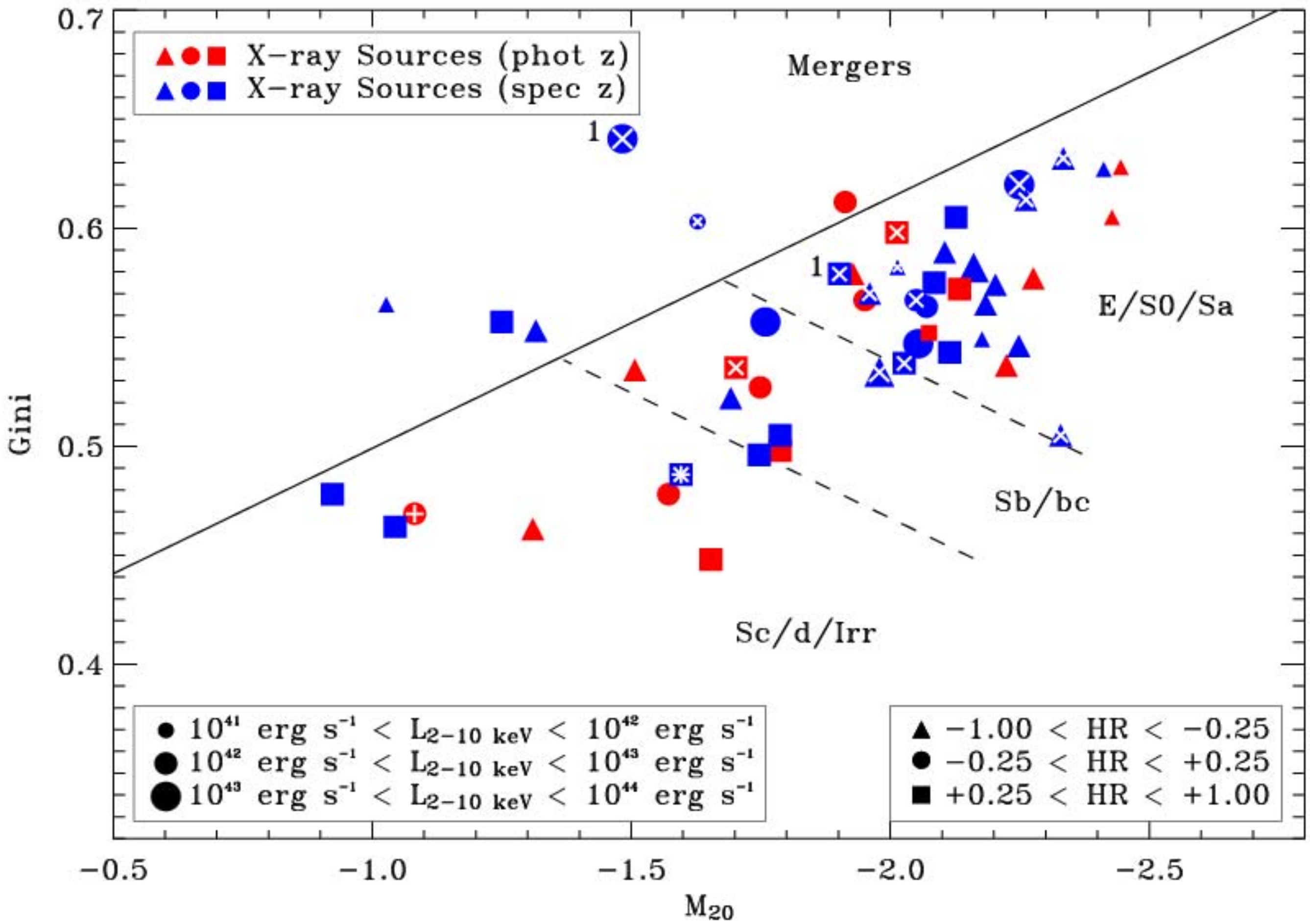

The highest fraction of EGS galaxies hosting AGN are early-types, not mergers. This suggests that the AGN activity is delayed, rather than occurring mainly during and immediately following mergers as the Hopkins et al. simulations predicted. (Christy Pierce et al., ApJ Letters, in press May 2007).

Color-Magnitude Diagram of EGS X-ray selected AGN

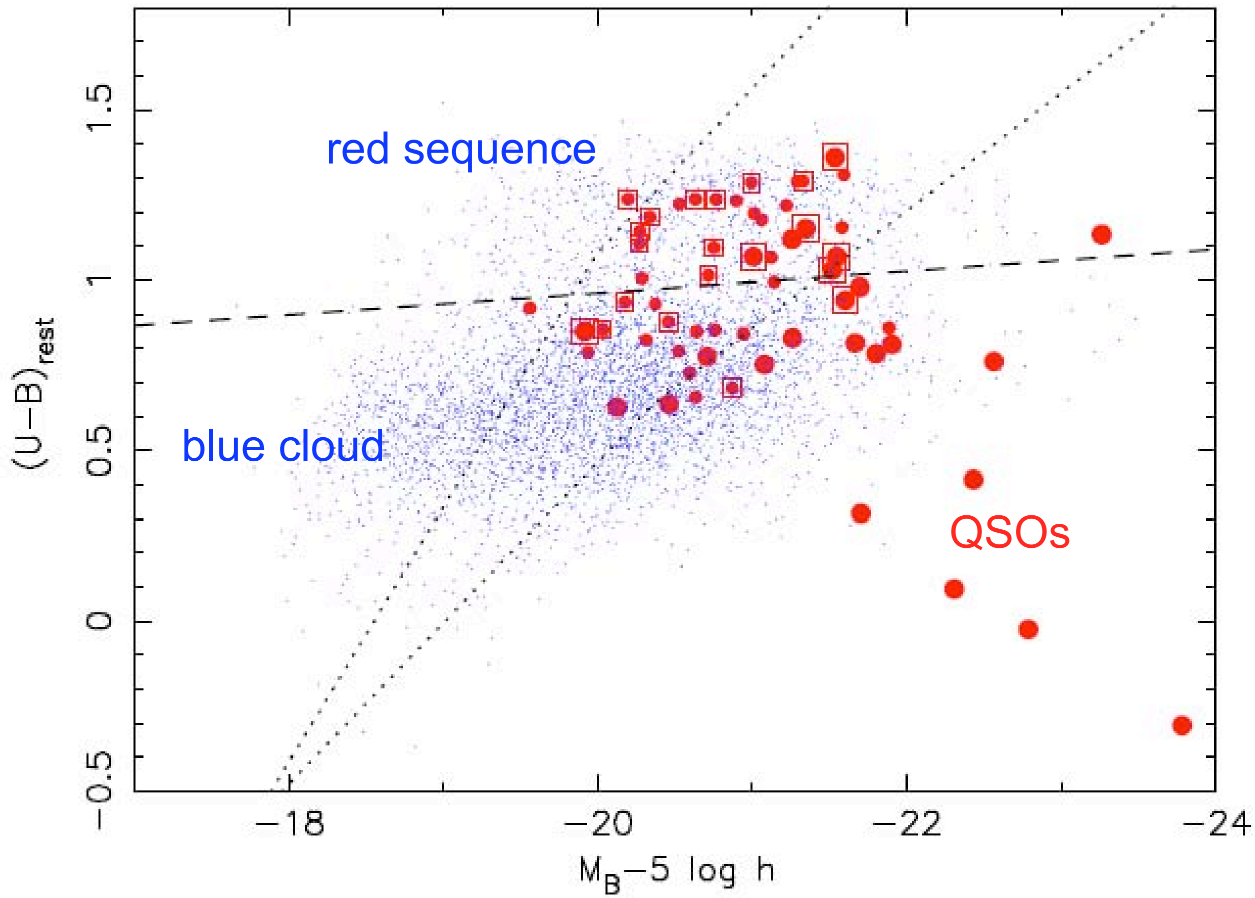

Rest-frame U-B colour is plotted against the B-band absolute magnitude for DEEP2 comparison galaxies (small blue dots) and X-ray sources (filled red circles) in the EGS in the range $0.7 < z < 1.4$. Squares around the symbols indicate hard X-ray sources, and more luminous systems ($L_X > 10^{43}$ erg s^{-1}) are plotted with larger symbols. The dashed line separates red and blue galaxies, and the dotted lines show the DEEP2 completeness limits at $z = 1.0$ and $z = 1.4$.
(Kirpal Nandra et al., ApJ Letters, in press.)

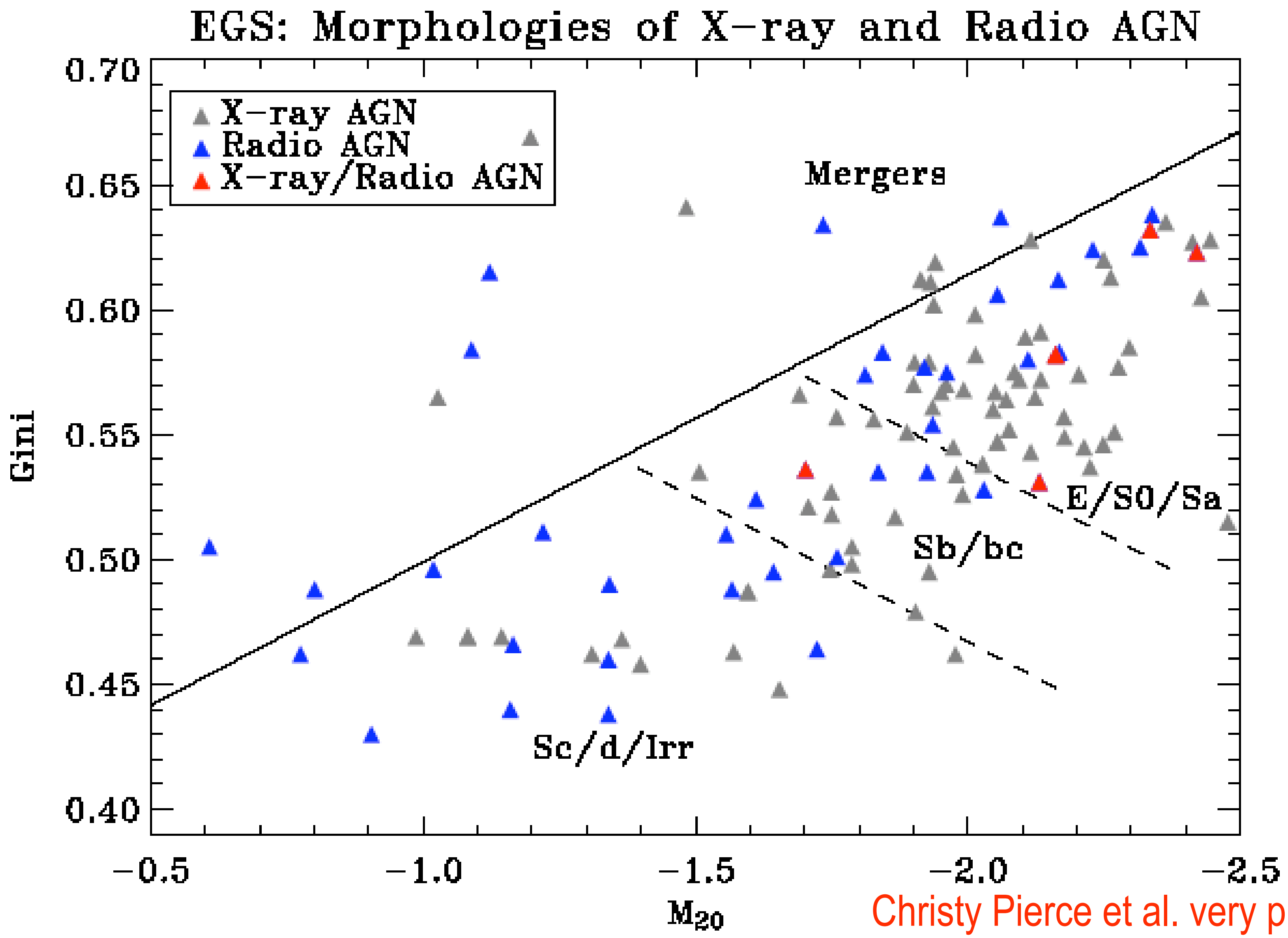

Christy Pierce et al. very preliminary

Fig. 1.— X-ray and radio-selected AGN in the EGS. AGN outside of either the X-ray region or the radio region are excluded. Thus, each X-ray AGN represented should have been detectable by the radio survey, if there was any radio signal to detect, and vice versa. The host galaxies have $I \leq 23.5$, $0.2 \leq z < 1.2$, $r_P \geq 0.''3$, $\langle S/N \rangle \geq 2.5$, and are not flagged as non-contiguous (i.e., they meet the criteria for use with $G - M_{20}$). The colors represent method of selection, as shown.

Conclusions on EGS X-ray Selected AGN

We find that most X-ray selected AGN are hosted by early-type galaxies, based both on G-M_{20} and on visual classification. Mergers and Sb/bc galaxies are represented at the same rate as the field population, and Sc/d/Irr galaxies are greatly underrepresented. Close kinematic pairs are 3 times as likely to host X-ray AGN.

Most X-ray AGN are in the red sequence, in the top half of the blue cloud, or in the transition region between them. This supports the idea that AGN terminate star formation. But many transition galaxies do not have AGN.

Many X-ray AGN are bright (>10^{42} erg/s) for 1 Gyr or more after a starburst. Many hard AGN are on the red sequence, disfavoring star-forming gas as a main source of obscuration.

Radio AGN appear to have similar morphology as X-ray AGN. Lack of enhanced likelihood of mergers suggests that bright AGN phase is delayed by ~100s of My after starburst peak.

Multiple Merger Simulations